Eur. Phys. J. C (2023) 83:438
https://doi.org/10.1140/epjc/s10052-023-11427-9

THE EUROPEAN PHYSICAL JOURNAL C

Regular Article - Experimental Physics

Measurement of the nuclear modification factor of *b*-jets in 5.02 TeV Pb+Pb collisions with the ATLAS detector

ATLAS Collaboration[*]

CERN, 1211 Geneva 23, Switzerland

Received: 29 April 2022 / Accepted: 9 August 2022

Abstract This paper presents a measurement of *b*-jet production in Pb+Pb and *pp* collisions at $\sqrt{s_{\mathrm{NN}}} = 5.02$ TeV with the ATLAS detector at the LHC. The measurement uses 260 pb^{-1} of *pp* collisions collected in 2017 and 1.4 nb^{-1} of Pb+Pb collisions collected in 2018. In both collision systems, jets are reconstructed via the anti-k_t algorithm. The *b*-jets are identified from a sample of jets containing muons from the semileptonic decay of *b*-quarks using template fits of the muon momentum relative to the jet axis. In *pp* collisions, *b*-jets are reconstructed for radius parameters $R = 0.2$ and $R = 0.4$, and only $R = 0.2$ jets are used in Pb+Pb collisions. For comparison, inclusive $R = 0.2$ jets are also measured using 1.7 nb^{-1} of Pb+Pb collisions collected in 2018 and the same *pp* collision data as the *b*-jet measurement. The nuclear modification factor, R_{AA}, is calculated for both *b*-jets and inclusive jets with $R = 0.2$ over the transverse momentum range of 80–290 GeV. The nuclear modification factor for *b*-jets decreases from peripheral to central collisions. The ratio of the *b*-jet R_{AA} to inclusive jet R_{AA} is also presented and suggests that the R_{AA} for *b*-jets is larger than that for inclusive jets in central Pb+Pb collisions. The measurements are compared with theoretical calculations and suggest a role for mass and colour-charge effects in partonic energy loss in heavy-ion collisions.

Contents

1 Introduction

The primary physics aim of the heavy-ion programme at the Large Hadron Collider (LHC) is to produce and study the quark–gluon plasma (QGP), the high-temperature state of quantum-chromodynamic (QCD) matter in which quarks and gluons are no longer confined within protons and neutrons (for a recent review, see Ref. [1]). Measurements of jets arising from hard-scattered partons produced in the early stages of heavy-ion collisions provide information about the short-distance-scale interactions of high-energy partons with the QGP. The overall rate of jets in central Pb+Pb collisions at a given transverse momentum, p_{T}, is found to be significantly lower than expectations based on *pp* collisions, up to a p_{T} of approximately 1 TeV [2–4]. The showering partons which give rise to jets undergo medium-induced gluon radiation and elastic scattering off the QGP constituents; both processes broaden the angular distribution of the energy from the parton shower [5]. This leads to the measurement of lower-energy jets than in *pp* collisions as some of the parton's energy is moved outside of the jet cone.

The interactions between high-energy partons and the QGP are expected to depend on the parton's QCD colour charge and mass. Thus, jets originating from *b*-quarks, *b*-jets, (for a recent review, see Ref. [6]) are of particular interest because the quark mass is large compared to light quarks. Additionally, the QCD colour charge is controlled; this contrasts with inclusive jets, which mostly originate from a mixture of light quarks and gluons. The *b*-jets produced

[*] e-mail: atlas.publications@cern.ch

Published online: 25 May 2023

in hadronic collisions consist of jets in which the b-quark is directly produced in the hard scattering (e.g. $gg \rightarrow b\bar{b}$) and jets in which a hard-scattered gluon splits into a $b\bar{b}$ pair ($g \rightarrow b\bar{b}$) as part of the showering process.

Inclusive jets and b-jets are expected to be sensitive to different effects in the QGP. Medium-induced gluon radiation is expected to be suppressed for heavy quarks by the dead-cone effect [7]. As the velocity of the b-quark increases the importance of the dead-cone effect decreases. Calculations for Pb+Pb collisions show that the dead-cone effect reduces the suppression of B-mesons up to transverse momenta of approximately 50 GeV [8]. This does not simply translate to a specific jet p_{T} range because b-quarks in jets from gluon splitting tend to have lower momentum than those directly from hard scattering at the same jet p_{T}. Differences in the interactions between the QGP and the developing parton shower between b-jets and inclusive jets could also arise from differences in how quarks and gluons interact with the QGP [9]. Measurements of heavy-quark jets in heavy-ion collisions are also expected to be sensitive to the mixture of radiative and collisional energy loss in the QGP [10–12]. Due to these different effects, which are expected to lead to differences between b-jets and inclusive jets in Pb+Pb collisions, it is important to compare the b-jet and inclusive-jet suppression in Pb+Pb collisions over as wide a kinematic range as possible.

Prior measurements have investigated the effects of energy loss for heavy quarks. Many measurements are based on electrons or muons from the semileptonic decay of charm and bottom hadrons [13–17]. Other measurements have partially [18–21] or fully [22–27] reconstructed the heavy-flavour hadrons. One limitation of these measurements is that they do not provide direct information about the total jet energy. This is important because the fragmentation functions of b-jets are very different from those of inclusive jets [28]; thus, it is not possible to directly compare the suppression of b-quarks with that of light quarks and gluons without full jet measurements. CMS has measured the suppression of b-jets in Pb+Pb collisions at 2.76 TeV and found it to be consistent with that of inclusive jets over the jet transverse momentum, $p_{\mathrm{T}}^{\mathrm{jet}}$, range of 70–250 GeV [29], although the uncertainties are large.

For the measurements reported in this article, jets are clustered with the anti-k_t algorithm [30] using radius parameters $R = 0.2$ (in both Pb+Pb and pp collisions) and $R = 0.4$ (only in pp collisions). At generator level, a jet is considered as a b-jet if a b-hadron with $p_{\mathrm{T}} > 5$ GeV is found within an angular distance[1] of $\Delta R = 0.3$ from the jet axis. The b-jets are identified statistically from a sample of jets containing muons. The muons from b-hadron decays are distinguished from muons arising from charm- and light-hadron decays by the difference between their transverse momenta, p_{T}^{μ}, relative to the jet+μ axis. The jet+μ axis is defined in the transverse plane by

$$\vec{u}_{\mathrm{T}}^{\,\mathrm{jet}+\mu} = \frac{\vec{p}_{\mathrm{T}}^{\,\mu} + \vec{p}_{\mathrm{T}}^{\,\mathrm{jet}}}{\left|\vec{p}_{\mathrm{T}}^{\,\mu} + \vec{p}_{\mathrm{T}}^{\,\mathrm{jet}}\right|} \tag{1}$$

(where the vector notation indicates the vector quantity is meant instead of the magnitude of the vector), and the transverse momentum of the muon relative to the jet axis, $p_{\mathrm{T}}^{\mathrm{rel}}$, is defined as

$$p_{\mathrm{T}}^{\mathrm{rel}} = \left|\vec{p}_{\mathrm{T}}^{\,\mu} \times \vec{u}_{\mathrm{T}}^{\,\mathrm{jet}+\mu}\right|. \tag{2}$$

This method was used previously by ATLAS for pp collisions at 7 TeV and the results were compared with those based on the reconstruction of secondary vertices [31]. Only $R = 0.2$ jets are used in Pb+Pb collisions because they have better angular resolution and have a smaller contribution from accidental jet–muon overlaps in Pb+Pb collisions; both of these features improve the performance of the $p_{\mathrm{T}}^{\mathrm{rel}}$ method.

This paper reports measurements of inclusive jet and b-jet cross-sections in pp collisions and the per-event yield for inclusive jets and b-jets in Pb+Pb collisions at 5.02 TeV. In both collision systems, the spectra are corrected to the generator level (just before the b-hadron decays for b-jets). For $R = 0.2$ jets the nuclear modification factor, R_{AA}, is calculated for b-jets as

$$R_{\mathrm{AA}}^{b\text{-jet}} \equiv \left.\frac{1}{N_{\mathrm{evt}}}\frac{\mathrm{d}^2 N_{\mathrm{AA}}^{b\text{-jet}}}{\mathrm{d}p_{\mathrm{T}}\mathrm{d}y}\right|_{\mathrm{cent}} \Bigg/ \langle T_{\mathrm{AA}}\rangle \frac{\mathrm{d}^2\sigma_{pp}^{b\text{-jet}}}{\mathrm{d}p_{\mathrm{T}}\mathrm{d}y}$$

where $\mathrm{d}^2 N_{\mathrm{AA}}^{b\text{-jet}}/\mathrm{d}p_{\mathrm{T}}\mathrm{d}y$ is the yield of b-jets in Pb+Pb collisions for the centrality, p_{T}, and rapidity range of interest; $\mathrm{d}^2\sigma_{pp}^{b\text{-jet}}/\mathrm{d}p_{\mathrm{T}}\mathrm{d}y$ is the b-jet cross-section in pp collisions; $\langle T_{\mathrm{AA}}\rangle$ is the nuclear thickness function [32]; and N_{evt} is the number of minimum-bias (MB) Pb+Pb events for the central-

[1] ATLAS uses a right-handed coordinate system with its origin at the nominal interaction point (IP) in the centre of the detector, and the z-axis along the beam pipe. The x-axis points from the IP to the centre of the LHC ring, and the y-axis points upward. Cylindrical coordinates (r, ϕ) are used in the transverse plane, ϕ being the azimuthal angle around the z-axis. The pseudorapidity is defined in terms of the polar angle θ as $\eta = -\ln\tan(\theta/2)$. The rapidity is defined as $y = 0.5\ln[(E + p_z)/(E - p_z)]$ where E and p_z are the energy and z-component of the momentum along the beam direction, respectively. Transverse momentum and transverse energy are defined as $p_{\mathrm{T}} = p\sin\theta$ and $E_{\mathrm{T}} = E\sin\theta$, respectively. The angular distance between two objects with relative differences $\Delta\eta$ in pseudorapidity and $\Delta\phi$ in azimuth is given by $\Delta R = \sqrt{(\Delta\eta)^2 + (\Delta\phi)^2}$.

ity selection under consideration. Analogously, the nuclear modification factor for inclusive jets is defined as

$$R_{\mathrm{AA}}^{\text{inclusive jet}} \equiv \frac{1}{N_{\mathrm{evt}}} \frac{\mathrm{d}^2 N_{\mathrm{AA}}^{\text{inclusive jet}}}{\mathrm{d}p_{\mathrm{T}}\mathrm{d}y}\bigg|_{\mathrm{cent}} \Big/ \langle T_{\mathrm{AA}} \rangle \frac{\mathrm{d}^2 \sigma_{pp}^{\text{inclusive jet}}}{\mathrm{d}p_{\mathrm{T}}\mathrm{d}y}$$

where the yield and cross-section are for inclusive jets and the other quantities remain the same.

The measurements are performed in Pb+Pb collisions at $\sqrt{s_{\mathrm{NN}}} = 5.02$ TeV collected during 2018, with an integrated luminosity of 1.4 nb^{-1} for the b-jet sample and 1.7 nb^{-1} for the inclusive jet sample, and in pp collisions at $\sqrt{s} = 5.02$ TeV collected during 2017, with an integrated luminosity of 260 pb^{-1}. The measurements are presented for jets with $80 < p_{\mathrm{T}} < 290$ GeV and $|y| < 2.1$.

The paper is structured as follows. Section 2 describes the ATLAS detector, and Sect. 3 discusses the selection procedure applied to the data. The data analysis is presented in Sect. 4 and the systematic uncertainties are presented in Sect. 5. The results and a summary are presented in Sects. 6 and 7.

2 ATLAS detector

The ATLAS detector [33] at the LHC covers nearly the entire solid angle around the collision point. It consists of an inner tracking detector surrounded by a thin superconducting solenoid, electromagnetic and hadronic calorimeters, and a muon spectrometer incorporating three large superconducting toroidal magnets.

The inner-detector system (ID) is immersed in a 2 T axial magnetic field and provides charged-particle tracking in the range $|\eta| < 2.5$. The high-granularity silicon pixel detector covers the vertex region, and is composed of four layers including the insertable B-layer [34,35]. It is followed by the silicon microstrip tracker, which usually provides four two-dimensional measurement points per track. These silicon detectors are complemented by the transition radiation tracker (TRT), which enables radially extended track reconstruction up to $|\eta| = 2.0$.

The calorimeter system covers the pseudorapidity range $|\eta| < 4.9$. Within the region $|\eta| < 3.2$, electromagnetic calorimetry is provided by barrel and endcap high-granularity lead/liquid-argon (LAr) electromagnetic calorimeters, with an additional thin LAr presampler covering $|\eta| < 1.8$ to correct for energy loss in material upstream of the calorimeters. The hadronic calorimeters have three sampling layers longitudinal in shower depth in $|\eta| < 1.7$ and four sampling layers in $1.5 < |\eta| < 3.2$, with a slight overlap in η. The solid angle coverage is completed with forward copper/LAr and tungsten/LAr calorimeter modules (FCal) optimised for electromagnetic and hadronic measurements respectively.

The muon spectrometer (MS) comprises separate trigger and high-precision tracking chambers measuring the deflection of muons in a magnetic field generated by the superconducting air-core toroids. The field integral of the toroids ranges between 2.0 and 6.0 T m across most of the detector. A set of precision chambers covers the region $|\eta| < 2.7$ with three layers of monitored drift tubes, complemented by cathode strip chambers in the forward region, where the background is highest. The muon trigger system covers the range $|\eta| < 2.4$ with resistive plate chambers in the barrel, and thin gap chambers in the endcap regions.

The zero-degree calorimeters (ZDCs) are located symmetrically at $z = \pm 140$ m and cover $|\eta| > 8.3$ during the Pb+Pb data-taking period. The ZDCs use tungsten plates as absorbers and quartz rods sandwiched between the tungsten plates as the active medium. In Pb+Pb collisions the ZDCs primarily measure spectator neutrons, which are neutrons that do not interact hadronically when the incident nuclei collide. A ZDC coincidence trigger is implemented by requiring the pulse height from each ZDC to be above a threshold set to accept the energy of a single neutron.

A two-level trigger system is used to select interesting events [36]. The first-level trigger is implemented in hardware and uses a subset of detector information, including ZDC coincidences in Pb+Pb collisions, to reduce the event rate to a design value of at most 100 kHz. This is followed by a software-based high-level trigger which reduces the event rate to several kHz. An extensive software suite [37] is used in the reconstruction and analysis of real and simulated data, in detector operations, and in the trigger and data acquisition systems of the experiment.

3 Data selection and Monte Carlo samples

All events are required to have at least one reconstructed vertex, to have been collected during stable beam conditions, and to satisfy detector and data-quality requirements [38].

These events were selected by two sets of triggers: single-jet triggers, and muon–jet triggers requiring a muon spatially matched to a jet at the trigger level [39]. In both Pb+Pb and pp collisions, the muon–jet triggers require a muon with $p_{\mathrm{T}} > 4$ GeV matched to an $R = 0.4$ jet with various p_{T} thresholds. The spatial matching of the jet to the muon is made within a cone of size $\Delta R = 0.5$ around the jet axis; this matching is fully efficient. All events are in a kinematic range where the jet trigger is fully efficient.

The overlap area of two colliding nuclei in Pb+Pb collisions is characterized by the total transverse energy deposited in the FCal [40]. This analysis uses three centrality intervals which are defined according to successive percentiles of the

Table 1 The $\langle T_{AA} \rangle$ and $\langle N_{coll} \rangle$ values and uncertainties in each centrality bin. These are the results from the Glauber modelling of the summed transverse energy in the forward calorimeters, $\sum E_T^{FCal}$

Centrality (%)	$\langle T_{AA} \rangle$ (mb^{-1})	$\langle N_{coll} \rangle$
0–20	18.84 ± 0.18	1319 ± 90
20–50	5.41 ± 0.15	378 ± 23
50–80	0.69 ± 0.05	48 ± 4

$\sum E_T^{FCal}$ distribution obtained in MB collisions. The centrality regions used in this analysis, going from the most central (largest $\sum E_T^{FCal}$) collisions to the peripheral (lowest $\sum E_T^{FCal}$) collisions are 0–20%, 20–50%, and 50–80%. The values of $\langle T_{AA} \rangle$ and the number of binary nucleon–nucleon collisions, $\langle N_{coll} \rangle$, for each centrality interval are evaluated by a Monte Carlo (MC) Glauber model analysis [32,41] of the $\sum E_T^{FCal}$ distribution, and are shown in Table 1.

A small fraction of the triggered Pb+Pb events ($< 0.5\%$) contain multiple collisions, known as 'pile-up'. The expected anti-correlation between $\sum E_T^{FCal}$ and the number of neutrons detected in the ZDCs is used to reject these pile-up events. The pile-up contribution is not rejected in pp collisions.

This analysis uses several MC samples to evaluate the performance of the detector and the analysis procedure, and to correct the measured distributions for detector effects. All MC samples were produced with the full ATLAS detector simulation based on the GEANT44 toolkit [42,43]. Dijet samples were generated with PYTHIA 8 [44], using the parameter values of the A14 tune [45] with the NNPDF23LO set of parton distribution functions (PDFs) [46]. These were generated both with no additional requirements and with the requirement of a muon with $p_T > 3$ GeV at the generator level (such as from heavy-flavour hadron decays). The EVTGEN package [47] was used to fully simulate b-hadron decays.

In pp collisions, pile-up from additional interactions in the same bunch crossing was generated by PYTHIA 8, using the parameter values of the A3 tune [48] with the NNPDF23LO PDFs; the distribution of the number of extra collisions was matched to that of data. In Pb+Pb collisions the simulated events were overlaid with events from a dedicated sample of Pb+Pb data events. This sample was recorded with a combination of MB triggers and total energy triggers to increase the number of events from central collisions. This 'data overlay' sample was reweighted on an event-by-event basis to obtain the same centrality distribution as in the jet-triggered data sample.

For muon reconstruction studies, prompt ($pp \to J/\psi \to \mu\mu$) and non-prompt ($pp \to bb \to J/\psi \to \mu\mu$) samples of J/ψ events were produced with PYTHIA 8 and corrected for electromagnetic radiation with PHOTOS [49]. The A14 tune and CTEQ6L1 PDFs [50] were used. Generator-level pp HERWIG++ [51] events, using the UEEE5 tune [52] and the CTEQ6L1 PDFs [50], were used to study systematic uncertainties.

4 Analysis

4.1 Jet reconstruction

All jets are reconstructed using procedures which follow those used by ATLAS for previous jet measurements in Pb+Pb collisions [2,53]. Jets are reconstructed using the anti-k_t algorithm [30] implemented in the FastJet software package [54]. In both pp and Pb+Pb collisions, jets with $R = 0.2$ and $R = 0.4$ are formed by clustering calorimetric towers of spatial size $\Delta\eta \times \Delta\phi = 0.1 \times \pi/32$. The energies in the towers are obtained by summing the energies of calorimeter cells at the electromagnetic energy scale [55] within the tower boundaries. In Pb+Pb collisions, a background subtraction procedure is applied to estimate, within each event, the underlying event (UE) average transverse energy density, $\rho(\eta, \phi)$, where the ϕ dependence is due to global azimuthal correlations in the particle production from hydrodynamic flow [40]. The modulation accounts for the contribution to the UE of the second-, third-, and fourth-order azimuthal anisotropy harmonics characterized by values of flow coefficients v_n^{UE} [40]. Additionally, the UE is also corrected for η- and ϕ-dependent non-uniformities of the detector response by correction factors derived in MB Pb+Pb data. In pp collisions, the same background subtraction procedure is applied without the ϕ-dependent modulation and without the correction for η- and ϕ-dependent non-uniformities to remove the pile-up contribution to the jet.

An iterative procedure is used to remove the impact of jets on the estimated ρ and v_n^{UE} values. The first estimate of the average transverse energy density of the UE, $\rho(\eta)$, is evaluated in 0.1 intervals of η, excluding towers within $\Delta R = 0.4$ of 'seed' jets. In the first subtraction step, the seeds are defined to be an union of $R = 0.2$ jets and $R = 0.4$ track-jets. Track-jets are reconstructed by applying the anti-k_t algorithm with $R = 0.4$ to charged particles with $p_T > 4$ GeV. The $R = 0.2$ jets must pass a requirement on the minimum value of the tower E_T and on a ratio of maximum tower E_T to average tower E_T, while the track-jets are required to have $p_T > 7$ GeV. The background is then subtracted from each tower constituent and the jet kinematics are recalculated. After the first iteration, the ρ and v_n values are updated by excluding from the UE determination the regions within $\Delta R = 0.4$ of both the track-jets and the newly reconstructed $R = 0.2$ jets with $p_T > 25$ GeV (8 GeV) in Pb+Pb (pp) collisions. The updated ρ and v_n^{UE} values are used to update the jet kinematic properties in the second iteration.

Jet η- and p_{T}-dependent correction factors derived in simulations are applied to the measured jet energy to correct for the calorimeter energy response [56]. An additional correction based on in situ studies of jets recoiling against photons, Z bosons, and jets in other regions of the calorimeter is applied [57]. This calibration is followed by a cross-calibration which relates the jet energy scale of jets reconstructed by the procedure outlined in this section to the jet energy scale in 13 TeV pp collisions [58].

Jets are defined at the truth level in the MC sample before detector simulation by applying the anti-k_t algorithm with the appropriate R value to stable particles with a proper lifetime greater than 30 ps, but excluding muons and neutrinos, which do not leave significant energy deposits in the calorimeter. The ΔR between the truth jet and reconstructed jet is required to be $\Delta R < 0.15\,(0.30)$ for $R = 0.2\,(R = 0.4)$ jets. The corrections for muons and neutrinos from semileptonic decays are discussed below.

4.2 Muon reconstruction

Muon candidates in both Pb+Pb and pp collisions are formed by combining charged-particle tracks reconstructed in the ID and the MS that pass the 'tight' selection requirements detailed in Ref. [59], except the requirement on the number of TRT hits.

Muons are selected with $p_{\mathrm{T}}^{\mu} > 4$ GeV and $|\eta^{\mu}| < 2.4$ requirements. If the muon is required in the trigger, the data is corrected to account for the muon trigger inefficiency, and the reconstructed muon must be within $\Delta R = 0.01$ of the trigger muon object. The muon selection is the same in both pp collisions and Pb+Pb collisions. Muons and jets are judged to be associated if $\Delta R(\text{jet}, \mu)$ is less than the jet radius, R. If more than one muon passes this selection, the muon with the largest momentum is used.

The muon trigger efficiency with respect to reconstructed muons is estimated from pp data by using the tag-and-probe method [16,60] in bins of p_{T}^{μ} and η^{μ}. A small centrality dependence of the muon trigger efficiency was observed in Pb+Pb data; this is corrected by an extra factor, which is the Pb+Pb to pp data-driven efficiency ratio, applied to Pb+Pb data as a function of the centrality. In pp collisions, the trigger efficiency plateaus at 78% for $p_{\mathrm{T}}^{\mu} > 6$ GeV and $|\eta^{\mu}| < 1.05$, and at 90% for $p_{\mathrm{T}}^{\mu} > 9$ GeV and $|\eta^{\mu}| > 1.05$. In Pb+Pb collisions, the efficiency is lower than in pp collisions by 9% in the most central collisions; the efficiency in peripheral Pb+Pb collisions is the same as in pp collisions.

The muon reconstruction efficiency is estimated from simulated prompt and non-prompt $J/\psi \to \mu\mu$ events using the tag-and-probe method [16,59], in fine bins of p_{T}^{μ} and η^{μ}. Mis-modelling of the reconstruction performance in simulation, quantified by the ratio of measured efficiencies in pp data and the simulation, is accounted for by applying a multiplicative correction which changes the efficiency by less than 5%. For $p_{\mathrm{T}}^{\mu} > 10$ GeV in pp collisions, the muon reconstruction efficiency plateaus at 90% for $|\eta^{\mu}| < 1.05$ and at 95% for $|\eta^{\mu}| > 1.05$. No difference between the muon reconstruction efficiencies in pp and Pb+Pb collisions was observed and the same values were used in both collision systems.

4.3 b-jet yield reconstruction

4.3.1 Templates and fitting

At the generator level, the jet flavour is defined by matching jets to hadrons with $p_{\mathrm{T}} > 5$ GeV. The jet is considered a b-jet if a b-hadron is found within $\Delta R = 0.3$ of the jet axis; otherwise, if a c-hadron is found within the same distance the jet is labelled as a c-jet. All other jets are considered to be *light*-jets.

Since the muons in the momentum range of interest generally do not stop in the calorimeter, their momentum is not included in the calorimetric jet p_{T}. In order to better characterize the jets, the jet+μ scale is defined as the p_{T} of the sum of the muon and jet four-vectors. The $p_{\mathrm{T}}^{\mathrm{rel}}$ distributions in the data and MC samples are constructed for selections in this jet+μ object at the reconstruction level, $p_{\mathrm{T,reco}}^{\mathrm{jet}+\mu}$. In order to form a jet+μ pair, jets are required to have a minimum calorimetric $p_{\mathrm{T,reco}}^{\mathrm{jet}}$ of 40 GeV (58 GeV) in pp (Pb+Pb) collisions.

In semileptonic b-hadron decays, the p_{T} of the lepton relative to the jet+μ-axis (see Eqs. (1) and (2)), $p_{\mathrm{T}}^{\mathrm{rel}}$, is used to distinguish between b-, c-, and *light*-jets[31]. Due to the large mass of b-hadrons relative to hadrons containing charm or light quarks, their decay products are more energetic. Consequently, muons originating from b-hadron decays have a harder $p_{\mathrm{T}}^{\mathrm{rel}}$ spectrum than muons in c-jets and *light*-jets.

The templates distributions of $p_{\mathrm{T}}^{\mathrm{rel}}$ for b- and c-jets are extracted from the muon-filtered MC samples. The b-hadron mixture is taken from Tevatron measurements [61], which are consistent with those from the LHCb Collaboration [62]. The c-hadron mixture is taken from default PYTHIA 8 simulation. The *light*-jet template is obtained from track-jet pairs in the data inclusive-jet sample as in Refs. [31,63] (in the same centrality class as the jet+μ pair for Pb+Pb collisions). The tracks are selected with the standard selection, with no additional requirements on the distance of closest approach to the vertex. The p_{T} spectra of the tracks are reweighted to reproduce the muon p_{T} spectrum from *light*-jets from the inclusive dijet MC sample.

In pp collisions, these three templates are inputs to a template fit of the data $p_{\mathrm{T}}^{\mathrm{rel}}$ spectrum to obtain the fractions of b-, c-, and *light*-jets. A binned maximum-likelihood fit is performed using the RooFit framework [64]. The model for the fit is defined as a normalized sum of three templates: *light*-

jets ($F_{\mathrm{l},i}(p_{\mathrm{T}}^{\mathrm{rel}})$), c-jets ($F_{\mathrm{c},i}(p_{\mathrm{T}}^{\mathrm{rel}})$), and b-jets($F_{\mathrm{b},i}(p_{\mathrm{T}}^{\mathrm{rel}})$). The pp fit model, M^{pp}, is structured as

$$M_i^{pp}\left(p_{\mathrm{T}}^{\mathrm{rel}}\right) = f_{\mathrm{b},i}\,F_{\mathrm{b},i}\left(p_{\mathrm{T}}^{\mathrm{rel}}\right) + \left(1 - f_{\mathrm{b},i}\right) \times \left[f_{\mathrm{c},i}\,F_{\mathrm{c},i}\left(p_{\mathrm{T}}^{\mathrm{rel}}\right) + \left(1 - f_{\mathrm{c},i}\right)F_{\mathrm{l},i}\left(p_{\mathrm{T}}^{\mathrm{rel}}\right)\right]$$

where $f_{\mathrm{b},i}$ is the fraction of b-jets in the total sample, $f_{\mathrm{c},i}$ is the fraction of c-jets in the non-b-jet sample, and the index i denotes the p_{T} bin. The fit model has two free parameters, $f_{\mathrm{b},i}$ and $f_{\mathrm{c},i}$ for each $p_{\mathrm{T,reco}}^{\mathrm{jet}+\mu}$ bin.

In Pb+Pb collisions the model has an additional term which accounts for combinatoric muon–jet pairs. These are muon–jet pairs which pass the ΔR matching requirements, but the muon and jet do not come from the same hard scattering. These are the most common in central Pb+Pb collisions, where the multiplicity of jets and muons is the highest. In pp collisions, this effect is negligibly small. For the combinatoric pairs, both the shape, $F_{\mathrm{mix},i}$, and the amplitude, $f_{\mathrm{mix},i}$, are determined by event mixing in the Pb+Pb data. This procedure uses a muon from one event and a jet from another event; all the analysis selections are applied, including the requirement on the ΔR separation between the muon and jet. Events which are mixed together are required to have $\sum E_{\mathrm{T}}^{\mathrm{FCal}}$ values that agree within 0.05 TeV and vertex z-positions that agree within 10 mm. The nominal data sample and mixed-event sample are found to agree well in the large ΔR region where there is no correlated signal. The Pb+Pb model, $M^{\mathrm{Pb+Pb}}$, is structured as

$$M_i^{\mathrm{Pb+Pb}}\left(p_{\mathrm{T}}^{\mathrm{rel}}\right) = \left(1 - f_{\mathrm{mix},i}\right) \times M_i^{pp}\left(p_{\mathrm{T}}^{\mathrm{rel}}\right) + f_{\mathrm{mix},i} \times F_{\mathrm{mix},i}\left(p_{\mathrm{T}}^{\mathrm{rel}}\right).$$

The background fraction is largest in central collisions and is always less than 1.5%.

The data $p_{\mathrm{T}}^{\mathrm{rel}}$ distributions are resampled 500 times and the mean and width of the range of results are used to set the central value and uncertainties in the fit. The statistical uncertainty of the templates is taken to be part of the statistical uncertainty of the yield. Example fits for pp and Pb+Pb collisions are shown in Figs. 1 and 2, for low and high $p_{\mathrm{T,reco}}^{\mathrm{jet}+\mu}$ respectively.

The raw b-jet p_{T} spectrum is constructed in each Pb+Pb centrality bin and in pp collisions by taking each $f_{\mathrm{b},i}$ value and multiplying it by the number of jets in i-th bin in the total $p_{\mathrm{T,reco}}^{\mathrm{jet}+\mu}$ spectrum.

4.3.2 *Comparing muon momentum distributions in the data and simulations*

The b-jet fragmentation function in Pb+Pb collisions has not been measured. Significant modification to the b-hadron longitudinal momentum due to jet quenching could bias the b-jet template. In order to ensure that the simulations reproduce the data sufficiently well, a check of the longitudinal momentum distribution of the muon with respect to the jet+μ axis is performed. The fitting results as a function of centrality and $p_{\mathrm{T,reco}}^{\mathrm{jet}+\mu}$ from the previous subsection are used to weight the jet+μ pairs from the MC samples (used for the charm and bottom templates) and those used in constructing the data-driven *light*-jet template to have the same flavour fractions as the data. Muons which have a transverse distance to the primary vertex, d_0, greater than 0.25 mm are selected; this requirement further enhances the heavy-flavour fractions relative to the light jets. For these jet+μ pairs, the distribution of

$$z \equiv p_{\mathrm{T}}^{\mu}\cos(\theta)\,/\,p_{\mathrm{T,reco}}^{\mathrm{jet}+\mu}$$

where θ is the angle between the muon and the jet+μ axis, is constructed. This combined distribution from the pairs in the charm-, bottom-, and *light*-jet templates is compared with the data distribution for the same quantity. Since the *light*-jet template is data-driven, it should agree between the data and the template, and thus the comparison between data and simulations is sensitive to the degree to which the MC modelling of the charm and bottom templates agrees with the data. These distributions are shown in Fig. 3 for pp and 0–20% centrality Pb+Pb collisions. The data and the simulations (including the data-driven *light*-jet template) agree in both pp and Pb+Pb collisions. Thus, within the current uncertainties, the longitudinal momentum fraction of the muon is unmodified in Pb+Pb collisions and the $p_{\mathrm{T}}^{\mathrm{rel}}$ distributions are largely sensitive to the b-hadron decay kinematics.

4.4 Corrections to the raw spectra

The raw jet spectra are constructed from all the measured jets for the inclusive jets and from the muon–jet pairs, scaled by the $f_{\mathrm{b},i}$ values, for the b-jets after correction for the muon trigger efficiency. The raw spectra are unfolded to account for bin migrations due to the finite jet energy resolution, and any reconstruction inefficiency for the jets and muons (and muon and neutrino energies in the b-jet sample). Both the b-jet and inclusive jet p_{T} spectra are unfolded using the one-dimensional (1D) Bayesian unfolding [65] from the RooUnfold software package [66]. The b-jet response matrices are built from the muon-filtered MC samples using truth-level b-jets (including the muon and neutrino momenta) that are matched to reconstructed jets in simulations and have $|y_{\mathrm{truth}}^{b\text{-jet}}| < 2.1$. The inclusive jet response matrices are built from the dijet MC samples using all truth jets and not including any muon or neutrino momenta.

The response matrices are generated separately for pp collisions and for each centrality interval in Pb+Pb collisions. To better represent the data, the response matrices are

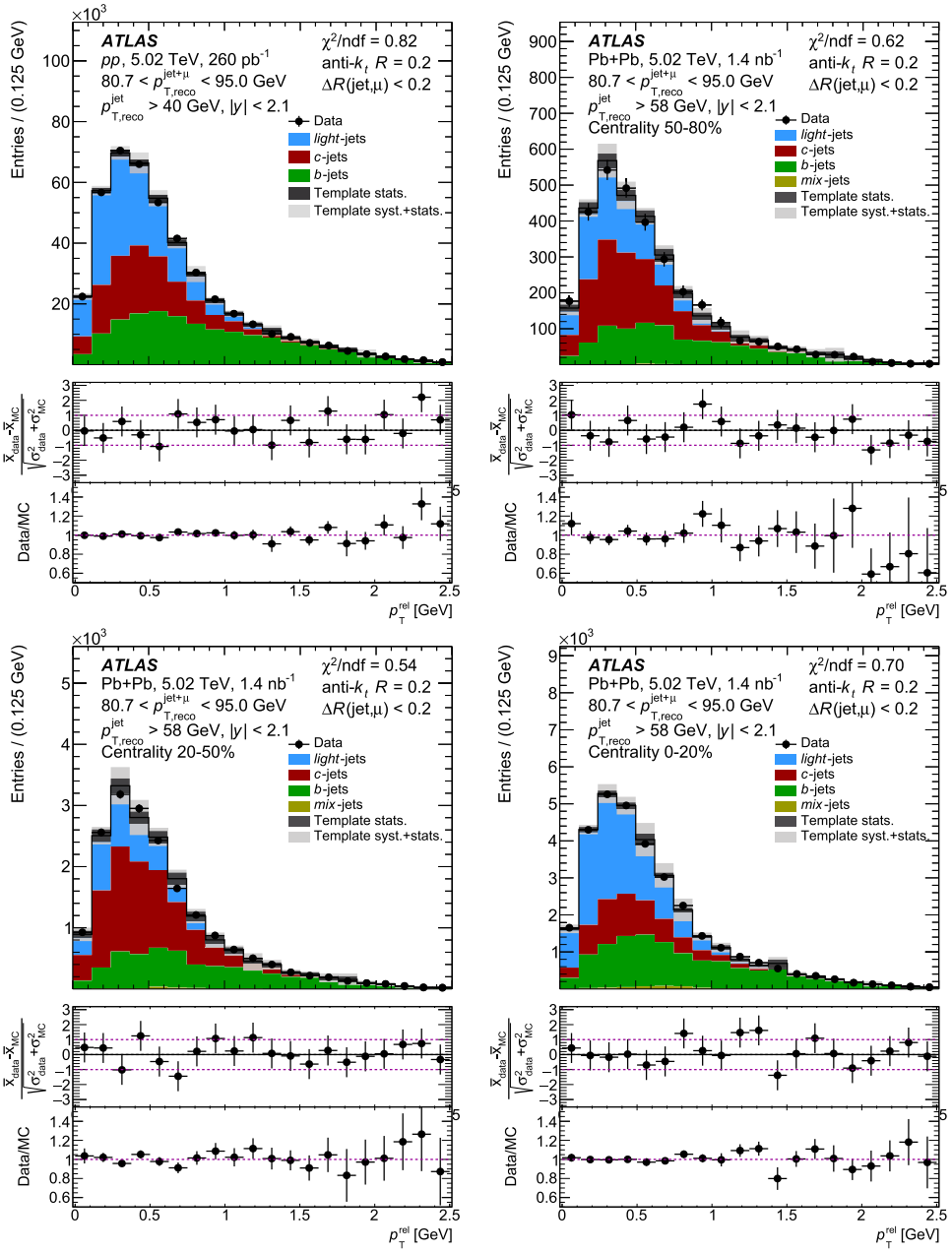

Fig. 1 The $p_{\mathrm{T}}^{\mathrm{rel}}$ distributions in pp collisions (top left) and 50–80% (top right), 20–50% (bottom left), and 0–20% (bottom right) centrality Pb+Pb collisions. The data are shown for the range $80.7 < p_{\mathrm{T,reco}}^{\mathrm{jet}+\mu} < 95.0$ GeV. The stacked histograms show the fit results. Middle and bottom panels of each plot show the pulls and data-to-fit ratios, respectively. The error bars in the ratio plots show the statistical uncertainties of the data and MC samples

reweighted along the truth-$p_{\mathrm{T}}^{\mathrm{jet}}$ axis by the reconstruction-level data to simulation ratio. The number of iterations in the unfolding was chosen such that the result is stable when changing the number of iterations while minimizing the amplification of statistical uncertainties. Four iterations are used in all cases presented here. The reconstructed $p_{\mathrm{T,reco}}^{\mathrm{jet}+\mu}$ values are required to be larger than 72 GeV in Pb+Pb collisions and 64 GeV in pp collisions for both $R = 0.2$ and $R = 0.4$ jets. The inclusive-jet minimum reconstructed p_{T} is required to be larger than 72 GeV for both Pb+Pb and pp collisions. Reconstructed jets below these thresholds that match to truth-p_{T} values in the measurement region are corrected via the unfolding procedure. Fully unfolded results are presented starting from 80 GeV for both categories of jets.

As described in Sect. 3, the main MC sample used in the b-jet analysis required the truth-muon p_{T} to be larger than 3 GeV. The missing part of the cross-section from b-jets with muons below this threshold is addressed through an acceptance correction based on the PYTHIA 8 dijet MC samples which is applied after unfolding. The size of the correction is approximately 22% (25%) at 80 GeV and 19% (23%) at 250 GeV for $R = 0.2$ ($R = 0.4$) jets.

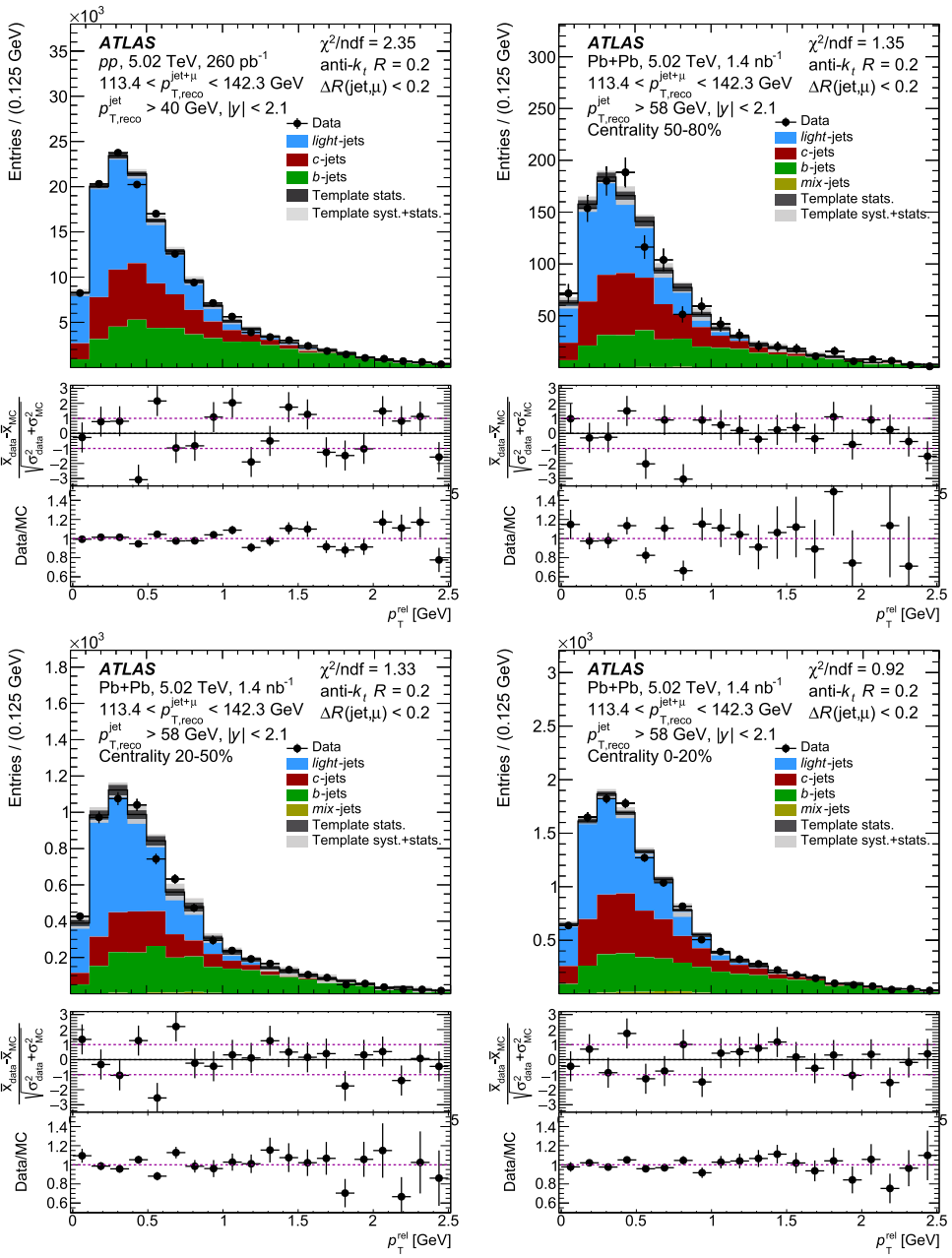

Fig. 2 The $p_{\mathrm{T}}^{\mathrm{rel}}$ distributions in pp collisions (top left) and 50–80% (top right), 20–50% (bottom left), and 0–20% (bottom right) centrality Pb+Pb collisions. The data are shown for the range $113.4 < p_{\mathrm{T,reco}}^{\mathrm{jet}+\mu} < 142.3$ GeV. The stacked histograms show the fit results. Middle and bottom panels of each plot show the pulls and data-to-fit ratios, respectively. The error bars in the ratio plots show the statistical uncertainties of the data and MC samples

4.5 Observables

The b-jet cross-section in pp collisions is defined as

$$\frac{\mathrm{d}^2\sigma_{b\text{-jet}}}{\mathrm{d}p_{\mathrm{T}}\mathrm{d}y} = \frac{1}{L_{\mathrm{int}}\mathcal{B}}\frac{N_{b\text{-jet}}^{\mathrm{Unfol.}}}{\Delta p_{\mathrm{T}}\Delta y} \tag{3}$$

where L_{int} is the integrated luminosity and $\mathcal{B}$ is the branching ratio which includes direct ($b \to \mu$) and cascade ($b \to c \to \mu$) semileptonic decays. The value of $\mathcal{B}$ is (20.6±0.6)% [28]. The quantity $N_{b\text{-jet}}^{\mathrm{Unfol.}}$ is the b-jet yield after the unfolding and acceptance correction described above, and Δp_{T} and Δy are the widths of the p_{T} and y bins. Following the same approach, the per-event yield of b-jets measured in Pb+Pb collisions is calculated as

$$\frac{1}{N_{\mathrm{evt}}}\frac{\mathrm{d}^2N_{b\text{-jet}}}{\mathrm{d}p_{\mathrm{T}}\mathrm{d}y}\bigg|_{\mathrm{cent}} = \frac{1}{N_{\mathrm{evt}}\mathcal{B}}\frac{N_{b\text{-jet}}^{\mathrm{Unfol.}}}{\Delta p_{\mathrm{T}}\Delta y}\bigg|_{\mathrm{cent}}, \tag{4}$$

where N_{evt} is the number of MB events in the centrality class 'cent'. The inclusive jet cross-section and per-event yields are defined in the same way as in Eq. (3) and Eq. (4) but without the $\mathcal{B}$ factor.

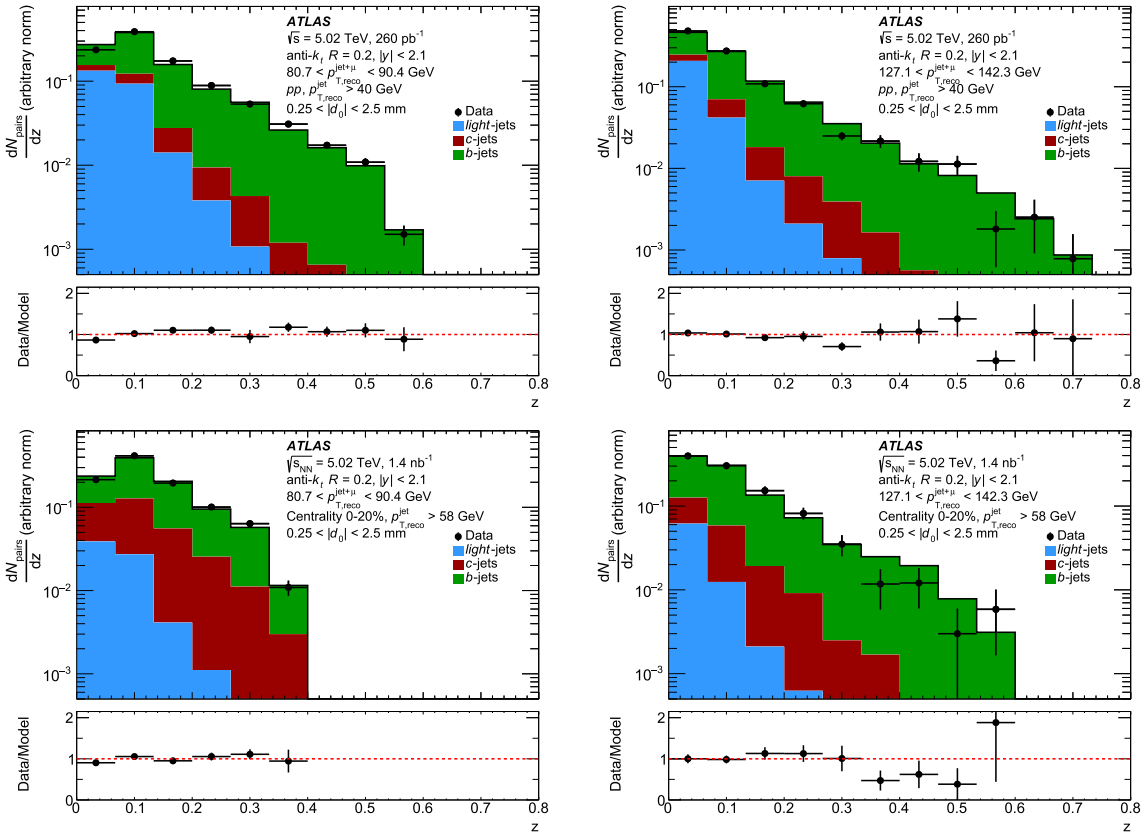

Fig. 3 The z distributions for data and simulations (including the data-driven *light*-jet template) for pp collisions (top row) and 0–20% centrality Pb+Pb collisions (bottom row) for two $p_{\mathrm{T,reco}}^{\mathrm{jet}+\mu}$ selections. In each figure the top panel shows the distributions themselves and the bottom panel shows the ratio of data to simulations. The error bars in the ratio plots show the statistical uncertainties on the data and MC samples

5 Systematic uncertainties

The systematic uncertainties of the jet cross-sections and per-event yields common to both the inclusive jet and the b-jet measurements arise from the jet energy scale and resolution, the unfolding procedure, luminosity (pp only), and $\langle T_{\mathrm{AA}} \rangle$ determination (Pb+Pb only). There are additional contributions to the b-jet measurements from the modelling of the $p_{\mathrm{T}}^{\mathrm{rel}}$ distributions, the fitting procedure, the branching ratio of b-hadrons to muons, and the muon performance. The uncertainties are discussed in detail below.

The systematic uncertainty of the jet energy scale (JES) has five parts. First, there is a centrality-independent baseline component that is determined from in situ studies of the calorimeter response for jets reconstructed with the procedure used in 13 TeV pp collisions [55,67], including an additional term for b-jet energy scale [55]. The second is a centrality-independent component which accounts for the relative energy scale difference between the jet reconstruction procedure used in this paper and that in 13 TeV pp collisions [58]. Potential inaccuracies in the MC description of the relative abundances of jets initiated by quarks and gluons and of the calorimetric response to quark and gluon jets are accounted for by a third, JES flavour, component; this component is estimated independently for the inclusive-jet and b-jet energy scale by varying the quark and gluon fractions from their PYTHIA 8 values to those extracted from HERWIG++. The fourth, centrality-dependent, component (in Pb+Pb collisions only) accounts for a different structure [68], and possibly a different detector response, for jets in Pb+Pb collisions that is not modelled by the simulations. It is evaluated by the method used for 2015 and 2011 data [58] that compares the calorimetric jet p_{T} and the sum of the transverse momentum of charged particles within the jet in data and MC samples. The size of the centrality-dependent uncertainty in the JES reaches 1.2% in the most central collisions; it is smaller for more peripheral collisions. The systematic uncertainties from the JES discussed above are derived for $R = 0.4$ jets and applied to both $R = 0.4$ and $R = 0.2$ jets. An additional component applies only to $R = 0.2$ jets and accounts for a potential uncertainty difference between $R = 0.4$ and $R = 0.2$ jets. The uncertainty is assessed by comparing the ratio of $R = 0.2$ jet p_{T} to $R = 0.4$ jet p_{T} in data and simulations.

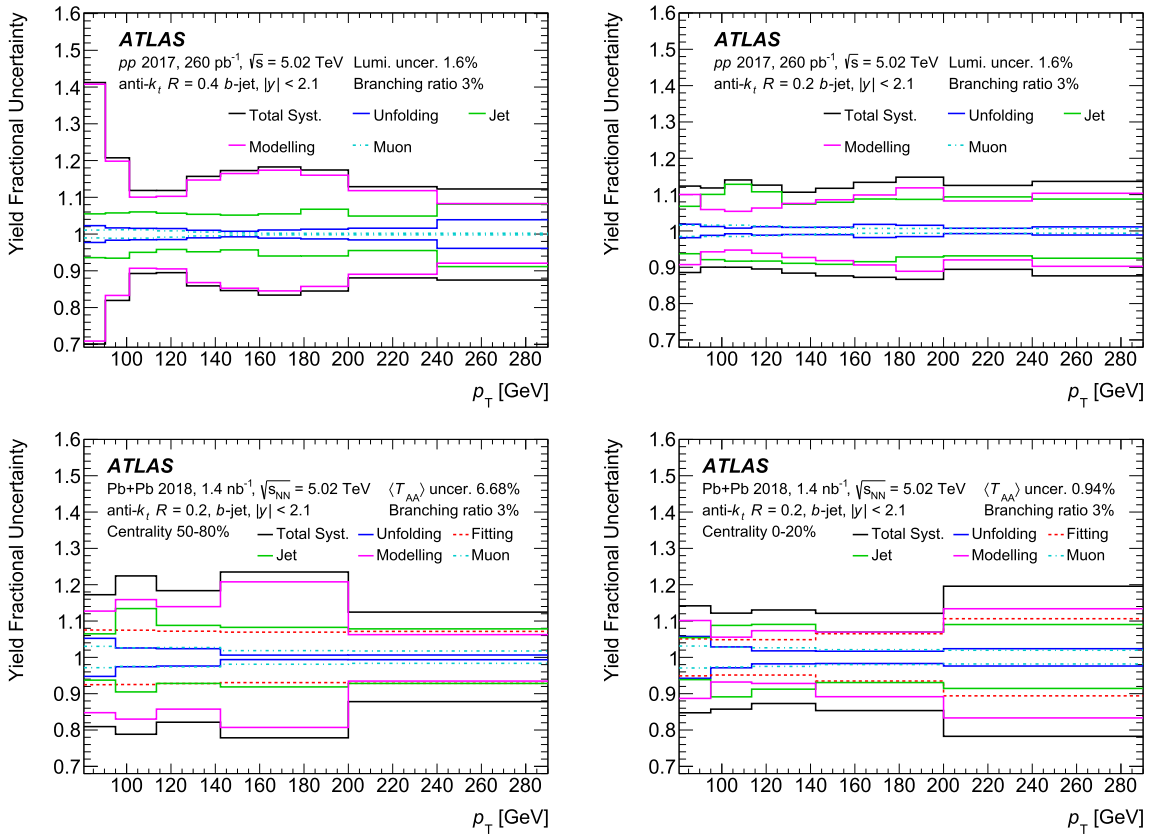

Fig. 4 The relative systematic uncertainties for several categories, as a function of b-jet p_{T} for (top) the pp cross-section for $R = 0.4$ (left) and $R = 0.2$ (right) jets, and (bottom) the Pb+Pb per-event-yield in peripheral (left) and central (right) collisions for $R = 0.2$ jets

The uncertainty due to the jet energy resolution (JER) is evaluated by repeating the unfolding procedure with modified response matrices, where an additional contribution is added to the resolution of the reconstructed p_{T} using a Gaussian smearing procedure. The smearing factor is evaluated using an in situ technique in 13 TeV pp data that involves studies of dijet p_{T} balance [69,70]. Additionally, an uncertainty is included to account for differences between the tower-based jet reconstruction and the jet reconstruction used in analyses of 13 TeV pp data, as well as differences in calibration procedures. Similarly to the JES, an additional uncertainty in the JER accounting for differences between $R = 0.2$ and $R = 0.4$ jets is added. The resulting uncertainty from the JER is symmetrized.

Uncertainties related to muons are associated with the trigger and reconstruction efficiency measurement. The systematic uncertainties are estimated by varying the tag-and-probe method as described in Refs. [59,60]. Additionally, the statistical uncertainty of the factor used to correct the centrality dependence of the trigger efficiency in Pb+Pb collisions and the difference between the data-driven reconstruction efficiencies in Pb+Pb and pp collisions are taken as muon systematic uncertainties that apply only to Pb+Pb collisions.

The uncertainties in modelling the $p_{\mathrm{T}}^{\mathrm{rel}}$ distributions come from several sources, which are common to pp and Pb+Pb collisions. For the fraction of b-hadrons which arise from gluon splitting, the analysis uses that from PYTHIA 8 simulation as the central value. In pp collisions, the gluon-splitting fraction is reweighted to the value obtained from the HERWIG++ sample [71]. In Pb+Pb collisions, there is no information about the modification of the gluon-splitting contribution to b-jets. Additionally, the fragmentation functions of b-jets in Pb+Pb collisions have not been measured. In order to cover both of these effects, the gluon-splitting fraction is conservatively varied between zero and 100%. For the c-jets, the gluon-splitting uncertainty is estimated by varying the PYTHIA 8 value of the gluon-splitting fraction by a factor of two, based on measurements in Ref. [72]. The fraction of muons which arise from b-hadron decays which include an intermediate D-meson is varied in accord with Ref. [28]. The fractions of the various b-hadron species are varied according to the world average values in Ref. [61]. The fraction of c-baryons was varied according to ALICE measurement [27] with negligible impact on the results. The modelling of the muon momentum in the b-hadron rest frame is crucial for the $p_{\mathrm{T}}^{\mathrm{rel}}$ method. The modelling in PYTHIA 8 is used for the central values. The PYTHIA 8 distributions were compared

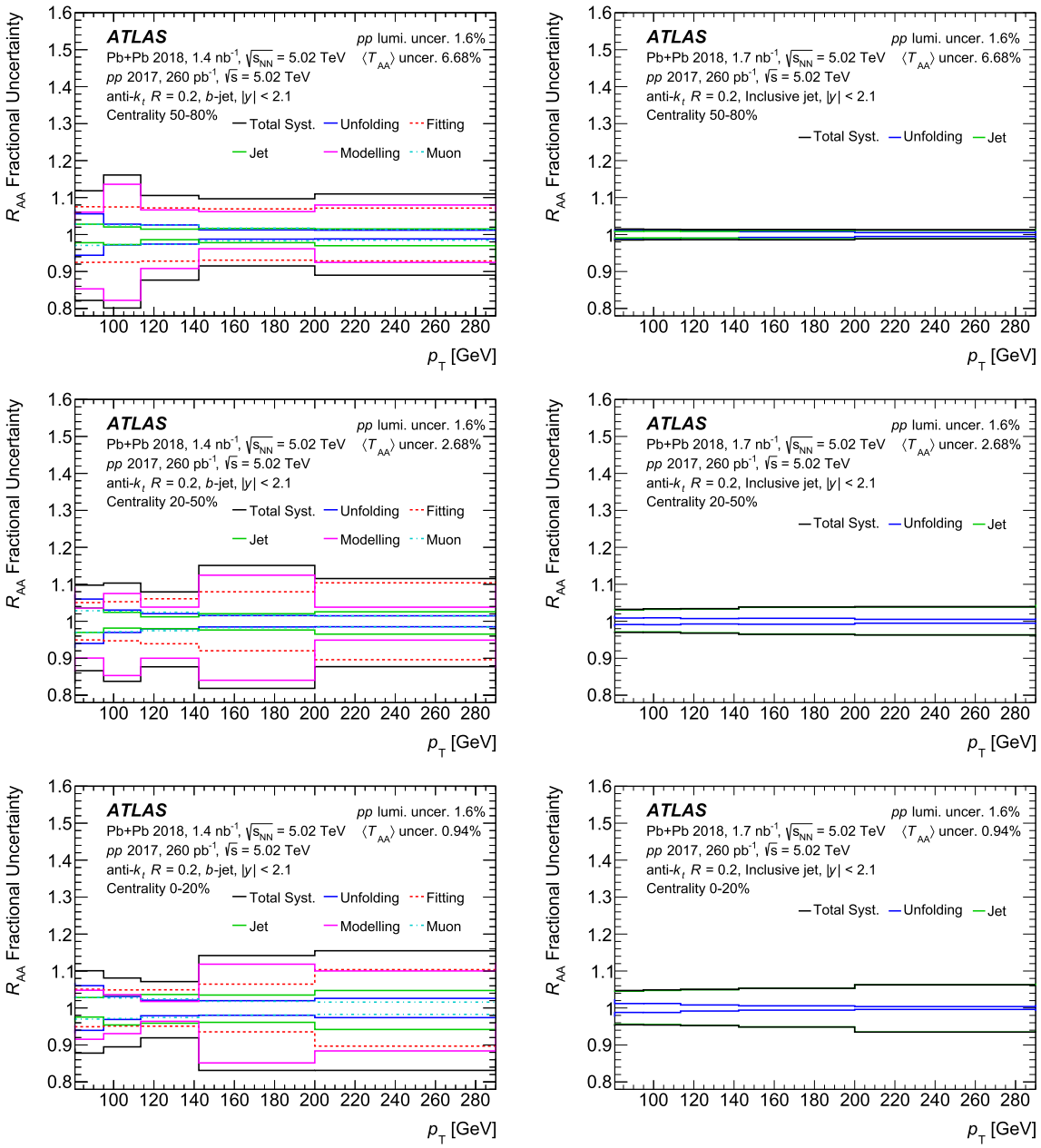

Fig. 5 Relative size of systematic uncertainties for several categories, as a function of jet p_T for b-jet R_{AA} (left column) and inclusive jet R_{AA} (right column), in peripheral (top row), semi-central (middle row) and central (bottom row) Pb+Pb collisions

with the measurement from DELPHI [73] and the difference between PYTHIA 8 and the DELPHI measurement is used as a systematic uncertainty. The uncertainty in the *light*-jet template is evaluated by using muons with a distance of closest approach to the collision vertex smaller than 0.01 mm, to minimize the contribution from heavy-flavour jets, and remaking the templates. In $R = 0.2$ jets in pp collisions, the dominant components of modelling uncertainties stem from the *light*-jet template and the fraction of b-hadrons; for $R = 0.4$ jets, the *light*-jet template uncertainty dominates. For Pb+Pb collisions, the dominant modelling uncertainties stem from the *light*-jet template and gluon-splitting components.

The uncertainty in the unfolding procedure is determined in all cases by constructing response matrices from the MC distributions without the reweighting factors that are used to match the MC distributions to those in data. The uncertainty due to using a particular MC model in unfolding b-jets is addressed by reweighting the 2D $(p_T^{\text{jet}}, p_T^{\mu})$ distribution in PYTHIA 8 to that observed in HERWIG++. The inclusive jet analysis has an uncertainty associated with the non-closure of the unfolding procedure when the MC sample is divided

and one portion is used in place of the data and the other portion used to generate a response matrix; in the b-jet analysis the closure was found to be consistent with unity within the statistical uncertainties and no uncertainty is added.

Uncertainties from the finite size of the MC samples are combined with the data statistical uncertainties. A systematic uncertainty associated with the template fit procedure is addressed by allowing the templates to deform in Pb+Pb collisions by convolving the nominal template with a Gaussian function where the width parameter is free. Deformations of the templates account for mismodelling due to the large UE, such as via the jet position resolution, muon momentum resolution, or other effects. A similar uncertainty was applied in Ref. [16]. The small non-closure of the fitting procedure, when the $f_{\mathrm{b},i}$ extraction is tested in simulations, is also included in the systematic uncertainties.

For each uncertainty component discussed above, the entire analysis procedure is repeated with the variation under consideration and the resulting changes are added in quadrature to form the total systematic uncertainty of the measurement. A summary of the systematic uncertainties for the $R = 0.4$ and $R = 0.2$ b-jet cross-sections is shown in Fig. 4. For the $R = 0.4$ jets, the largest contribution is the modelling component, while for $R = 0.2$ jets, the jet and modelling components have similar magnitudes.

The integrated luminosity determined for 2017 pp data was calibrated using data from dedicated beam-separation scans, also known as van der Meer scans [74]. Sources of systematic uncertainty similar to those examined in the 2012 pp luminosity calibration [74] were studied in order to assess the systematic uncertainties for the 2017 data. The combination of these systematic uncertainties results in a relative uncertainty of 1.6%. The uncertainty of the mean nuclear thickness function arises from geometric modelling uncertainties (nucleon–nucleon inelastic cross-section, Woods–Saxon parameterization of the nucleon distribution) and the uncertainty in the fraction of selected inelastic Pb+Pb collisions. The values of these uncertainties are taken from Ref. [2]. The branching ratio for b-hadrons into muons is $(20.6 \pm 0.6)\%$ and is taken from Ref. [28].

The uncertainties which are common to pp and Pb+Pb collisions are treated as correlated when determining the uncertainty in the R_{AA} value, with the exception of gluon splitting, where the uncertainties account for possible production and fragmentation mechanism differences between pp and Pb+Pb collisions, and the unfolding. Similarly, the uncertainties which are common to inclusive jets and b-jets cancel out when ratios of cross-sections or R_{AA} values are taken; the remaining uncertainties are the JES flavour component, the b-jet-specific JES uncertainty, and the unfolding. A summary of the systematic uncertainties for inclusive jet and b-jet R_{AA} is shown in Fig. 5. The uncertainties in the

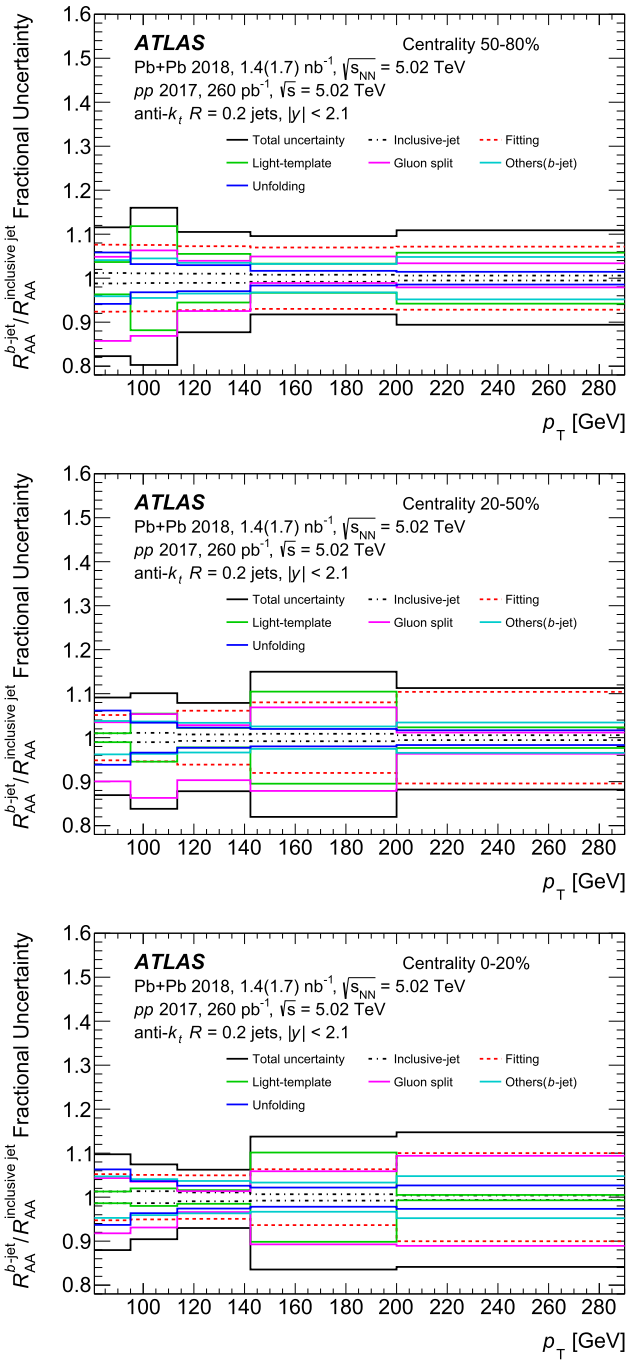

Fig. 6 Relative size of systematic uncertainties of the ratio $R_{\mathrm{AA}}^{b\text{-jet}}/R_{\mathrm{AA}}^{\text{inclusive jet}}$ shown for the most relevant components, as a function of jet p_{T} for 50–80% (top), 20–50% (middle), and 0–20% (bottom) centrality Pb+Pb collisions

$R_{\mathrm{AA}}^{b\text{-jet}}/R_{\mathrm{AA}}^{\text{inclusive jet}}$ ratio are shown in Fig. 6; the uncertainties in the gluon-splitting contribution and deformation of the templates in Pb+Pb collisions dominate in most cases.

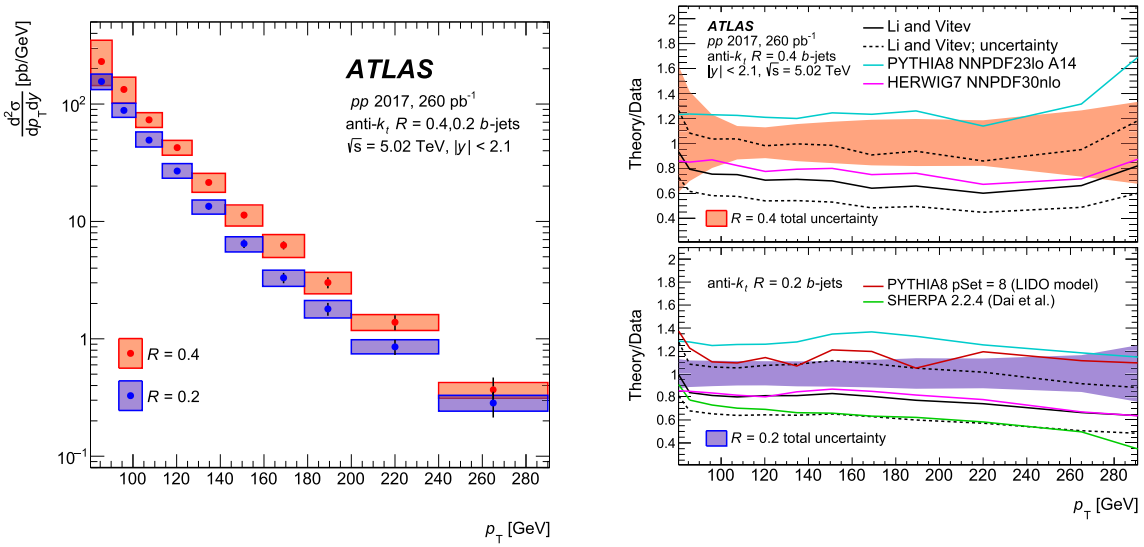

Fig. 7 (Left) Differential cross-section for b-jet production for $R = 0.2$ and $R = 0.4$ jets with $|y| < 2.1$ as a function of p_{T} in 5.02 TeV pp data. (right) Ratio of the predictions to the measured b-jet cross-section in pp collisions at 5.02 TeV for $R = 0.4$ (top) and $R = 0.2$ (bottom) jets. The $R = 0.4$ jets are compared with calculations from Ref. [75] and $R = 0.2$ jets are compared with calculations from Refs. [11,12,75,76]. Both cross-sections are compared with PYTHIA 8 and HERWIG++ calculations. The bands around unity represent the total uncertainty of the data. The text provides additional discussion

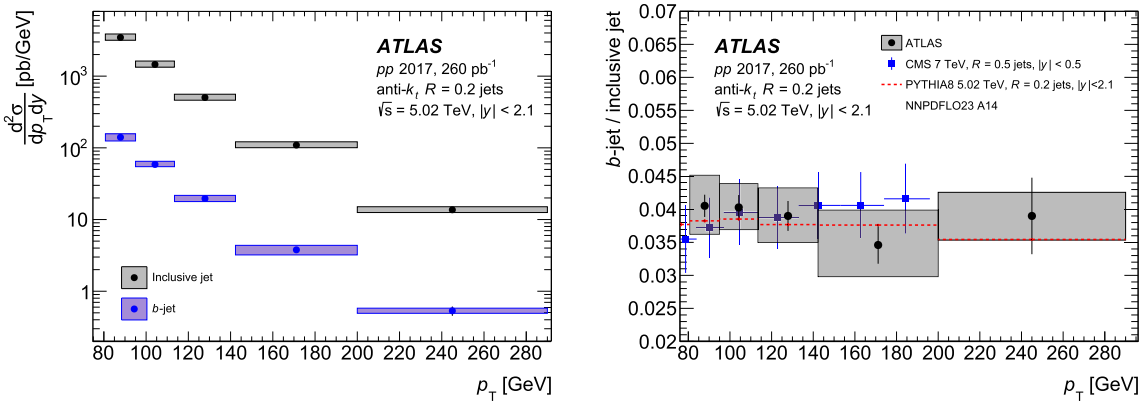

Fig. 8 (Left) Cross-section of $R = 0.2$ b-jet and inclusive jet production in pp collisions at 5.02 TeV, and (right) the b-jet to inclusive jet cross-section ratio, together with PYTHIA 8 simulation and measurements from the CMS Collaboration at 7 TeV for $R = 0.5$ jets [78]. For the current measurement, the boxes represent the systematic uncertainties and the error bars represent the statistical uncertainties. For the CMS data the bars represent the total uncertainty

6 Results

6.1 Cross-section in pp collisions

Figure 7 shows the b-jet cross-section as a function of b-jet p_{T} in pp collisions at 5.02 TeV for $R = 0.2$ and $R = 0.4$ jets with $|y| < 2.1$. Additionally, b-jet cross-sections for both $R = 0.2$ and $R = 0.4$ jets are compared with theory and generator calculations. The data is in good agreement with the calculations by Li and Vitev [75] for both $R = 0.4$ and $R = 0.2$ jets. This calculation is based on semi-inclusive jet functions where the cross-section is expressed in terms of the parton distribution functions, the hard kernel and the jet functions. The jet functions have terms in $\ln(R)$, which are resummed. The SHERPA 2.2.4 calculations [12] for $R = 0.2$ jets underestimate the measured b-jet cross-sections by an amount which increases with p_{T}. A calculation [11,76] which is based on PYTHIA 8 where the PDFs and $\alpha_s(M_Z)$ is set with pSet = 8 [44] is approximately consistent with the upper edge of the uncertainty band of the $R = 0.2$ jet yields. The PYTHIA 8 calculation using the NNPDF23LO PDF [46] and the A14 tune [45] is 20–30% higher than data for both $R =$

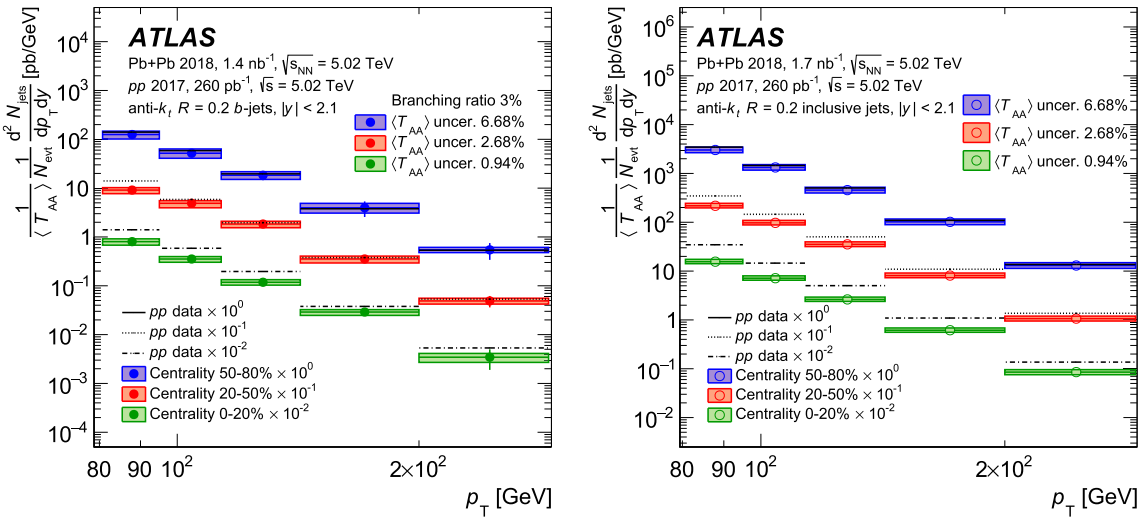

Fig. 9 Per-event yields scaled by $\langle T_{AA}\rangle$ in Pb+Pb collisions for three centrality classes for $R = 0.2$ b-jets (left) and inclusive jets (right). The boxes show the systematic uncertainties and the bars represent the statistical uncertainties. The different centrality classes are offset by the factors shown on the plot for clarity. The values of the pp cross-sections are shown by the black lines; they are offset by the factors shown on the plot. The size of the T_{AA} uncertainties are noted in the legend

0.4 and $R = 0.2$ jets. The HERWIG++ calculations [77] using the NNPDF30NLO PDF underestimate the measured cross-sections at both jet radii. There is no uncertainty estimate for the generator calculations, and the sensitivity of the results to the choice of parameter values has not been investigated.

Figure 8 shows a comparison of the b-jet and inclusive jet cross-sections for $R = 0.2$ jets and their ratio. The figure also shows the same ratio from the PYTHIA 8 MC sample; it agrees with the data. The cross-section ratio measured at 7 TeV for $R = 0.5$ jets with $|y| < 0.5$ by the CMS Collaboration [78] is also shown; the jet radii in this measurement are larger than in the present analysis but the results are qualitatively similar. No significant p_T dependence of the b-jet to inclusive jet cross-section ratio is observed.

6.2 Per-event yields and R_{AA} in Pb+Pb collisions

The inclusive jet and b-jet per-event yields in Pb+Pb collisions scaled by $\langle T_{AA}\rangle$ are shown in Fig. 9 for the three centrality classes used in this analysis overlaid with the values of the pp cross-sections. Figure 10 shows a direct comparison of the inclusive jet and b-jet R_{AA} for each centrality class. The R_{AA} values for both types of jets decrease going from peripheral to central collisions. Both are consistent with unity in peripheral collisions. In central and semi-central collisions the R_{AA} central values for inclusive jets are lower than those for b-jets. A difference between the slopes of the inclusive jet and b-jet differential cross-sections could cause the R_{AA} values to differ between the two categories of jets; however, the ratio of the b-jet to inclusive jet cross-section, shown in Fig. 8, does not vary with p_T.

The R_{AA} values for both inclusive jets and b-jets are compared with two theory calculations. The first calculation is the LIDO model [11,76,79], which includes both energy loss and diffusion of heavy quarks. The dead-cone effect for b-jets is included and the medium is implemented via (2+1)D viscous hydrodynamics with averaged initial conditions. The parameter which controls the coupling between the jet and the medium, $\mu_{\min}$, is varied between $1.3\pi T$ and $1.8\pi T$, where T is the temperature of the QGP in the model, in the calculation shown here. The choice of $\mu_{\min}$ values is motivated by comparisons with other jet measurements. These parameters have been shown [79] to provide a reasonable description of measurements of the R_{AA} values of B- and D-mesons [22,23]. The calculation by Dai et al. in Ref. [12] is based on a Langevin transport model describing the evolution of b-quarks and their collisional energy loss and a higher-twist description of radiative energy loss for both heavy and light partons. This model also includes the dead-cone effect for b-jets and also uses a (2+1)D viscous hydrodynamic medium with averaged initial conditions. The parameter controlling the coupling of the jet to the medium, q_0, is set to be 1.2 GeV^2/fm. The LIDO model shows good agreement with the data for both inclusive jet and b-jet R_{AA}, although with the inclusive jets on the low side and the b-jet case on the high side, for all three centralities considering model and data uncertainties. The calculation in Ref. [12] is below the measured R_{AA} in central and semi-central collisions for both b-jets and inclusive jets.

In order to assess any difference between the b-jet and inclusive jet R_{AA}, the ratio $R_{AA}^{b\text{-jet}}/R_{AA}^{\text{inclusive jet}}$ is presented in

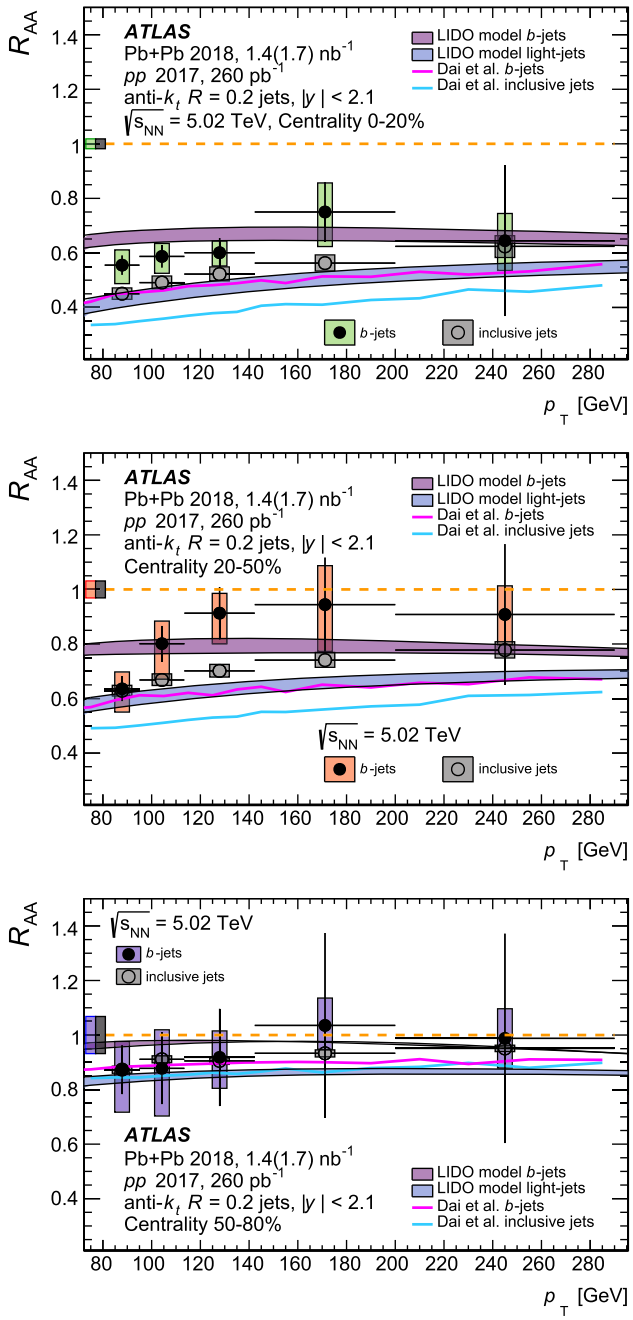

Fig. 10 b-jet (filled points) R_{AA} for three centrality classes compared with the inclusive jet R_{AA} (open points) at 5.02 TeV. Both R_{AA} measurements are compared with theory calculations [11,12,76]. The boxes represent the systematic uncertainties and the error bars represent the statistical uncertainties. For the LIDO calculation, the width of the band shows the variation of the μ_{min} parameter from $1.3\pi T$ (lower edge) to $1.8\pi T$ (upper edge). The boxes at unity represent the scale uncertainties from $\langle T_{\mathrm{AA}} \rangle$ and the luminosity determination

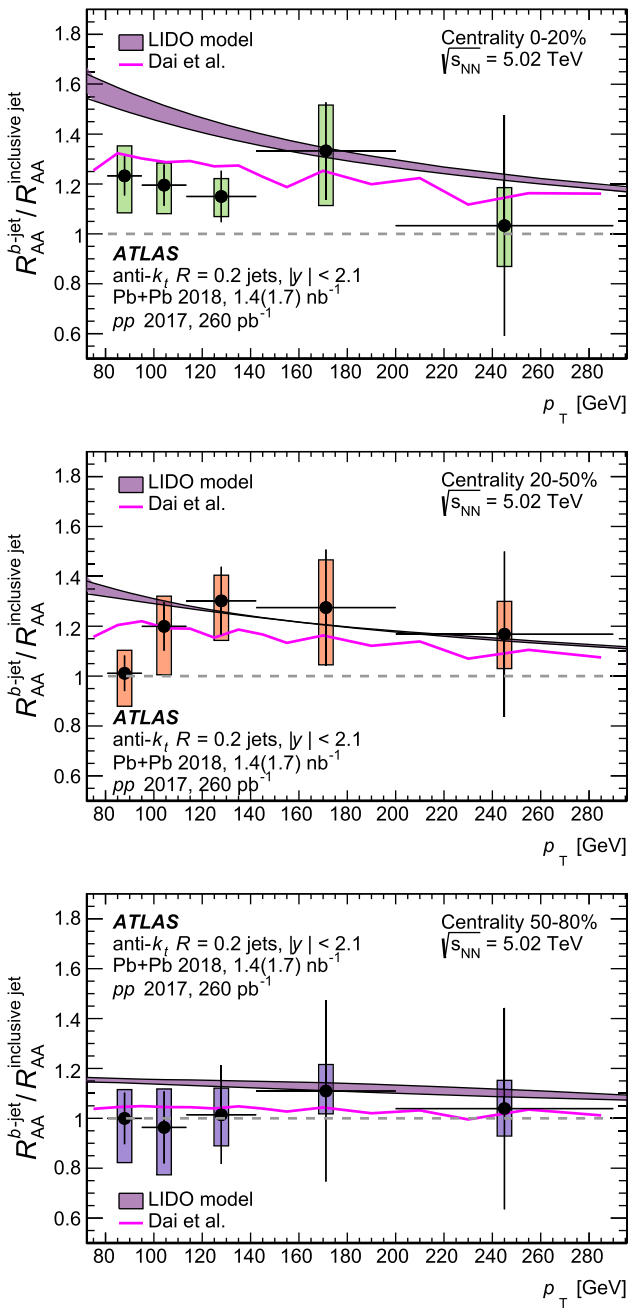

Fig. 11 Ratio of b-jet R_{AA} to the inclusive jet R_{AA} for each centrality class. Ratios are compared with theory calculations [11,12,76]. The boxes represent the systematic uncertainties and the error bars represent the statistical uncertainties. For the LIDO calculation, the width of the band shows the variation of the μ_{min} parameter from $1.3\pi T$ (upper edge) to $1.8\pi T$ (lower edge)

Fig. 11 for each centrality class. This provides a more precise comparison of the R_{AA} values than in Fig. 10. The results suggest that in central collisions the suppression of b-jets is less than that of inclusive jets, with an overall significance of approximately 1.7σ. The calculation by Dai et al. [12] agrees well with the ratio in all centrality classes, while LIDO model calculations tend to overestimate the double ratio at low p_{T}, especially in central collisions, but agree well with the data at higher p_{T}. In the LIDO model, the difference between the inclusive jet and b-jet R_{AA} values is not expected

to be entirely a result of the large mass of the b-quark, and qualitatively similar differences are seen between the two R_{AA} values in that model with and without the inclusion of the dead-cone effect [79].

Differences in the internal structure of the b-jets, such as those that come from gluon-splitting processes, are also expected to be important in determining the b-jet R_{AA} value. Based on the PYTHIA 8 MC samples, the fractions of jets which are initiated by gluons in the inclusive jet and b-jet samples have opposite trends with p_{T}. The fraction increases from 23% to 45% over the range of 80 to 250 GeV for the b-jets and decreases from 61% to 47% over the same range for the inclusive jets.

These results are compatible with previous results from CMS [29] (although both the collision energy and jet radius are different) but have better precision. Additional measurements of the fragmentation functions of b-jets in heavy-ion collisions would improve the uncertainties in future measurements using the method used in this article.

7 Summary

This paper reports cross-sections for b-jets and inclusive jets in Pb+Pb and pp collisions, both at $\sqrt{s_{\mathrm{NN}}} = 5.02$ TeV, and recorded by the ATLAS detector at the LHC. The measurement uses three datasets: 1.4 nb^{-1} and 1.7 nb^{-1} of Pb+Pb collisions collected in 2018 for $R = 0.2$ b-jets and inclusive jets respectively, and 260 pb^{-1} of pp collisions collected in 2017 for $R = 0.2$ and $R = 0.4$ b-jets and $R = 0.2$ inclusive jets. The b-jet cross-section in pp collisions is compared with a theoretical calculation and Monte Carlo generator predictions. The b-jet and inclusive jet per-event yields for $R = 0.2$ jets and the corresponding nuclear modification factor, R_{AA}, are also reported for Pb+Pb collisions at the same per-nucleon collision energy. The R_{AA} values are found to decrease with increasing collision centrality for both b-jets and inclusive jets. In order to more directly compare the suppression of b-jets and inclusive jets, the ratio of the R_{AA} values is presented. The central values of this ratio suggest that the R_{AA} for b-jets is larger than that for inclusive jets in central Pb+Pb collisions. The observed differences may arise primarily from the different mixture of quark and gluon jets in the inclusive jets and b-jets, and the b-quark mass effect may be subdominant in the kinematic range measured here. However, the current systematic uncertainties do not permit a more definitive statement. This highlights the need for more precise measurements of this quantity, mainly the necessity to measure the fragmentation functions of b-jets in heavy-ion collisions. The measurements are compared with theoretical calculations and suggest a role for mass and colour-charge effects in partonic energy loss in heavy-ion collisions.

Acknowledgements We thank CERN for the very successful operation of the LHC, as well as the support staff from our institutions without whom ATLAS could not be operated efficiently. We acknowledge the support of ANPCyT, Argentina; YerPhI, Armenia; ARC, Australia; BMWFW and FWF, Austria; ANAS, Azerbaijan; CNPq and FAPESP, Brazil; NSERC, NRC and CFI, Canada; CERN; ANID, Chile; CAS, MOST and NSFC, China; Minciencias, Colombia; MEYS CR, Czech Republic; DNRF and DNSRC, Denmark; IN2P3-CNRS and CEA-DRF/IRFU, France; SRNSFG, Georgia; BMBF, HGF and MPG, Germany; GSRI, Greece; RGC and Hong Kong SAR, China; ISF and Benoziyo Center, Israel; INFN, Italy; MEXT and JSPS, Japan; CNRST, Morocco; NWO, Netherlands; RCN, Norway; MEiN, Poland; FCT, Portugal; MNE/IFA, Romania; MESTD, Serbia; MSSR, Slovakia; ARRS and MIZŠ, Slovenia; DSI/NRF, South Africa; MICINN, Spain; SRC and Wallenberg Foundation, Sweden; SERI, SNSF and Cantons of Bern and Geneva, Switzerland; MOST, Taiwan; TENMAK, Türkiye; STFC, United Kingdom; DOE and NSF, United States of America. In addition, individual groups and members have received support from BCKDF, CANARIE, Compute Canada and CRC, Canada; PRIMUS 21/SCI/017 and UNCE SCI/013, Czech Republic; COST, ERC, ERDF, Horizon 2020 and Marie Skłodowska-Curie Actions, European Union; Investissements d'Avenir Labex, Investissements d'Avenir Idex and ANR, France; DFG and AvH Foundation, Germany; Herakleitos, Thales and Aristeia programmes co-financed by EU-ESF and the Greek NSRF, Greece; BSF-NSF and MINERVA, Israel; Norwegian Financial Mechanism 2014–2021, Norway; NCN and NAWA, Poland; La Caixa Banking Foundation, CERCA Programme Generalitat de Catalunya and PROMETEO and GenT Programmes Generalitat Valenciana, Spain; Göran Gustafssons Stiftelse, Sweden; The Royal Society and Leverhulme Trust, United Kingdom. The crucial computing support from all WLCG partners is acknowledged gratefully, in particular from CERN, the ATLAS Tier-1 facilities at TRIUMF (Canada), NDGF (Denmark, Norway, Sweden), CC-IN2P3 (France), KIT/GridKA (Germany), INFN-CNAF (Italy), NL-T1 (Netherlands), PIC (Spain), ASGC (Taiwan), RAL (UK) and BNL (USA), the Tier-2 facilities worldwide and large non-WLCG resource providers. Major contributors of computing resources are listed in Ref. [80].

Data Availability Statement This manuscript has no associated data or the data will not be deposited. [Authors' comment: All ATLAS scientific output is published in journals, and preliminary results are made available in Conference Notes. All are openly available, without restriction on use by external parties beyond copyright law and the standard conditions agreed by CERN. Data associated with journal publications are also made available: tables and data from plots (e.g. cross section values, likelihood profiles, selection efficiencies, cross section limits, ...) are stored in appropriate repositories such as HEPDATA (http://hepdata.cedar.ac.uk/). ATLAS also strives to make additional material related to the paper available that allows a reinterpretation of the data in the context of new theoretical models. For example, an extended encapsulation of the analysis is often provided for measurements in the framework of RIVET (http://rivet.hepforge.org/). This information is taken from the ATLAS Data Access Policy, which is a public document that can be downloaded from http://opendata.cern.ch/record/413 [opendata.cern.ch].].

Funded by SCOAP[3]. SCOAP[3] supports the goals of the International Year of Basic Sciences for Sustainable Development.

References

1. W. Busza, K. Rajagopal, W. van der Schee, Heavy ion collisions: the big picture, and the big questions. Annu. Rev. Nucl. Part. Sci. **68**, 339 (2018). https://doi.org/10.1146/annurev-nucl-101917-020852. arXiv: 1802.04801 [hep-ph]
2. ATLAS Collaboration, Measurement of the nuclear modification factor for inclusive jets in Pb+Pb collisions at $\sqrt{s_{\rm NN}} = 5.02$ TeV with the ATLAS detector. Phys. Lett. B **790**, 108 (2019). https://doi.org/10.1016/j.physletb.2018.10.076. arXiv:1805.05635 [nucl-ex]
3. ALICE Collaboration, Measurements of inclusive jet spectra in pp and central Pb-Pb collisions at $\sqrt{s_{NN}}$ = 5.02 TeV. Phys. Rev. C **101**, 034911 (2020). https://doi.org/10.1103/PhysRevC.101.034911. arXiv:1909.09718 [nucl-ex]
4. CMS Collaboration, First measurement of large area jet transverse momentum spectra in heavy-ion collisions. JHEP **05**, 284 (2021). https://doi.org/10.1007/JHEP05(2021)284. arXiv:2102.13080 [hep-ex]
5. ATLAS Collaboration, Measurement of angular and momentum distributions of charged particles within and around jets in Pb+Pb and pp collisions at $\sqrt{s_{\rm NN}} = 5.02$ TeV with the ATLAS detector. Phys. Rev. C **100**, 064901 (2019). https://doi.org/10.1103/PhysRevC.100.064901. arXiv:1908.05264 [nucl-ex] [Erratum: Phys. Rev. C 101, 059903 (2020)]
6. X. Dong, Y.-J. Lee, R. Rapp, Open heavy-flavor production in heavy-ion collisions. Annu. Rev. Nucl. Part. Sci. **69**, 417 (2019). https://doi.org/10.1146/annurev-nucl-101918-023806. arXiv:1903.07709 [nucl-ex]
7. Y.L. Dokshitzer, D.E. Kharzeev, Heavy quark colorimetry of QCD matter. Phys. Lett. B **519**, 199 (2001). https://doi.org/10.1016/S0370-2693(01)01130-3. arXiv:hep-ph/0106202
8. D. Zigic, I. Salom, J. Auvinen, M. Djordjevic, M. Djordjevic, DREENA-B framework: first predictions of R_{AA} and v_2 within dynamical energy loss formalism in evolving QCD medium. Phys. Lett. B **791**, 236 (2019). https://doi.org/10.1016/j.physletb.2019.02.020. arXiv:1805.04786 [nucl-th]
9. M. Spousta, B. Cole, Interpreting single jet measurements in Pb + Pb collisions at the LHC. Eur. Phys. J. C **76**, 50 (2016). https://doi.org/10.1140/epjc/s10052-016-3896-0. arXiv:1504.05169 [hep-ph]
10. S. Wicks, W. Horowitz, M. Djordjevic, M. Gyulassy, Elastic, inelastic, and path length fluctuations in jet tomography. Nucl. Phys. A **784**, 426 (2007). https://doi.org/10.1016/j.nuclphysa.2006.12.048. arXiv:nucl-th/0512076
11. W. Ke, Y. Xu, S.A. Bass, Linearized Boltzmann–Langevin model for heavy quark transport in hot and dense QCD matter. Phys. Rev. C **98**, 064901 (2018). https://doi.org/10.1103/PhysRevC.98.064901. arXiv:1806.08848 [nucl-th]
12. W. Dai, S. Wang, S.-L. Zhang, B.-W. Zhang, E. Wang, Transverse momentum balance and angular distribution of $b\bar{b}$ dijets in Pb+Pb collisions. Chin. Phys. C **44**, 104105 (2020). https://doi.org/10.1088/1674-1137/abab8f. arXiv:1806.06332 [nucl-th]
13. PHENIX Collaboration, Energy Loss and Flow of Heavy Quarks in Au+Au Collisions at $\sqrt{s_{\rm NN}}$ = 200 GeV. Phys. Rev. Lett. **98**, 172301 (2007). https://doi.org/10.1103/PhysRevLett.98.172301. arXiv:nucl-ex/0611018 [nucl-ex]
14. PHENIX Collaboration, Single electron yields from semileptonic charm and bottom hadron decays in Au+Au collisions at $\sqrt{s_{\rm NN}} =$ 200 GeV. Phys. Rev. C **93**, 034904 (2016). https://doi.org/10.1103/PhysRevC.93.034904. arXiv:1509.04662 [nucl-ex]
15. ALICE Collaboration, Production of muons from heavy-flavour hadron decays at high transverse momentum in Pb–Pb collisions at $\sqrt{s_{\rm NN}} =$ 5.02 and 2.76 TeV. Phys. Lett. B **820**, 136558 (2021). https://doi.org/10.1016/j.physletb.2021.136558. arXiv:2011.05718 [nucl-ex]
16. ATLAS Collaboration, Measurement of the nuclear modification factor for muons from charm and bottom hadrons in Pb+Pb collisions at 5.02 TeV with the ATLAS detector (2021). arXiv:2109.00411 [nucl-ex]
17. STAR Collaboration, Evidence of mass ordering of charm and bottom quark energy loss in Au+Au collisions at RHIC (2021). arXiv:2111.14615 [nucl-ex]
18. ATLAS Collaboration, Prompt and non-prompt J/ψ and $\psi(2S)$ suppression at high transverse momentum in 5.02 TeV Pb+Pb collisions with the ATLAS experiment. Eur. Phys. J. C **78**, 762 (2018). https://doi.org/10.1140/epjc/s10052-018-6219-9. arXiv:1805.04077 [nucl-ex]
19. CMS Collaboration, Suppression of non-prompt J/ψ, prompt J/ψ, and Υ(1S) in PbPb collisions at $\sqrt{s_{NN}} =$ 2.76 TeV. JHEP **05**, 063 (2012). https://doi.org/10.1007/JHEP05(2012)063. arXiv:1201.5069 [nucl-ex]
20. CMS Collaboration, Suppression and azimuthal anisotropy of prompt and nonprompt J/ψ production in PbPb collisions at $\sqrt{s_{NN}} = 2.76$ TeV. Eur. Phys. J. C **77**, 252 (2017). https://doi.org/10.1140/epjc/s10052-017-4781-1. arXiv:1610.00613 [nucl-ex]
21. CMS Collaboration, Studies of beauty suppression via nonprompt D^0 mesons in Pb–Pb collisions at $\sqrt{s_{\rm NN}} = 5.02$ TeV. Phys. Rev. Lett. **123**, 022001 (2019). https://doi.org/10.1103/PhysRevLett.123.022001. arXiv:1810.11102 [hep-ex]
22. CMS Collaboration, Nuclear modification factor of D^0 mesons in PbPb collisions at $\sqrt{s_{\rm NN}} =$ 5.02 TeV. Phys. Lett. B **782**, 474 (2018). https://doi.org/10.1016/j.physletb.2018.05.074. arXiv:1708.04962 [nucl-ex]
23. CMS Collaboration, Measurement of the $B^{\pm}$ meson nuclear modification factor in Pb–Pb collisions at $\sqrt{s_{NN}} = 5.02$TeV. Phys. Rev. Lett **119**, 152301 (2017). https://doi.org/10.1103/PhysRevLett.119.152301. arXiv:1705.04727 [hep-ex]
24. STAR Collaboration, Centrality and transverse momentum dependence of D^0-meson production at mid-rapidity in Au+Au collisions at $\sqrt{s_{\rm NN}} = 200$ GeV. Phys. Rev. C **99**, 034908 (2019). https://doi.org/10.1103/PhysRevC.99.034908. arXiv:1812.10224 [nucl-ex]
25. ALICE Collaboration, Prompt D^0, D^+, and D^{*+} production in Pb–Pb collisions at $\sqrt{s_{\rm NN}}$ = 5.02 TeV. JHEP **01**, 174 (2022). https://doi.org/10.1007/JHEP01(2022)174. arXiv:2110.09420 [nucl-ex]
26. ALICE Collaboration, Measurement of prompt D_s^+-meson production and azimuthal anisotropy in Pb–Pb collisions at $\sqrt{s_{NN}} = 5.02$ TeV. Phys. Lett. B **827**, 136986 (2022). https://doi.org/10.1016/j.physletb.2022.136986. arXiv:2110.10006 [nucl-ex]
27. ALICE Collaboration, Constraining hadronization mechanisms with Λ_c^+/D^0 production ratios in Pb–Pb collisions at $\sqrt{s_{NN}} = 5.02$ TeV (2021). arXiv:2112.08156 [nucl-ex]
28. Particle Data Group, Review of Particle Physics. PTEP **2020**, 083C01 (2020)
29. CMS Collaboration, Evidence of b-Jet Quenching in PbPb Collisions at $\sqrt{s_{NN}} =$ 2.76 TeV. Phys. Rev. Lett. **113**, 132301 (2014). https://doi.org/10.1103/PhysRevLett.113.132301. arXiv:1312.4198 [nucl-ex] [Erratum: Phys. Rev. Lett. 115 (2015) 029903]
30. M. Cacciari, G.P. Salam, G. Soyez, The anti-k_t jet clustering algorithm. JHEP **04**, 063 (2008). https://doi.org/10.1088/1126-6708/2008/04/063. arXiv:0802.1189 [hep-ph]
31. ATLAS Collaboration, Measurement of the inclusive and dijet cross-sections of $b-$jets in pp collisions at $\sqrt{s} =$ 7 TeV with

the ATLAS detector. Eur. Phys. J. C **71**, 1846 (2011). https://doi.org/10.1140/epjc/s10052-011-1846-4. arXiv:1109.6833 [hep-ex]
32. M.L. Miller, K. Reygers, S.J. Sanders, P. Steinberg, Glauber modeling in high-energy nuclear collisions. Annu. Rev. Nucl. Part. Sci. **57**, 205 (2007). https://doi.org/10.1146/annurev.nucl.57.090506.123020. arXiv:nucl-ex/0701025
33. ATLAS Collaboration, The ATLAS Experiment at the CERN Large Hadron Collider. JINST **3**, S08003 (2008)
34. ATLAS Collaboration, ATLAS Insertable B-Layer: Technical Design Report, ATLAS-TDR-19; CERN-LHCC-2010-013, 2010, https://cds.cern.ch/record/1291633,Addendum: ATLAS-TDR-19-ADD-1; CERN-LHCC-2012-009, 2012, https://cds.cern.ch/record/1451888
35. B. Abbott et al., Production and integration of the ATLAS Insertable B-Layer. JINST **13**, T05008 (2018). https://doi.org/10.1088/1748-0221/13/05/T05008. arXiv:1803.00844 [physics.ins-det]
36. ATLAS Collaboration, Operation of the ATLAS trigger system in Run 2. JINST **15**, P10004 (2020). https://doi.org/10.1088/1748-0221/15/10/P10004. arXiv:2007.12539 [physics.ins-det]
37. The ATLAS Collaboration Software and Firmware, tech. rep., CERN (2021). http://cds.cern.ch/record/2767187
38. ATLAS Collaboration, ATLAS data quality operations and performance for 2015–2018 data–taking. JINST **15**, P04003 (2020). https://doi.org/10.1088/1748-0221/15/04/P04003. arXiv:1911.04632 [physics.ins-det]
39. ATLAS Collaboration, Configuration and performance of the ATLAS b-jet triggers in Run 2. Eur. Phys. J. C **81**, 1087 (2021). https://doi.org/10.1140/epjc/s10052-021-09775-5. arXiv:2106.03584 [hep-ex]
40. ATLAS Collaboration, Measurement of the azimuthal anisotropy of charged particles produced in $\sqrt{s_{NN}} = 5.02$ TeV Pb+Pb collisions with the ATLAS detector. Eur. Phys. J. C **78**, 997 (2018). https://doi.org/10.1140/epjc/s10052-018-6468-7. arXiv:1808.03951 [hep-ex]
41. C. Loizides, J. Nagle, P. Steinberg, Improved version of the PHOBOS Glauber Monte Carlo. SoftwareX **1–2**, 13 (2015). https://doi.org/10.1016/j.softx.2015.05.001. arXiv:1408.2549 [nucl-ex]
42. GEANT4 Collaboration, S. Agostinelli et al., GEANT4—a simulation toolkit. Nucl. Instrum. Meth. A **506**, 250 (2003)
43. ATLAS Collaboration, The ATLAS Simulation Infrastructure. Eur. Phys. J. C **70**, 823 (2010). https://doi.org/10.1140/epjc/s10052-010-1429-9. arXiv:1005.4568 [physics.ins-det]
44. T. Sjöstrand et al., An introduction to PYTHIA 8.2. Comput. Phys. Commun. **191**, 159 (2015). https://doi.org/10.1016/j.cpc.2015.01.024. arXiv:1410.3012 [hep-ph]
45. ATLAS Collaboration, ATLAS Pythia 8 tunes to 7 TeV data (2014), ATLAS–PHYS-PUB-2014-021. https://cds.cern.ch/record/1966419
46. R.D. Ball et al., Parton distributions with LHC data. Nucl. Phys. B **867**, 244 (2013). https://doi.org/10.1016/j.nuclphysb.2012.10.003. arXiv:1207.1303 [hep-ph]
47. D.J. Lange, The EvtGen particle decay simulation package. Nucl. Instrum. Meth. A **462**, 152 (2001)
48. ATLAS Collaboration, The Pythia 8 A3 tune description of ATLAS minimum bias and inelastic measurements incorporating the Donnachie–Landshoff diffractive model, ATL-PHYS-PUB-2016-017 (2016). https://cds.cern.ch/record/2206965
49. E. Barberio, Z. Was, PHOTOS—a universal Monte Carlo for QED radiative corrections: version 2.0. Comput. Phys. **79**, 291 (1994). ISSN: 0010-4655
50. J. Pumplin et al., New generation of parton distributions with uncertainties from global QCD analysis. JHEP **07**, 012 (2002). https://doi.org/10.1088/1126-6708/2002/07/012. arXiv:hep-ph/0201195
51. M. Bähr et al., Herwig++ physics and manual. Eur. Phys. J. C **58**, 639 (2008). https://doi.org/10.1140/epjc/s10052-008-0798-9. arXiv:0803.0883 [hep-ph]
52. S. Gieseke, C. Röhr, A. Siødmok, Colour reconnections in Herwig++. Eur. Phys. J. C **72**, 2225 (2012). https://doi.org/10.1140/epjc/s10052-012-2225-5. arXiv:1206.0041 [hep-ph]
53. ATLAS Collaboration, Measurements of azimuthal anisotropies of jet production in Pb+Pb collisions at $\sqrt{s_{NN}} = 5.02$ TeV with the ATLAS detector (2021). arXiv:2111.06606 [nucl-ex]
54. M. Cacciari, G.P. Salam, G. Soyez, FastJet user manual. Eur. Phys. J. C **72**, 1896 (2012). https://doi.org/10.1140/epjc/s10052-012-1896-2. arXiv:1111.6097 [hep-ph]
55. ATLAS Collaboration, Jet energy measurement with the ATLAS detector in proton–proton collisions at $\sqrt{s} = 7$ TeV. Eur. Phys. J. C **73**, 2304 (2013). https://doi.org/10.1140/epjc/s10052-013-2304-2. arXiv:1112.6426 [hep-ex]
56. ATLAS Collaboration, Jet energy measurement and its systematic uncertainty in proton–proton collisions at $\sqrt{s} = 7$ TeV with the ATLAS detector. Eur. Phys. J. C **75**, 17 (2015). https://doi.org/10.1140/epjc/s10052-014-3190-y. arXiv:1406.0076 [hep-ex]
57. ATLAS Collaboration, Measurement of photon–jet transverse momentum correlations in 5.02 TeV Pb+Pb and pp collisions with ATLAS. Phys. Lett. B **789**, 167 (2019). https://doi.org/10.1016/j.physletb.2018.12.023. arXiv:1809.07280 [hep-ex]
58. ATLAS Collaboration, Jet energy scale and its uncertainty for jets reconstructed using the ATLAS heavy ion jet algorithm, ATLAS-CONF-2015-016 (2015). https://cds.cern.ch/record/2008677
59. ATLAS Collaboration, Muon reconstruction performance of the ATLAS detector in proton–proton collision data at $\sqrt{s}$ =13 TeV. Eur. Phys. J. C **76**, 292 (2016). https://doi.org/10.1140/epjc/s10052-016-4120-y. arXiv:1603.05598 [hep-ex]
60. ATLAS Collaboration, Performance of the ATLAS muon triggers in Run 2. JINST **15**, P09015 (2020). https://doi.org/10.1088/1748-0221/15/09/p09015. arXiv:2004.13447 [hep-ex]
61. Y.S. Amhis et al., Averages of b-hadron, c-hadron, and τ-lepton properties as of 2018. Eur. Phys. J. C **81**, 226 (2021). https://doi.org/10.1140/epjc/s10052-020-8156-7. arXiv: 1909.12524 [hep-ex]
62. Measurement of b hadron fractions in 13 TeV pp collisions. Phys. Rev. D **100**, 031102 (2019). https://doi.org/10.1103/PhysRevD.100.031102. arXiv:1902.06794 [hep-ex]
63. CMS Collaboration, Inclusive b-hadron production cross section with muons in pp collisions at $\sqrt{s} = 7$ TeV. JHEP **03**, 090 (2011). https://doi.org/10.1007/JHEP03(2011)090. arXiv:1101.3512 [hep-ex]
64. W. Verkerke, D.P. Kirkby, The RooFit toolkit for data modeling (2003). arXiv:physics/0306116
65. G. D'Agostini, A multidimensional unfolding method based on Bayes' theorem. Nucl. Instrum. Meth. A **362**, 487 (1995)
66. T. Adye, Unfolding algorithms and tests using RooUnfold, 313 (2011). https://doi.org/10.5170/CERN-2011-006.313. arXiv:1105.1160 [physics.data-an]
67. ATLAS Collaboration, Jet energy scale measurements and their systematic uncertainties in proton–proton collisions at $\sqrt{s} = 13$ TeV with the ATLAS detector. Phys. Rev. D **96**, 072002 (2017). https://doi.org/10.1103/PhysRevD.96.072002. arXiv:1703.09665 [hep-ex]
68. ATLAS Collaboration, Measurement of jet fragmentation in Pb+Pb and pp collisions at $\sqrt{s_{NN}} = 5.02$ TeV with the ATLAS detector. Phys. Rev. C **98**, 024908 (2018). https://doi.org/10.1103/PhysRevC.98.024908. arXiv:1805.05424 [nucl-ex]
69. ATLAS Collaboration, Jet energy resolution in proton–proton collisions at $\sqrt{s} = 7$ TeV recorded in 2010 with the ATLAS detector. Eur. Phys. J. C **73**, 2306 (2013). https://doi.org/10.1140/epjc/s10052-013-2306-0. arXiv:1210.6210 [hep-ex]
70. ATLAS Collaboration, Determination of jet calibration and energy resolution in proton–proton collisions at $\sqrt{s} = 8$ TeV using the

76. W. Ke, Y. Xu, S.A. Bass, Modified Boltzmann approach for modeling the splitting vertices induced by the hot QCD medium in the deep Landau-Pomeranchuk-Migdal region. Phys. Rev. C **100**, 064911 (2019). https://doi.org/10.1103/PhysRevC.100.064911. arXiv:1810.08177 [nucl-th]
77. J. Bellm et al., Herwig 7.0/Herwig++ 3.0 release note. Eur. Phys. J. C **76**, 196 (2016). https://doi.org/10.1140/epjc/s10052-016-4018-8. arXiv:1512.01178 [hep-ph]
78. CMS Collaboration, Inclusive b-jet production in pp collisions at $\sqrt{s} = 7$ TeV. JHEP **04**, 084 (2012). https://doi.org/10.1007/JHEP04(2012)084. arXiv:1202.4617 [hep-ex]
79. W. Ke, X.–N. Wang, W. Fan, S. Bass, Study of heavy-flavor jets in a transport approach (2020). arXiv:2008.07622 [nucl-th]
80. ATLAS Collaboration, ATLAS Computing Acknowledgements, ATL-SOFT-PUB-2021-003 (2021). https://cds.cern.ch/record/2776662

ATLAS Collaboration*

G. Aad[101], B. Abbott[119], D. C. Abbott[102], K. Abeling[55], S. H. Abidi[29], A. Aboulhorma[35e], H. Abramowicz[150], H. Abreu[149], Y. Abulaiti[116], A. C. Abusleme Hoffman[136a], B. S. Acharya[68a,68b,o], B. Achkar[55], L. Adam[99], C. Adam Bourdarios[4], L. Adamczyk[84a], L. Adamek[154], S. V. Addepalli[26], J. Adelman[114], A. Adiguzel[21c], S. Adorni[56], T. Adye[133], A. A. Affolder[135], Y. Afik[36], M. N. Agaras[13], J. Agarwala[72a,72b], A. Aggarwal[99], C. Agheorghiesei[27c], J. A. Aguilar-Saavedra[129f], A. Ahmad[36], F. Ahmadov[38,w], W. S. Ahmed[103], X. Ai[48], G. Aielli[75a,75b], I. Aizenberg[167], M. Akbiyik[99], T. P. A. Åkesson[97], A. V. Akimov[37], K. Al Khoury[41], G. L. Alberghi[23b], J. Albert[163], P. Albicocco[53], M. J. Alconada Verzini[89], S. Alderweireldt[52], M. Aleksa[36], I. N. Aleksandrov[38], C. Alexa[27b], T. Alexopoulos[10], A. Alfonsi[113], F. Alfonsi[23b], M. Alhroob[119], B. Ali[131], S. Ali[147], M. Aliev[37], G. Alimonti[70a], C. Allaire[36], B. M. M. Allbrooke[145], P. P. Allport[20], A. Aloisio[71a,71b], F. Alonso[89], C. Alpigiani[137], E. Alunno Camelia[75a,75b], M. Alvarez Estevez[98], M. G. Alviggi[71a,71b], Y. Amaral Coutinho[81b], A. Ambler[103], C. Amelung[36], C. G. Ames[108], D. Amidei[105], S. P. Amor Dos Santos[129a], S. Amoroso[48], K. R. Amos[161], C. S. Amrouche[56], V. Ananiev[124], C. Anastopoulos[138], N. Andari[134], T. Andeen[11], J. K. Anders[19], S. Y. Andrean[47a,47b], A. Andreazza[70a,70b], S. Angelidakis[9], A. Angerami[41,y], A. V. Anisenkov[37], A. Annovi[73a], C. Antel[56], M. T. Anthony[138], E. Antipov[120], M. Antonelli[53], D. J. A. Antrim[17a], F. Anulli[74a], M. Aoki[82], J. A. Aparisi Pozo[161], M. A. Aparo[145], L. Aperio Bella[48], C. Appelt[18], N. Aranzabal[36], V. Araujo Ferraz[81a], C. Arcangeletti[53], A. T. H. Arce[51], E. Arena[91], J.-F. Arguin[107], S. Argyropoulos[54], J.-H. Arling[48], A. J. Armbruster[36], O. Arnaez[154], H. Arnold[113], Z. P. Arrubarrena Tame[108], G. Artoni[74a,74b], H. Asada[110], K. Asai[117], S. Asai[152], N. A. Asbah[61], E. M. Asimakopoulou[159], J. Assahsah[35d], K. Assamagan[29], R. Astalos[28a], R. J. Atkin[33a], M. Atkinson[160], N. B. Atlay[18], H. Atmani[62b], P. A. Atmasiddha[105], K. Augsten[131], S. Auricchio[71a,71b], A. D. Auriol[20], V. A. Austrup[169], G. Avner[149], G. Avolio[36], K. Axiotis[56], M. K. Ayoub[14c], G. Azuelos[107,ac], D. Babal[28a], H. Bachacou[134], K. Bachas[151,q], A. Bachiu[34], F. Backman[47a,47b], A. Badea[61], P. Bagnaia[74a,74b], M. Bahmani[18], A. J. Bailey[161], V. R. Bailey[160], J. T. Baines[133], C. Bakalis[10], O. K. Baker[170], P. J. Bakker[113], E. Bakos[15], D. Bakshi Gupta[8], S. Balaji[146], R. Balasubramanian[113], E. M. Baldin[37], P. Balek[132], E. Ballabene[70a,70b], F. Balli[134], L. M. Baltes[63a], W. K. Balunas[32], J. Balz[99], E. Banas[85], M. Bandieramonte[128], A. Bandyopadhyay[24], S. Bansal[24], L. Barak[150], E. L. Barberio[104], D. Barberis[57a,57b], M. Barbero[101], G. Barbour[95], K. N. Barends[33a], T. Barillari[109], M.-S. Barisits[36], J. Barkeloo[122], T. Barklow[142], R. M. Barnett[17a], P. Baron[121], D. A. Baron Moreno[100], A. Baroncelli[62a], G. Barone[29], A. J. Barr[125], L. Barranco Navarro[47a,47b], F. Barreiro[98], J. Barreiro Guimarães da Costa[14a], U. Barron[150], M. G. Barros Teixeira[129a], S. Barsov[37], F. Bartels[63a], R. Bartoldus[142], A. E. Barton[90], P. Bartos[28a], A. Basalaev[48], A. Basan[99], M. Baselga[49], I. Bashta[76a,76b], A. Bassalat[66,z], M. J. Basso[154], C. R. Basson[100], R. L. Bates[59], S. Batlamous[35e], J. R. Batley[32], B. Batool[140], M. Battaglia[135], M. Bauce[74a,74b], P. Bauer[24], A. Bayirli[21a], J. B. Beacham[51], T. Beau[126], P. H. Beauchemin[157], F. Becherer[54], P. Bechtle[24], H. P. Beck[19,p], K. Becker[165], C. Becot[48], A. J. Beddall[21d], V. A. Bednyakov[38], C. P. Bee[144], L. J. Beemster[15], T. A. Beermann[36], M. Begalli[81b], M. Begel[29], A. Behera[144], J. K. Behr[48], C. Beirao Da Cruz E Silva[36], J. F. Beirer[36,55], F. Beisiegel[24], M. Belfkir[115b], G. Bella[150], L. Bellagamba[23b], A. Bellerive[34], P. Bellos[20], K. Beloborodov[37], K. Belotskiy[37], N. L. Belyaev[37], D. Benchekroun[35a], F. Bendebba[35a], Y. Benhammou[150], D. P. Benjamin[29], M. Benoit[29], J. R. Bensinger[26], S. Bentvelsen[113], L. Beresford[36], M. Beretta[53], D. Berge[18], E. Bergeaas Kuutmann[159], N. Berger[4], B. Bergmann[131], J. Beringer[17a], S. Berlendis[7], G. Bernardi[5], C. Bernius[142], F. U. Bernlochner[24], T. Berry[94], P. Berta[132], A. Berthold[50], I. A. Bertram[90], O. Bessidskaia Bylund[169], S. Bethke[109], A. Betti[44], A. J. Bevan[93], M. Bhamjee[33c],

S. Bhatta[144], D. S. Bhattacharya[164], P. Bhattarai[26], V. S. Bhopatkar[6], R. Bi[128], R. Bi[29,af], R. M. Bianchi[128], O. Biebel[108], R. Bielski[122], N. V. Biesuz[73a,73b], M. Biglietti[76a], T. R. V. Billoud[131], M. Bindi[55], A. Bingul[21b], C. Bini[74a,74b], S. Biondi[23a,23b], A. Biondini[91], C. J. Birch-sykes[100], G. A. Bird[20,133], M. Birman[167], T. Bisanz[36], D. Biswas[168,k], A. Bitadze[100], K. Bjørke[124], I. Bloch[48], C. Blocker[26], A. Blue[59], U. Blumenschein[93], J. Blumenthal[99], G. J. Bobbink[113], V. S. Bobrovnikov[37], M. Boehler[54], D. Bogavac[36], A. G. Bogdanchikov[37], C. Bohm[47a], V. Boisvert[94], P. Bokan[48], T. Bold[84a], M. Bomben[5], M. Bona[93], M. Boonekamp[134], C. D. Booth[94], A. G. Borbély[59], H. M. Borecka-Bielska[107], L. S. Borgna[95], G. Borissov[90], D. Bortoletto[125], D. Boscherini[23b], M. Bosman[13], J. D. Bossio Sola[36], K. Bouaouda[35a], J. Boudreau[128], E. V. Bouhova-Thacker[90], D. Boumediene[40], R. Bouquet[5], A. Boveia[118], J. Boyd[36], D. Boye[29], I. R. Boyko[38], J. Bracinik[20], N. Brahimi[62d,62c], G. Brandt[169], O. Brandt[32], F. Braren[48], B. Brau[102], J. E. Brau[122], W. D. Breaden Madden[59], K. Brendlinger[48], R. Brener[167], L. Brenner[36], R. Brenner[159], S. Bressler[167], B. Brickwedde[99], D. Britton[59], D. Britzger[109], I. Brock[24], G. Brooijmans[41], W. K. Brooks[136f], E. Brost[29], P. A. Bruckman de Renstrom[85], B. Brüers[48], D. Bruncko[28b,*], A. Bruni[23b], G. Bruni[23b], M. Bruschi[23b], N. Bruscino[74a,74b], L. Bryngemark[142], T. Buanes[16], Q. Buat[137], P. Buchholz[140], A. G. Buckley[59], I. A. Budagov[38,*], M. K. Bugge[124], O. Bulekov[37], B. A. Bullard[61], S. Burdin[91], C. D. Burgard[48], A. M. Burger[40], B. Burghgrave[8], J. T. P. Burr[32], C. D. Burton[11], J. C. Burzynski[141], E. L. Busch[41], V. Büscher[99], P. J. Bussey[59], J. M. Butler[25], C. M. Buttar[59], J. M. Butterworth[95], W. Buttinger[133], C. J. Buxo Vazquez[106], A. R. Buzykaev[37], G. Cabras[23b], S. Cabrera Urbán[161], D. Caforio[58], H. Cai[128], Y. Cai[14a,14d], V. M. M. Cairo[36], O. Cakir[3a], N. Calace[36], P. Calafiura[17a], G. Calderini[126], P. Calfayan[67], G. Callea[59], L. P. Caloba[81b], D. Calvet[40], S. Calvet[40], T. P. Calvet[101], M. Calvetti[73a,73b], R. Camacho Toro[126], S. Camarda[36], D. Camarero Munoz[98], P. Camarri[75a,75b], M. T. Camerlingo[76a,76b], D. Cameron[124], C. Camincher[163], M. Campanelli[95], A. Camplani[42], V. Canale[71a,71b], A. Canesse[103], M. Cano Bret[79], J. Cantero[161], Y. Cao[160], F. Capocasa[26], M. Capua[43a,43b], A. Carbone[70a,70b], R. Cardarelli[75a], J. C. J. Cardenas[8], F. Cardillo[161], T. Carli[36], G. Carlino[71a], B. T. Carlson[128,r], E. M. Carlson[155a,163], L. Carminati[70a,70b], M. Carnesale[74a,74b], S. Caron[112], E. Carquin[136f], S. Carrá[70a,70b], G. Carratta[23a,23b], J. W. S. Carter[154], T. M. Carter[52], M. P. Casado[13,h], A. F. Casha[154], E. G. Castiglia[170], F. L. Castillo[63a], L. Castillo Garcia[13], V. Castillo Gimenez[161], N. F. Castro[129a,129e], A. Catinaccio[36], J. R. Catmore[124], V. Cavaliere[29], N. Cavalli[23a,23b], V. Cavasinni[73a,73b], E. Celebi[21a], F. Celli[125], M. S. Centonze[69a,69b], K. Cerny[121], A. S. Cerqueira[81a], A. Cerri[145], L. Cerrito[75a,75b], F. Cerutti[17a], A. Cervelli[23b], S. A. Cetin[21d], Z. Chadi[35a], D. Chakraborty[114], M. Chala[129f], J. Chan[168], W. S. Chan[113], W. Y. Chan[152], J. D. Chapman[32], B. Chargeishvili[148b], D. G. Charlton[20], T. P. Charman[93], M. Chatterjee[19], S. Chekanov[6], S. V. Chekulaev[155a], G. A. Chelkov[38,a], A. Chen[105], B. Chen[150], B. Chen[163], C. Chen[62a], H. Chen[14c], H. Chen[29], J. Chen[62c], J. Chen[26], S. Chen[152], S. J. Chen[14c], X. Chen[62c], X. Chen[14b,ab], Y. Chen[62a], C. L. Cheng[168], H. C. Cheng[64a], A. Cheplakov[38], E. Cheremushkina[48], E. Cherepanova[113], R. Cherkaoui El Moursli[35e], E. Cheu[7], K. Cheung[65], L. Chevalier[134], V. Chiarella[53], G. Chiarelli[73a], G. Chiodini[69a], A. S. Chisholm[20], A. Chitan[27b], Y. H. Chiu[163], M. V. Chizhov[38], K. Choi[11], A. R. Chomont[74a,74b], Y. Chou[102], E. Y. S. Chow[113], T. Chowdhury[33g], L. D. Christopher[33g], K. L. Chu[64a], M. C. Chu[64a], X. Chu[14a,14d], J. Chudoba[130], J. J. Chwastowski[85], D. Cieri[109], K. M. Ciesla[84a], V. Cindro[92], A. Ciocio[17a], F. Cirotto[71a,71b], Z. H. Citron[167,l], M. Citterio[70a], D. A. Ciubotaru[27b], B. M. Ciungu[154], A. Clark[56], P. J. Clark[52], J. M. Clavijo Columbie[48], S. E. Clawson[100], C. Clement[47a,47b], J. Clercx[48], L. Clissa[23a,23b], Y. Coadou[101], M. Cobal[68a,68c], A. Coccaro[57b], R. F. Coelho Barrue[129a], R. Coelho Lopes De Sa[102], S. Coelli[70a], H. Cohen[150], A. E. C. Coimbra[70a,70b], B. Cole[41], J. Collot[60], P. Conde Muiño[129a,129g], S. H. Connell[33c], I. A. Connelly[59], E. I. Conroy[125], F. Conventi[71a,ad], H. G. Cooke[20], A. M. Cooper-Sarkar[125], F. Cormier[162], L. D. Corpe[36], M. Corradi[74a,74b], E. E. Corrigan[97], F. Corriveau[103,v], A. Cortes-Gonzalez[18], M. J. Costa[161], F. Costanza[4], D. Costanzo[138], B. M. Cote[118], G. Cowan[94], J. W. Cowley[32], K. Cranmer[116], S. Crépé-Renaudin[60], F. Crescioli[126], M. Cristinziani[140], M. Cristoforetti[77a,77b,c], V. Croft[157], G. Crosetti[43a,43b], A. Cueto[36], T. Cuhadar Donszelmann[158], H. Cui[14a,14d], Z. Cui[7], A. R. Cukierman[142], W. R. Cunningham[59], F. Curcio[43a,43b], P. Czodrowski[36], M. M. Czurylo[63b], M. J. Da Cunha Sargedas De Sousa[62a], J. V. Da Fonseca Pinto[81b], C. Da Via[100], W. Dabrowski[84a], T. Dado[49], S. Dahbi[33g], T. Dai[105], C. Dallapiccola[102], M. Dam[42], G. D'amen[29], V. D'Amico[76a,76b], J. Damp[99], J. R. Dandoy[127], M. F. Daneri[30], M. Danninger[141], V. Dao[36], G. Darbo[57b], S. Darmora[6], S. J. Das[29], A. Dattagupta[122], S. D'Auria[70a,70b], C. David[155b], T. Davidek[132], D. R. Davis[51], B. Davis-Purcell[34], I. Dawson[93], K. De[8], R. De Asmundis[71a], M. De Beurs[113], S. De Castro[23a,23b],

N. De Groot[112], P. de Jong[113], H. De la Torre[106], A. De Maria[14c], A. De Salvo[74a], U. De Sanctis[75a,75b], M. De Santis[75a,75b], A. De Santo[145], J. B. De Vivie De Regie[60], D. V. Dedovich[38], J. Degens[113], A. M. Deiana[44], F. Del Corso[23a,23b], J. Del Peso[98], F. Del Rio[63a], F. Deliot[134], C. M. Delitzsch[49], M. Della Pietra[71a,71b], D. Della Volpe[56], A. Dell'Acqua[36], L. Dell'Asta[70a,70b], M. Delmastro[4], P. A. Delsart[60], S. Demers[170], M. Demichev[38], S. P. Denisov[37], L. D'Eramo[114], D. Derendarz[85], F. Derue[126], P. Dervan[91], K. Desch[24], K. Dette[154], C. Deutsch[24], P. O. Deviveiros[36], F. A. Di Bello[74a,74b], A. Di Ciaccio[75a,75b], L. Di Ciaccio[4], A. Di Domenico[74a,74b], C. Di Donato[71a,71b], A. Di Girolamo[36], G. Di Gregorio[73a,73b], A. Di Luca[77a,77b], B. Di Micco[76a,76b], R. Di Nardo[76a,76b], C. Diaconu[101], F. A. Dias[113], T. Dias Do Vale[141], M. A. Diaz[136a,136b], F. G. Diaz Capriles[24], M. Didenko[161], E. B. Diehl[105], L. Diehl[54], S. Díez Cornell[48], C. Diez Pardos[140], C. Dimitriadi[24,159], A. Dimitrievska[17a], W. Ding[14b], J. Dingfelder[24], I.-M. Dinu[27b], S. J. Dittmeier[63b], F. Dittus[36], F. Djama[101], T. Djobava[148b], J. I. Djuvsland[16], D. Dodsworth[26], C. Doglioni[97,100], J. Dolejsi[132], Z. Dolezal[132], M. Donadelli[81c], B. Dong[62c], J. Donini[40], A. D'Onofrio[14c], M. D'Onofrio[91], J. Dopke[133], A. Doria[71a], M. T. Dova[89], A. T. Doyle[59], M. A. Draguet[125], E. Drechsler[141], E. Dreyer[167], I. Drivas-koulouris[10], A. S. Drobac[157], D. Du[62a], T. A. du Pree[113], F. Dubinin[37], M. Dubovsky[28a], E. Duchovni[167], G. Duckeck[108], O. A. Ducu[36], D. Duda[109], A. Dudarev[36], M. D'uffizi[100], L. Duflot[66], M. Dührssen[36], C. Dülsen[169], A. E. Dumitriu[27b], M. Dunford[63a], S. Dungs[49], K. Dunne[47a,47b], A. Duperrin[101], H. Duran Yildiz[3a], M. Düren[58], A. Durglishvili[148b], B. L. Dwyer[114], G. I. Dyckes[17a], M. Dyndal[84a], S. Dysch[100], B. S. Dziedzic[85], B. Eckerova[28a], M. G. Eggleston[51], E. Egidio Purcino De Souza[81b], L. F. Ehrke[56], G. Eigen[16], K. Einsweiler[17a], T. Ekelof[159], P. A. Ekman[97], Y. El Ghazali[35b], H. El Jarrari[35e,147], A. El Moussaouy[35a], V. Ellajosyula[159], M. Ellert[159], F. Ellinghaus[169], A. A. Elliot[93], N. Ellis[36], J. Elmsheuser[29], M. Elsing[36], D. Emeliyanov[133], A. Emerman[41], Y. Enari[152], I. Ene[17a], S. Epari[13], J. Erdmann[49], A. Ereditato[19], P. A. Erland[85], M. Errenst[169], M. Escalier[66], C. Escobar[161], E. Etzion[150], G. Evans[129a], H. Evans[67], M. O. Evans[145], A. Ezhilov[37], S. Ezzarqtouni[35a], F. Fabbri[59], L. Fabbri[23a,23b], G. Facini[95], V. Fadeyev[135], R. M. Fakhrutdinov[37], S. Falciano[74a], P. J. Falke[24], S. Falke[36], J. Faltova[132], Y. Fan[14a], Y. Fang[14a,14d], G. Fanourakis[46], M. Fanti[70a,70b], M. Faraj[68a,68b], A. Farbin[8], A. Farilla[76a], T. Farooque[106], S. M. Farrington[52], F. Fassi[35e], D. Fassouliotis[9], M. Faucci Giannelli[75a,75b], W. J. Fawcett[32], L. Fayard[66], O. L. Fedin[37,a], G. Fedotov[37], M. Feickert[160], L. Feligioni[101], A. Fell[138], D. E. Fellers[122], C. Feng[62b], M. Feng[14b], M. J. Fenton[158], A. B. Fenyuk[37], L. Ferencz[48], S. W. Ferguson[45], J. A. Fernandez Pretel[54], J. Ferrando[48], A. Ferrari[159], P. Ferrari[113], R. Ferrari[72a], D. Ferrere[56], C. Ferretti[105], F. Fiedler[99], A. Filipčič[92], E. K. Filmer[1], F. Filthaut[112], M. C. N. Fiolhais[129a,129c,b], L. Fiorini[161], F. Fischer[140], W. C. Fisher[106], T. Fitschen[20,66], I. Fleck[140], P. Fleischmann[105], T. Flick[169], L. Flores[127], M. Flores[33d], L. R. Flores Castillo[64a], F. M. Follega[77a,77b], N. Fomin[16], J. H. Foo[154], B. C. Forland[67], A. Formica[134], A. C. Forti[100], E. Fortin[101], A. W. Fortman[61], M. G. Foti[17a], L. Fountas[9], D. Fournier[66], H. Fox[90], P. Francavilla[73a,73b], S. Francescato[61], M. Franchini[23a,23b], S. Franchino[63a], D. Francis[36], L. Franco[112], L. Franconi[19], M. Franklin[61], G. Frattari[26], A. C. Freegard[93], P. M. Freeman[20], W. S. Freund[81b], N. Fritzsche[50], A. Froch[54], D. Froidevaux[36], J. A. Frost[125], Y. Fu[62a], M. Fujimoto[117], E. Fullana Torregrosa[161,*], J. Fuster[161], A. Gabrielli[23a,23b], A. Gabrielli[36], P. Gadow[48], G. Gagliardi[57a,57b], L. G. Gagnon[17a], G. E. Gallardo[125], E. J. Gallas[125], B. J. Gallop[133], R. Gamboa Goni[93], K. K. Gan[118], S. Ganguly[152], J. Gao[62a], Y. Gao[52], F. M. Garay Walls[136a,136b], B. Garcia[29,af], C. García[161], J. E. García Navarro[161], J. A. García Pascual[14a], M. Garcia-Sciveres[17a], R. W. Gardner[39], D. Garg[79], R. B. Garg[142], S. Gargiulo[54], C. A. Garner[154], V. Garonne[29], S. J. Gasiorowski[137], P. Gaspar[81b], G. Gaudio[72a], P. Gauzzi[74a,74b], I. L. Gavrilenko[37], A. Gavrilyuk[37], C. Gay[162], G. Gaycken[48], E. N. Gazis[10], A. A. Geanta[27b], C. M. Gee[135], J. Geisen[97], M. Geisen[99], C. Gemme[57b], M. H. Genest[60], S. Gentile[74a,74b], S. George[94], W. F. George[20], T. Geralis[46], L. O. Gerlach[55], P. Gessinger-Befurt[36], M. Ghasemi Bostanabad[163], M. Ghneimat[140], A. Ghosal[140], A. Ghosh[158], A. Ghosh[7], B. Giacobbe[23b], S. Giagu[74a,74b], N. Giangiacomi[154], P. Giannetti[73a], A. Giannini[62a], S. M. Gibson[94], M. Gignac[135], D. T. Gil[84b], A. K. Gilbert[84a], B. J. Gilbert[41], D. Gillberg[34], G. Gilles[113], N. E. K. Gillwald[48], L. Ginabat[126], D. M. Gingrich[2,ac], M. P. Giordani[68a,68c], P. F. Giraud[134], G. Giugliarelli[68a,68c], D. Giugni[70a], F. Giuli[36], I. Gkialas[9,i], L. K. Gladilin[37], C. Glasman[98], G. R. Gledhill[122], M. Glisic[122], I. Gnesi[43b,e], Y. Go[29,af], M. Goblirsch-Kolb[26], D. Godin[107], S. Goldfarb[104], T. Golling[56], M. G. D. Gololo[33g], D. Golubkov[37], J. P. Gombas[106], A. Gomes[129a,129b], A. J. Gomez Delegido[161], R. Goncalves Gama[55], R. Gonçalo[129a,129c], G. Gonella[122], L. Gonella[20], A. Gongadze[38], F. Gonnella[20], J. L. Gonski[41], S. González de la Hoz[161], S. Gonzalez Fernandez[13],

R. Gonzalez Lopez[91], C. Gonzalez Renteria[17a], R. Gonzalez Suarez[159], S. Gonzalez-Sevilla[56], G. R. Gonzalvo Rodriguez[161], R. Y. González Andana[52], L. Goossens[36], N. A. Gorasia[20], P. A. Gorbounov[37], B. Gorini[36], E. Gorini[69a,69b], A. Gorišek[92], A. T. Goshaw[51], M. I. Gostkin[38], C. A. Gottardo[112], M. Gouighri[35b], V. Goumarre[48], A. G. Goussiou[137], N. Govender[33c], C. Goy[4], I. Grabowska-Bold[84a], K. Graham[34], E. Gramstad[124], S. Grancagnolo[18], M. Grandi[145], V. Gratchev[37,*], P. M. Gravila[27f], F. G. Gravili[69a,69b], H. M. Gray[17a], M. Greco[69a,69b], C. Grefe[24], I. M. Gregor[48], P. Grenier[142], C. Grieco[13], A. A. Grillo[135], K. Grimm[31,m], S. Grinstein[13,t], J.-F. Grivaz[66], E. Gross[167], J. Grosse-Knetter[55], C. Grud[105], A. Grummer[111], J. C. Grundy[125], L. Guan[105], W. Guan[168], C. Gubbels[162], J. G. R. Guerrero Rojas[161], G. Guerrieri[68a,68c], F. Guescini[109], R. Gugel[99], J. A. M. Guhit[105], A. Guida[48], T. Guillemin[4], E. Guilloton[133,165], S. Guindon[36], F. Guo[14a,14d], J. Guo[62c], L. Guo[66], Y. Guo[105], R. Gupta[48], S. Gurbuz[24], G. Gustavino[36], M. Guth[56], P. Gutierrez[119], L. F. Gutierrez Zagazeta[127], C. Gutschow[95], C. Guyot[134], C. Gwenlan[125], C. B. Gwilliam[91], E. S. Haaland[124], A. Haas[116], M. Habedank[48], C. Haber[17a], H. K. Hadavand[8], A. Hadef[99], S. Hadzic[109], M. Haleem[164], J. Haley[120], J. J. Hall[138], G. D. Hallewell[101], L. Halser[19], K. Hamano[163], H. Hamdaoui[35e], M. Hamer[24], G. N. Hamity[52], J. Han[62b], K. Han[62a], L. Han[14c], L. Han[62a], S. Han[17a], Y. F. Han[154], K. Hanagaki[82], M. Hance[135], D. A. Hangal[41,y], M. D. Hank[39], R. Hankache[100], J. B. Hansen[42], J. D. Hansen[42], P. H. Hansen[42], K. Hara[156], D. Harada[56], T. Harenberg[169], S. Harkusha[37], Y. T. Harris[125], P. F. Harrison[165], N. M. Hartman[142], N. M. Hartmann[108], Y. Hasegawa[139], A. Hasib[52], S. Haug[19], R. Hauser[106], M. Havranek[131], C. M. Hawkes[20], R. J. Hawkings[36], S. Hayashida[110], D. Hayden[106], C. Hayes[105], R. L. Hayes[162], C. P. Hays[125], J. M. Hays[93], H. S. Hayward[91], F. He[62a], Y. He[153], Y. He[126], M. P. Heath[52], V. Hedberg[97], A. L. Heggelund[124], N. D. Hehir[93], C. Heidegger[54], K. K. Heidegger[54], W. D. Heidorn[80], J. Heilman[34], S. Heim[48], T. Heim[17a], J. G. Heinlein[127], J. J. Heinrich[122], L. Heinrich[36], J. Hejbal[130], L. Helary[48], A. Held[116], S. Hellesund[124], C. M. Helling[162], S. Hellman[47a,47b], C. Helsens[36], R. C. W. Henderson[90], L. Henkelmann[32], A. M. Henriques Correia[36], H. Herde[142], Y. Hernández Jiménez[144], H. Herr[99], M. G. Herrmann[108], T. Herrmann[50], G. Herten[54], R. Hertenberger[108], L. Hervas[36], N. P. Hessey[155a], H. Hibi[83], E. Higón-Rodriguez[161], S. J. Hillier[20], I. Hinchliffe[17a], F. Hinterkeuser[24], M. Hirose[123], S. Hirose[156], D. Hirschbuehl[169], B. Hiti[92], J. Hobbs[144], R. Hobincu[27e], N. Hod[167], M. C. Hodgkinson[138], B. H. Hodkinson[32], A. Hoecker[36], J. Hofer[48], D. Hohn[54], T. Holm[24], M. Holzbock[109], L. B. A. H. Hommels[32], B. P. Honan[100], J. Hong[62c], T. M. Hong[128], Y. Hong[55], J. C. Honig[54], A. Hönle[109], B. H. Hooberman[160], W. H. Hopkins[6], Y. Horii[110], S. Hou[147], J. Howarth[59], J. Hoya[89], M. Hrabovsky[121], A. Hrynevich[37], T. Hryn'ova[4], P. J. Hsu[65], S.-C. Hsu[137], Q. Hu[41,y], Y. F. Hu[14a,14d,ae], D. P. Huang[95], S. Huang[64b], X. Huang[14c], Y. Huang[62a], Y. Huang[14a], Z. Huang[100], Z. Hubacek[131], M. Huebner[24], F. Huegging[24], T. B. Huffman[125], M. Huhtinen[36], S. K. Huiberts[16], R. Hulsken[103], N. Huseynov[12,a], J. Huston[106], J. Huth[61], R. Hyneman[142], S. Hyrych[28a], G. Iacobucci[56], G. Iakovidis[29], I. Ibragimov[140], L. Iconomidou-Fayard[66], P. Iengo[71a,71b], R. Iguchi[152], T. Iizawa[56], Y. Ikegami[82], A. Ilg[19], N. Ilic[154], H. Imam[35a], T. Ingebretsen Carlson[47a,47b], G. Introzzi[72a,72b], M. Iodice[76a], V. Ippolito[74a,74b], M. Ishino[152], W. Islam[168], C. Issever[18,48], S. Istin[21a,ag], H. Ito[166], J. M. Iturbe Ponce[64a], R. Iuppa[77a,77b], A. Ivina[167], J. M. Izen[45], V. Izzo[71a], P. Jacka[130,131], P. Jackson[1], R. M. Jacobs[48], B. P. Jaeger[141], C. S. Jagfeld[108], G. Jäkel[169], K. Jakobs[54], T. Jakoubek[167], J. Jamieson[59], K. W. Janas[84a], G. Jarlskog[97], A. E. Jaspan[91], T. Javůrek[36], M. Javurkova[102], F. Jeanneau[134], L. Jeanty[122], J. Jejelava[148a,x], P. Jenni[54,f], C. E. Jessiman[34], S. Jézéquel[4], J. Jia[144], X. Jia[61], X. Jia[14a,14d], Z. Jia[14c], Y. Jiang[62a], S. Jiggins[52], J. Jimenez Pena[109], S. Jin[14c], A. Jinaru[27b], O. Jinnouchi[153], H. Jivan[33g], P. Johansson[138], K. A. Johns[7], C. A. Johnson[67], D. M. Jones[32], E. Jones[165], R. W. L. Jones[90], T. J. Jones[91], J. Jovicevic[15], X. Ju[17a], J. J. Junggeburth[36], A. Juste Rozas[13,t], S. Kabana[136e], A. Kaczmarska[85], M. Kado[74a,74b], H. Kagan[118], M. Kagan[142], A. Kahn[41], A. Kahn[127], C. Kahra[99], T. Kaji[166], E. Kajomovitz[149], N. Kakati[167], C. W. Kalderon[29], A. Kamenshchikov[154], N. J. Kang[135], Y. Kano[110], D. Kar[33g], K. Karava[125], M. J. Kareem[155b], E. Karentzos[54], I. Karkanias[151], S. N. Karpov[38], Z. M. Karpova[38], V. Kartvelishvili[90], A. N. Karyukhin[37], E. Kasimi[151], C. Kato[62d], J. Katzy[48], S. Kaur[34], K. Kawade[139], K. Kawagoe[88], T. Kawaguchi[110], T. Kawamoto[134], G. Kawamura[55], E. F. Kay[163], F. I. Kaya[157], S. Kazakos[13], V. F. Kazanin[37], Y. Ke[144], J. M. Keaveney[33a], R. Keeler[163], G. V. Kehris[61], J. S. Keller[34], A. S. Kelly[95], D. Kelsey[145], J. J. Kempster[20], J. Kendrick[20], K. E. Kennedy[41], O. Kepka[130], B. P. Kerridge[165], S. Kersten[169], B. P. Kerševan[92], L. Keszeghova[28a], S. Ketabchi Haghighat[154], M. Khandoga[126], A. Khanov[120], A. G. Kharlamov[37], T. Kharlamova[37], E. E. Khoda[137], T. J. Khoo[18], G. Khoriauli[164], J. Khubua[148b], Y. A. R. Khwaira[66], M. Kiehn[36], A. Kilgallon[122], E. Kim[153], Y. K. Kim[39],

N. Kimura[95], A. Kirchhoff[55], D. Kirchmeier[50], C. Kirfel[24], J. Kirk[133], A. E. Kiryunin[109], T. Kishimoto[152], D. P. Kisliuk[154], C. Kitsaki[10], O. Kivernyk[24], M. Klassen[63a], C. Klein[34], L. Klein[164], M. H. Klein[105], M. Klein[91], U. Klein[91], P. Klimek[36], A. Klimentov[29], F. Klimpel[109], T. Klingl[24], T. Klioutchnikova[36], F. F. Klitzner[108], P. Kluit[113], S. Kluth[109], E. Kneringer[78], T. M. Knight[154], A. Knue[54], D. Kobayashi[88], R. Kobayashi[86], M. Kocian[142], T. Kodama[152], P. Kodyš[132], D. M. Koeck[145], P. T. Koenig[24], T. Koffas[34], N. M. Köhler[36], M. Kolb[134], I. Koletsou[4], T. Komarek[121], K. Köneke[54], A. X. Y. Kong[1], T. Kono[117], N. Konstantinidis[95], B. Konya[97], R. Kopeliansky[67], S. Koperny[84a], K. Korcyl[85], K. Kordas[151], G. Koren[150], A. Korn[95], S. Korn[55], I. Korolkov[13], N. Korotkova[37], B. Kortman[113], O. Kortner[109], S. Kortner[109], W. H. Kostecka[114], V. V. Kostyukhin[140], A. Kotsokechagia[66], A. Kotwal[51], A. Koulouris[36], A. Kourkoumeli-Charalampidi[72a,72b], C. Kourkoumelis[9], E. Kourlitis[6], O. Kovanda[145], R. Kowalewski[163], W. Kozanecki[134], A. S. Kozhin[37], V. A. Kramarenko[37], G. Kramberger[92], P. Kramer[99], M. W. Krasny[126], A. Krasznahorkay[36], J. A. Kremer[99], J. Kretzschmar[91], K. Kreul[18], P. Krieger[154], F. Krieter[108], S. Krishnamurthy[102], A. Krishnan[63b], M. Krivos[132], K. Krizka[17a], K. Kroeninger[49], H. Kroha[109], J. Kroll[130], J. Kroll[127], K. S. Krowpman[106], U. Kruchonak[38], H. Krüger[24], N. Krumnack[80], M. C. Kruse[51], J. A. Krzysiak[85], A. Kubota[153], O. Kuchinskaia[37], S. Kuday[3a], D. Kuechler[48], J. T. Kuechler[48], S. Kuehn[36], T. Kuhl[48], V. Kukhtin[38], Y. Kulchitsky[37,a], S. Kuleshov[136b,136d], M. Kumar[33g], N. Kumari[101], M. Kuna[60], A. Kupco[130], T. Kupfer[49], A. Kupich[37], O. Kuprash[54], H. Kurashige[83], L. L. Kurchaninov[155a], Y. A. Kurochkin[37], A. Kurova[37], E. S. Kuwertz[36], M. Kuze[153], A. K. Kvam[102], J. Kvita[121], T. Kwan[103], K. W. Kwok[64a], C. Lacasta[161], F. Lacava[74a,74b], H. Lacker[18], D. Lacour[126], N. N. Lad[95], E. Ladygin[38], B. Laforge[126], T. Lagouri[136e], S. Lai[55], I. K. Lakomiec[84a], N. Lalloue[60], J. E. Lambert[119], S. Lammers[67], W. Lampl[7], C. Lampoudis[151], A. N. Lancaster[114], E. Lançon[29], U. Landgraf[54], M. P. J. Landon[93], V. S. Lang[54], R. J. Langenberg[102], A. J. Lankford[158], F. Lanni[29], K. Lantzsch[24], A. Lanza[72a], A. Lapertosa[57a,57b], J. F. Laporte[134], T. Lari[70a], F. Lasagni Manghi[23b], M. Lassnig[36], V. Latonova[130], T. S. Lau[64a], A. Laudrain[99], A. Laurier[34], S. D. Lawlor[94], Z. Lawrence[100], M. Lazzaroni[70a,70b], B. Le[100], B. Leban[92], A. Lebedev[80], M. LeBlanc[36], T. LeCompte[6], F. Ledroit-Guillon[60], A. C. A. Lee[95], G. R. Lee[16], L. Lee[61], S. C. Lee[147], S. Lee[47a,47b], L. L. Leeuw[33c], H. P. Lefebvre[94], M. Lefebvre[163], C. Leggett[17a], K. Lehmann[141], G. Lehmann Miotto[36], W. A. Leight[102], A. Leisos[151,s], M. A. L. Leite[81c], C. E. Leitgeb[48], R. Leitner[132], K. J. C. Leney[44], T. Lenz[24], S. Leone[73a], C. Leonidopoulos[52], A. Leopold[143], C. Leroy[107], R. Les[106], C. G. Lester[32], M. Levchenko[37], J. Levêque[4], D. Levin[105], L. J. Levinson[167], D. J. Lewis[20], B. Li[14b], B. Li[62b], C. Li[62a], C.-Q. Li[62c,62d], H. Li[62a], H. Li[62b], H. Li[14c], H. Li[62b], J. Li[62c], K. Li[137], L. Li[62c], M. Li[14a,14d], Q. Y. Li[62a], S. Li[62d,62c,d], T. Li[62b], X. Li[103], Z. Li[62b], Z. Li[125], Z. Li[103], Z. Li[91], Z. Liang[14a], M. Liberatore[48], B. Liberti[75a], K. Lie[64c], J. Lieber Marin[81b], K. Lin[106], R. A. Linck[67], R. E. Lindley[7], J. H. Lindon[2], A. Linss[48], E. Lipeles[127], A. Lipniacka[16], T. M. Liss[160,aa], A. Lister[162], J. D. Little[4], B. Liu[14a], B. X. Liu[141], D. Liu[62d,62c], J. B. Liu[62a], J. K. K. Liu[32], K. Liu[62d,62c], M. Liu[62a], M. Y. Liu[62a], P. Liu[14a], Q. Liu[62c,62d,137], X. Liu[62a], Y. Liu[48], Y. Liu[14c,14d], Y. L. Liu[105], Y. W. Liu[62a], M. Livan[72a,72b], J. Llorente Merino[141], S. L. Lloyd[93], E. M. Lobodzinska[48], P. Loch[7], S. Loffredo[75a,75b], T. Lohse[18], K. Lohwasser[138], M. Lokajicek[130], J. D. Long[160], I. Longarini[74a,74b], L. Longo[69a,69b], R. Longo[160], I. Lopez Paz[36], A. Lopez Solis[48], J. Lorenz[108], N. Lorenzo Martinez[4], A. M. Lory[108], A. Lösle[54], X. Lou[47a,47b], X. Lou[14a,14d], A. Lounis[66], J. Love[6], P. A. Love[90], J. J. Lozano Bahilo[161], G. Lu[14a,14d], M. Lu[79], S. Lu[127], Y. J. Lu[65], H. J. Lubatti[137], C. Luci[74a,74b], F. L. Lucio Alves[14c], A. Lucotte[60], F. Luehring[67], I. Luise[144], O. Lukianchuk[66], O. Lundberg[143], B. Lund-Jensen[143], N. A. Luongo[122], M. S. Lutz[150], D. Lynn[29], H. Lyons[91], R. Lysak[130], E. Lytken[97], F. Lyu[14a], V. Lyubushkin[38], T. Lyubushkina[38], H. Ma[29], L. L. Ma[62b], Y. Ma[95], D. M. Mac Donell[163], G. Maccarrone[53], J. C. MacDonald[138], R. Madar[40], W. F. Mader[50], J. Maeda[83], T. Maeno[29], M. Maerker[50], V. Magerl[54], J. Magro[68a,68c], H. Maguire[138], D. J. Mahon[41], C. Maidantchik[81b], A. Maio[129a,129b,129d], K. Maj[84a], O. Majersky[28a], S. Majewski[122], N. Makovec[66], V. Maksimovic[15], B. Malaescu[126], Pa. Malecki[85], V. P. Maleev[37], F. Malek[60], D. Malito[43a,43b], U. Mallik[79], C. Malone[32], S. Maltezos[10], S. Malyukov[38], J. Mamuzic[119], G. Mancini[53], J. P. Mandalia[93], I. Mandić[92], L. Manhaes de Andrade Filho[81a], I. M. Maniatis[151], M. Manisha[134], J. Manjarres Ramos[50], D. C. Mankad[167], K. H. Mankinen[97], A. Mann[108], A. Manousos[78], B. Mansoulie[134], S. Manzoni[36], A. Marantis[151], G. Marchiori[5], M. Marcisovsky[130], L. Marcoccia[75a,75b], C. Marcon[97], M. Marinescu[20], M. Marjanovic[119], Z. Marshall[17a], S. Marti-Garcia[161], T. A. Martin[165], V. J. Martin[52], B. Martin dit Latour[16], L. Martinelli[74a,74b], M. Martinez[13,t], P. Martinez Agullo[161], V. I. Martinez Outschoorn[102], P. Martinez Suarez[13],

S. Martin-Haugh[133], V. S. Martoiu[27b], A. C. Martyniuk[95], A. Marzin[36], S. R. Maschek[109], L. Masetti[99], T. Mashimo[152], J. Masik[100], A. L. Maslennikov[37], L. Massa[23b], P. Massarotti[71a,71b], P. Mastrandrea[73a,73b], A. Mastroberardino[43a,43b], T. Masubuchi[152], T. Mathisen[159], A. Matic[108], N. Matsuzawa[152], J. Maurer[27b], B. Maček[92], D. A. Maximov[37], R. Mazini[147], I. Maznas[151], M. Mazza[106], S. M. Mazza[135], C. Mc Ginn[29,af], J. P. Mc Gowan[103], S. P. Mc Kee[105], T. G. McCarthy[109], W. P. McCormack[17a], E. F. McDonald[104], A. E. McDougall[113], J. A. Mcfayden[145], G. Mchedlidze[148b], R. P. Mckenzie[33g], D. J. Mclaughlin[95], K. D. McLean[163], S. J. McMahon[133], P. C. McNamara[104], R. A. McPherson[163,v], J. E. Mdhluli[33g], S. Meehan[36], T. Megy[40], S. Mehlhase[108], A. Mehta[91], B. Meirose[45], D. Melini[149], B. R. Mellado Garcia[33g], A. H. Melo[55], F. Meloni[48], E. D. Mendes Gouveia[129a], A. M. Mendes Jacques Da Costa[20], H. Y. Meng[154], L. Meng[90], S. Menke[109], M. Mentink[36], E. Meoni[43a,43b], C. Merlassino[125], L. Merola[71a,71b], C. Meroni[70a], G. Merz[105], O. Meshkov[37], J. K. R. Meshreki[140], J. Metcalfe[6], A. S. Mete[6], C. Meyer[67], J.-P. Meyer[134], M. Michetti[18], R. P. Middleton[133], L. Mijović[52], G. Mikenberg[167], M. Mikestikova[130], M. Mikuž[92], H. Mildner[138], A. Milic[154], C. D. Milke[44], D. W. Miller[39], L. S. Miller[34], A. Milov[167], D. A. Milstead[47a,47b], T. Min[14c], A. A. Minaenko[37], I. A. Minashvili[148b], L. Mince[59], A. I. Mincer[116], B. Mindur[84a], M. Mineev[38], Y. Minegishi[152], Y. Mino[86], L. M. Mir[13], M. Miralles Lopez[161], M. Mironova[125], T. Mitani[166], A. Mitra[165], V. A. Mitsou[161], O. Miu[154], P. S. Miyagawa[93], Y. Miyazaki[88], A. Mizukami[82], J. U. Mjörnmark[97], T. Mkrtchyan[63a], M. Mlynarikova[114], T. Moa[47a,47b], S. Mobius[55], K. Mochizuki[107], P. Moder[48], P. Mogg[108], A. F. Mohammed[14a,14d], S. Mohapatra[41], G. Mokgatitswane[33g], B. Mondal[140], S. Mondal[131], K. Mönig[48], E. Monnier[101], L. Monsonis Romero[161], J. Montejo Berlingen[36], M. Montella[118], F. Monticelli[89], N. Morange[66], A. L. Moreira De Carvalho[129a], M. Moreno Llácer[161], C. Moreno Martinez[13], P. Morettini[57b], S. Morgenstern[165], M. Morii[61], M. Morinaga[152], V. Morisbak[124], A. K. Morley[36], F. Morodei[74a,74b], L. Morvaj[36], P. Moschovakos[36], B. Moser[36], M. Mosidze[148b], T. Moskalets[54], P. Moskvitina[112], J. Moss[31,n], E. J. W. Moyse[102], S. Muanza[101], J. Mueller[128], D. Muenstermann[90], R. Müller[19], G. A. Mullier[97], J. J. Mullin[127], D. P. Mungo[70a,70b], J. L. Munoz Martinez[13], F. J. Munoz Sanchez[100], M. Murin[100], W. J. Murray[133,165], A. Murrone[70a,70b], J. M. Muse[119], M. Muškinja[17a], C. Mwewa[29], A. G. Myagkov[37,a], A. J. Myers[8], A. A. Myers[128], G. Myers[67], M. Myska[131], B. P. Nachman[17a], O. Nackenhorst[49], A.Nag Nag[50], K. Nagai[125], K. Nagano[82], J. L. Nagle[29,af], E. Nagy[101], A. M. Nairz[36], Y. Nakahama[82], K. Nakamura[82], H. Nanjo[123], R. Narayan[44], E. A. Narayanan[111], I. Naryshkin[37], M. Naseri[34], C. Nass[24], G. Navarro[22a], J. Navarro-Gonzalez[161], R. Nayak[150], P. Y. Nechaeva[37], F. Nechansky[48], T. J. Neep[20], A. Negri[72a,72b], M. Negrini[23b], C. Nellist[112], C. Nelson[103], K. Nelson[105], S. Nemecek[130], M. Nessi[36,g], M. S. Neubauer[160], F. Neuhaus[99], J. Neundorf[48], R. Newhouse[162], P. R. Newman[20], C. W. Ng[128], Y. S. Ng[18], Y. W. Y. Ng[158], B. Ngair[35e], H. D. N. Nguyen[107], R. B. Nickerson[125], R. Nicolaidou[134], J. Nielsen[135], M. Niemeyer[55], N. Nikiforou[36], V. Nikolaenko[37,a], I. Nikolic-Audit[126], K. Nikolopoulos[20], P. Nilsson[29], H. R. Nindhito[56], A. Nisati[74a], N. Nishu[2], R. Nisius[109], J.-E. Nitschke[50], E. K. Nkadimeng[33g], S. J. Noacco Rosende[89], T. Nobe[152], D. L. Noel[32], Y. Noguchi[86], T. Nommensen[146], M. A. Nomura[29], M. B. Norfolk[138], R. R. B. Norisam[95], B. J. Norman[34], J. Novak[92], T. Novak[48], O. Novgorodova[50], L. Novotny[131], R. Novotny[111], L. Nozka[121], K. Ntekas[158], E. Nurse[95], F. G. Oakham[34,ac], J. Ocariz[126], A. Ochi[83], I. Ochoa[129a], S. Oda[88], S. Oerdek[159], A. Ogrodnik[84a], A. Oh[100], C. C. Ohm[143], H. Oide[153], R. Oishi[152], M. L. Ojeda[48], Y. Okazaki[86], M. W. O'Keefe[91], Y. Okumura[152], A. Olariu[27b], L. F. Oleiro Seabra[129a], S. A. Olivares Pino[136e], D. Oliveira Damazio[29], D. Oliveira Goncalves[81a], J. L. Oliver[158], M. J. R. Olsson[158], A. Olszewski[85], J. Olszowska[85,*], Ö. O. Öncel[54], D. C. O'Neil[141], A. P. O'Neill[19], A. Onofre[129a,129e], P. U. E. Onyisi[11], M. J. Oreglia[39], G. E. Orellana[89], D. Orestano[76a,76b], N. Orlando[13], R. S. Orr[154], V. O'Shea[59], R. Ospanov[62a], G. Otero y Garzon[30], H. Otono[88], P. S. Ott[63a], G. J. Ottino[17a], M. Ouchrif[35d], J. Ouellette[29,af], F. Ould-Saada[124], M. Owen[59], R. E. Owen[133], K. Y. Oyulmaz[21a], V. E. Ozcan[21a], N. Ozturk[8], S. Ozturk[21d], J. Pacalt[121], H. A. Pacey[32], K. Pachal[51], A. Pacheco Pages[13], C. Padilla Aranda[13], G. Padovano[74a,74b], S. Pagan Griso[17a], G. Palacino[67], A. Palazzo[69a,69b], S. Palazzo[52], S. Palestini[36], M. Palka[84b], J. Pan[170], D. K. Panchal[11], C. E. Pandini[113], J. G. Panduro Vazquez[94], P. Pani[48], G. Panizzo[68a,68c], L. Paolozzi[56], C. Papadatos[107], S. Parajuli[44], A. Paramonov[6], C. Paraskevopoulos[10], D. Paredes Hernandez[64b], T. H. Park[154], M. A. Parker[32], F. Parodi[57a,57b], E. W. Parrish[114], V. A. Parrish[52], J. A. Parsons[41], U. Parzefall[54], B. Pascual Dias[107], L. Pascual Dominguez[150], V. R. Pascuzzi[17a], F. Pasquali[113], E. Pasqualucci[74a], S. Passaggio[57b], F. Pastore[94], P. Pasuwan[47a,47b], J. R. Pater[100], J. Patton[91], T. Pauly[36], J. Pearkes[142], M. Pedersen[124], R. Pedro[129a], S. V. Peleganchuk[37], O. Penc[130], C. Peng[64b], H. Peng[62a], M. Penzin[37], B. S. Peralva[81a], A. P. Pereira Peixoto[60], L. Pereira Sanchez[47a,47b], D. V. Perepelitsa[29,af],

E. Perez Codina[155a], M. Perganti[10], L. Perini[70a,70b,*], H. Pernegger[36], S. Perrella[36], A. Perrevoort[112], O. Perrin[40], K. Peters[48], R. F. Y. Peters[100], B. A. Petersen[36], T. C. Petersen[42], E. Petit[101], V. Petousis[131], C. Petridou[151], A. Petrukhin[140], M. Pettee[17a], N. E. Pettersson[36], A. Petukhov[37], K. Petukhova[132], A. Peyaud[134], R. Pezoa[136f], L. Pezzotti[36], G. Pezzullo[170], T. Pham[104], P. W. Phillips[133], M. W. Phipps[160], G. Piacquadio[144], E. Pianori[17a], F. Piazza[70a,70b], R. Piegaia[30], D. Pietreanu[27b], A. D. Pilkington[100], M. Pinamonti[68a,68c], J. L. Pinfold[2], C. Pitman Donaldson[95], D. A. Pizzi[34], L. Pizzimento[75a,75b], A. Pizzini[113], M.-A. Pleier[29], V. Plesanovs[54], V. Pleskot[132], E. Plotnikova[38], G. Poddar[4], R. Poettgen[97], R. Poggi[56], L. Poggioli[126], I. Pogrebnyak[106], D. Pohl[24], I. Pokharel[55], S. Polacek[132], G. Polesello[72a], A. Poley[141,155a], R. Polifka[131], A. Polini[23b], C. S. Pollard[125], Z. B. Pollock[118], V. Polychronakos[29], D. Ponomarenko[37], L. Pontecorvo[36], S. Popa[27a], G. A. Popeneciu[27d], D. M. Portillo Quintero[155a], S. Pospisil[131], P. Postolache[27c], K. Potamianos[125], I. N. Potrap[38], C. J. Potter[32], H. Potti[1], T. Poulsen[48], J. Poveda[161], G. Pownall[48], M. E. Pozo Astigarraga[36], A. Prades Ibanez[161], M. M. Prapa[46], D. Price[100], M. Primavera[69a], M. A. Principe Martin[98], M. L. Proffitt[137], N. Proklova[37], K. Prokofiev[64c], G. Proto[75a,75b], S. Protopopescu[29], J. Proudfoot[6], M. Przybycien[84a], J. E. Puddefoot[138], D. Pudzha[37], P. Puzo[66], D. Pyatiizbyantseva[37], J. Qian[105], Y. Qin[100], T. Qiu[93], A. Quadt[55], M. Queitsch-Maitland[24], G. Rabanal Bolanos[61], D. Rafanoharana[54], F. Ragusa[70a,70b], J. L. Rainbolt[39], J. A. Raine[56], S. Rajagopalan[29], E. Ramakoti[37], K. Ran[14a,14d], V. Raskina[126], D. F. Rassloff[63a], S. Rave[99], B. Ravina[59], I. Ravinovich[167], M. Raymond[36], A. L. Read[124], N. P. Readioff[138], D. M. Rebuzzi[72a,72b], G. Redlinger[29], K. Reeves[45], J. A. Reidelsturz[169], D. Reikher[150], A. Reiss[99], A. Rej[140], C. Rembser[36], A. Renardi[48], M. Renda[27b], M. B. Rendel[109], A. G. Rennie[59], S. Resconi[70a], M. Ressegotti[57a,57b], E. D. Resseguie[17a], S. Rettie[95], B. Reynolds[118], E. Reynolds[17a], M. Rezaei Estabragh[169], O. L. Rezanova[37], P. Reznicek[132], E. Ricci[77a,77b], R. Richter[109], S. Richter[47a,47b], E. Richter-Was[84b], M. Ridel[126], P. Rieck[116], P. Riedler[36], M. Rijssenbeek[144], A. Rimoldi[72a,72b], M. Rimoldi[48], L. Rinaldi[23a,23b], T. T. Rinn[29], M. P. Rinnagel[108], G. Ripellino[143], I. Riu[13], P. Rivadeneira[48], J. C. Rivera Vergara[163], F. Rizatdinova[120], E. Rizvi[93], C. Rizzi[56], B. A. Roberts[165], B. R. Roberts[17a], S. H. Robertson[103,v], M. Robin[48], D. Robinson[32], C. M. Robles Gajardo[136f], M. Robles Manzano[99], A. Robson[59], A. Rocchi[75a,75b], C. Roda[73a,73b], S. Rodriguez Bosca[63a], Y. Rodriguez Garcia[22a], A. Rodriguez Rodriguez[54], A. M. Rodríguez Vera[155b], S. Roe[36], J. T. Roemer[158], A. R. Roepe-Gier[119], J. Roggel[169], O. Røhne[124], R. A. Rojas[163], B. Roland[54], C. P. A. Roland[67], J. Roloff[29], A. Romaniouk[37], M. Romano[23b], A. C. Romero Hernandez[160], N. Rompotis[91], L. Roos[126], S. Rosati[74a], B. J. Rosser[39], E. Rossi[4], E. Rossi[71a,71b], L. P. Rossi[57b], L. Rossini[48], R. Rosten[118], M. Rotaru[27b], B. Rottler[54], D. Rousseau[66], D. Rousso[32], G. Rovelli[72a,72b], A. Roy[160], A. Rozanov[101], Y. Rozen[149], X. Ruan[33g], A. Rubio Jimenez[161], A. J. Ruby[91], T. A. Ruggeri[1], F. Rühr[54], A. Ruiz-Martinez[161], A. Rummler[36], Z. Rurikova[54], N. A. Rusakovich[38], H. L. Russell[163], J. P. Rutherfoord[7], E. M. Rüttinger[138], K. Rybacki[90], M. Rybar[132], E. B. Rye[124], A. Ryzhov[37], J. A. Sabater Iglesias[56], P. Sabatini[161], L. Sabetta[74a,74b], H.F.-W. Sadrozinski[135], F. Safai Tehrani[74a], B. Safarzadeh Samani[145], M. Safdari[142], S. Saha[103], M. Sahinsoy[109], M. Saimpert[134], M. Saito[152], T. Saito[152], D. Salamani[36], G. Salamanna[76a,76b], A. Salnikov[142], J. Salt[161], A. Salvador Salas[13], D. Salvatore[43a,43b], F. Salvatore[145], A. Salzburger[36], D. Sammel[54], D. Sampsonidis[151], D. Sampsonidou[62d,62c], J. Sánchez[161], A. Sanchez Pineda[4], V. Sanchez Sebastian[161], H. Sandaker[124], C. O. Sander[48], J. A. Sandesara[102], M. Sandhoff[169], C. Sandoval[22b], D. P. C. Sankey[133], A. Sansoni[53], C. Santoni[40], H. Santos[129a,129b], S. N. Santpur[17a], A. Santra[167], K. A. Saoucha[138], J. G. Saraiva[129a,129d], J. Sardain[101], O. Sasaki[82], K. Sato[156], C. Sauer[63b], F. Sauerburger[54], E. Sauvan[4], P. Savard[154,ac], R. Sawada[152], C. Sawyer[133], L. Sawyer[96], I. Sayago Galvan[161], C. Sbarra[23b], A. Sbrizzi[23a,23b], T. Scanlon[95], J. Schaarschmidt[137], P. Schacht[109], D. Schaefer[39], U. Schäfer[99], A. C. Schaffer[66], D. Schaile[108], R. D. Schamberger[144], E. Schanet[108], C. Scharf[18], V. A. Schegelsky[37], D. Scheirich[132], F. Schenck[18], M. Schernau[158], C. Scheulen[55], C. Schiavi[57a,57b], Z. M. Schillaci[26], E. J. Schioppa[69a,69b], M. Schioppa[43a,43b], B. Schlag[99], K. E. Schleicher[54], S. Schlenker[36], K. Schmieden[99], C. Schmitt[99], S. Schmitt[48], L. Schoeffel[134], A. Schoening[63b], P. G. Scholer[54], E. Schopf[125], M. Schott[99], J. Schovancova[36], S. Schramm[56], F. Schroeder[169], H.-C. Schultz-Coulon[63a], M. Schumacher[54], B. A. Schumm[135], Ph. Schune[134], A. Schwartzman[142], T. A. Schwarz[105], Ph. Schwemling[134], R. Schwienhorst[106], A. Sciandra[135], G. Sciolla[26], F. Scuri[73a], F. Scutti[104], C. D. Sebastiani[91], K. Sedlaczek[49], P. Seema[18], S. C. Seidel[111], A. Seiden[135], B. D. Seidlitz[41], T. Seiss[39], C. Seitz[48], J. M. Seixas[81b], G. Sekhniaidze[71a], S. J. Sekula[44], L. Selem[4], N. Semprini-Cesari[23a,23b], S. Sen[51], V. Senthilkumar[161], L. Serin[66], L. Serkin[68a,68b], M. Sessa[76a,76b], H. Severini[119], S. Sevova[142], F. Sforza[57a,57b], A. Sfyrla[56], E. Shabalina[55], R. Shaheen[143],

J. D. Shahinian[127], N. W. Shaikh[47a,47b], D. Shaked Renous[167], L. Y. Shan[14a], M. Shapiro[17a], A. Sharma[36], A. S. Sharma[162], P. Sharma[79], S. Sharma[48], P. B. Shatalov[37], K. Shaw[145], S. M. Shaw[100], Q. Shen[62c], P. Sherwood[95], L. Shi[95], C. O. Shimmin[170], Y. Shimogama[166], J. D. Shinner[94], I. P. J. Shipsey[125], S. Shirabe[60], M. Shiyakova[38], J. Shlomi[167], M. J. Shochet[39], J. Shojaii[104], D. R. Shope[143], S. Shrestha[118], E. M. Shrif[33g], M. J. Shroff[163], P. Sicho[130], A. M. Sickles[160], E. Sideras Haddad[33g], O. Sidiropoulou[36], A. Sidoti[23b], F. Siegert[50], Dj. Sijacki[15], R. Sikora[84a], F. Sili[89], J. M. Silva[20], M. V. Silva Oliveira[36], S. B. Silverstein[47a], S. Simion[66], R. Simoniello[36], E. L. Simpson[59], N. D. Simpson[97], S. Simsek[21d], S. Sindhu[55], P. Sinervo[154], V. Sinetckii[37], S. Singh[141], S. Singh[154], S. Sinha[48], S. Sinha[33g], M. Sioli[23a,23b], I. Siral[122], S.Yu. Sivoklokov[37,*], J. Sjölin[47a,47b], A. Skaf[55], E. Skorda[97], P. Skubic[119], M. Slawinska[85], V. Smakhtin[167], B. H. Smart[133], J. Smiesko[132], S.Yu. Smirnov[37], Y. Smirnov[37], L. N. Smirnova[37,a], O. Smirnova[97], E. A. Smith[39], H. A. Smith[125], J. L. Smith[91], R. Smith[142], M. Smizanska[90], K. Smolek[131], A. Smykiewicz[85], A. A. Snesarev[37], H. L. Snoek[113], S. Snyder[29], R. Sobie[163,v], A. Soffer[150], C. A. Solans Sanchez[36], E.Yu. Soldatov[37], U. Soldevila[161], A. A. Solodkov[37], S. Solomon[54], A. Soloshenko[38], K. Solovieva[54], O. V. Solovyanov[37], V. Solovyev[37], P. Sommer[36], A. Sonay[13], W. Y. Song[155b], A. Sopczak[131], A. L. Sopio[95], F. Sopkova[28b], V. Sothilingam[63a], S. Sottocornola[72a,72b], R. Soualah[115c], Z. Soumaimi[35e], D. South[48], S. Spagnolo[69a,69b], M. Spalla[109], F. Spanò[94], D. Sperlich[54], G. Spigo[36], M. Spina[145], S. Spinali[90], D. P. Spiteri[59], M. Spousta[132], E. J. Staats[34], A. Stabile[70a,70b], R. Stamen[63a], M. Stamenkovic[113], A. Stampekis[20], M. Standke[24], E. Stanecka[85], B. Stanislaus[17a], M. M. Stanitzki[48], M. Stankaityte[125], B. Stapf[48], E. A. Starchenko[37], G. H. Stark[135], J. Stark[101], D. M. Starko[155b], P. Staroba[130], P. Starovoitov[63a], S. Stärz[103], R. Staszewski[85], G. Stavropoulos[46], J. Steentoft[159], P. Steinberg[29], A. L. Steinhebel[122], B. Stelzer[141,155a], H. J. Stelzer[128], O. Stelzer-Chilton[155a], H. Stenzel[58], T. J. Stevenson[145], G. A. Stewart[36], M. C. Stockton[36], G. Stoicea[27b], M. Stolarski[129a], S. Stonjek[109], A. Straessner[50], J. Strandberg[143], S. Strandberg[47a,47b], M. Strauss[119], T. Strebler[101], P. Strizenec[28b], R. Ströhmer[164], D. M. Strom[122], L. R. Strom[48], R. Stroynowski[44], A. Strubig[47a,47b], S. A. Stucci[29], B. Stugu[16], J. Stupak[119], N. A. Styles[48], D. Su[142], S. Su[62a], W. Su[62c,62d,137], X. Su[62a,66], K. Sugizaki[152], V. V. Sulin[37], M. J. Sullivan[91], D. M. S. Sultan[77a,77b], L. Sultanaliyeva[37], S. Sultansoy[3b], T. Sumida[86], S. Sun[105], S. Sun[168], O. Sunneborn Gudnadottir[159], M. R. Sutton[145], M. Svatos[130], M. Swiatlowski[155a], T. Swirski[164], I. Sykora[28a], M. Sykora[132], T. Sykora[132], D. Ta[99], K. Tackmann[48,u], A. Taffard[158], R. Tafirout[155a], J. S. Tafoya Vargas[66], R. H. M. Taibah[126], R. Takashima[87], K. Takeda[83], E. P. Takeva[52], Y. Takubo[82], M. Talby[101], A. A. Talyshev[37], K. C. Tam[64b], N. M. Tamir[150], A. Tanaka[152], J. Tanaka[152], R. Tanaka[66], M. Tanasini[57a,57b], J. Tang[62c], Z. Tao[162], S. Tapia Araya[80], S. Tapprogge[99], A. Tarek Abouelfadl Mohamed[106], S. Tarem[149], K. Tariq[62b], G. Tarna[27b], G. F. Tartarelli[70a], P. Tas[132], M. Tasevsky[130], E. Tassi[43a,43b], A. C. Tate[160], G. Tateno[152], Y. Tayalati[35e], G. N. Taylor[104], W. Taylor[155b], H. Teagle[91], A. S. Tee[168], R. Teixeira De Lima[142], P. Teixeira-Dias[94], J. J. Teoh[154], K. Terashi[152], J. Terron[98], S. Terzo[13], M. Testa[53], R. J. Teuscher[154,v], N. Themistokleous[52], T. Theveneaux-Pelzer[18], O. Thielmann[169], D. W. Thomas[94], J. P. Thomas[20], E. A. Thompson[48], P. D. Thompson[20], E. Thomson[127], E. J. Thorpe[93], Y. Tian[55], V. Tikhomirov[37,a], Yu.A. Tikhonov[37], S. Timoshenko[37], E. X. L. Ting[1], P. Tipton[170], S. Tisserant[101], S. H. Tlou[33g], A. Tnourji[40], K. Todome[23a,23b], S. Todorova-Nova[132], S. Todt[50], M. Togawa[82], J. Tojo[88], S. Tokár[28a], K. Tokushuku[82], R. Tombs[32], M. Tomoto[82,110], L. Tompkins[142], P. Tornambe[102], E. Torrence[122], H. Torres[50], E. Torró Pastor[161], M. Toscani[30], C. Tosciri[39], D. R. Tovey[138], A. Traeet[16], I. S. Trandafir[27b], T. Trefzger[164], A. Tricoli[29], I. M. Trigger[155a], S. Trincaz-Duvoid[126], D. A. Trischuk[162], B. Trocmé[60], A. Trofymov[66], C. Troncon[70a], L. Truong[33c], M. Trzebinski[85], A. Trzupek[85], F. Tsai[144], M. Tsai[105], A. Tsiamis[151], P. V. Tsiareshka[37], S. Tsigaridas[155a], A. Tsirigotis[151,s], V. Tsiskaridze[144], E. G. Tskhadadze[148a], M. Tsopoulou[151], Y. Tsujikawa[86], I. I. Tsukerman[37], V. Tsulaia[17a], S. Tsuno[82], O. Tsur[149], D. Tsybychev[144], Y. Tu[64b], A. Tudorache[27b], V. Tudorache[27b], A. N. Tuna[36], S. Turchikhin[38], I. Turk Cakir[3a], R. Turra[70a], P. M. Tuts[41], S. Tzamarias[151], P. Tzanis[10], E. Tzovara[99], K. Uchida[152], F. Ukegawa[156], P. A. Ulloa Poblete[136c], G. Unal[36], M. Unal[11], A. Undrus[29], G. Unel[158], K. Uno[152], J. Urban[28b], P. Urquijo[104], G. Usai[8], R. Ushioda[153], M. Usman[107], Z. Uysal[21b], V. Vacek[131], B. Vachon[103], K. O. H. Vadla[124], T. Vafeiadis[36], C. Valderanis[108], E. Valdes Santurio[47a,47b], M. Valente[155a], S. Valentinetti[23a,23b], A. Valero[161], A. Vallier[101], J. A. Valls Ferrer[161], T. R. Van Daalen[137], P. Van Gemmeren[6], S. Van Stroud[95], I. Van Vulpen[113], M. Vanadia[75a,75b], W. Vandelli[36], M. Vandenbroucke[134], E. R. Vandewall[120], D. Vannicola[150], L. Vannoli[57a,57b], R. Vari[74a], E. W. Varnes[7], C. Varni[17a], T. Varol[147], D. Varouchas[66], L. Varriale[161], K. E. Varvell[146], M. E. Vasile[27b], L. Vaslin[40],

G. A. Vasquez[163], F. Vazeille[40], T. Vazquez Schroeder[36], J. Veatch[31], V. Vecchio[100], M. J. Veen[113], I. Veliscek[125], L. M. Veloce[154], F. Veloso[129a,129c], S. Veneziano[74a], A. Ventura[69a,69b], A. Verbytskyi[109], M. Verducci[73a,73b], C. Vergis[24], M. Verissimo De Araujo[81b], W. Verkerke[113], J. C. Vermeulen[113], C. Vernieri[142], P. J. Verschuuren[94], M. Vessella[102], M. L. Vesterbacka[116], M. C. Vetterli[141,ac], A. Vgenopoulos[151], N. Viaux Maira[136f], T. Vickey[138], O. E. Vickey Boeriu[138], G. H. A. Viehhauser[125], L. Vigani[63b], M. Villa[23a,23b], M. Villaplana Perez[161], E. M. Villhauer[52], E. Vilucchi[53], M. G. Vincter[34], G. S. Virdee[20], A. Vishwakarma[52], C. Vittori[23a,23b], I. Vivarelli[145], V. Vladimirov[165], E. Voevodina[109], F. Vogel[108], P. Vokac[131], J. Von Ahnen[48], E. Von Toerne[24], B. Vormwald[36], V. Vorobel[132], K. Vorobev[37], M. Vos[161], J. H. Vossebeld[91], M. Vozak[113], L. Vozdecky[93], N. Vranjes[15], M. Vranjes Milosavljevic[15], M. Vreeswijk[113], R. Vuillermet[36], O. Vujinovic[99], I. Vukotic[39], S. Wada[156], C. Wagner[102], W. Wagner[169], S. Wahdan[169], H. Wahlberg[89], R. Wakasa[156], M. Wakida[110], V. M. Walbrecht[109], J. Walder[133], R. Walker[108], W. Walkowiak[140], A. M. Wang[61], A. Z. Wang[168], C. Wang[62a], C. Wang[62c], H. Wang[17a], J. Wang[64a], P. Wang[44], R.-J. Wang[99], R. Wang[61], R. Wang[6], S. M. Wang[147], S. Wang[62b], T. Wang[62a], W. T. Wang[79], W. X. Wang[62a], X. Wang[14c], X. Wang[160], X. Wang[62c], Y. Wang[62d], Y. Wang[14c], Z. Wang[105], Z. Wang[62c,62d,51], Z. Wang[105], A. Warburton[103], R. J. Ward[20], N. Warrack[59], A. T. Watson[20], M. F. Watson[20], G. Watts[137], B. M. Waugh[95], A. F. Webb[11], C. Weber[29], M. S. Weber[19], S. A. Weber[34], S. M. Weber[63a], C. Wei[62a], Y. Wei[125], A. R. Weidberg[125], J. Weingarten[49], M. Weirich[99], C. Weiser[54], C. J. Wells[48], T. Wenaus[29], B. Wendland[49], T. Wengler[36], N. S. Wenke[109], N. Wermes[24], M. Wessels[63a], K. Whalen[122], A. M. Wharton[90], A. S. White[61], A. White[8], M. J. White[1], D. Whiteson[158], L. Wickremasinghe[123], W. Wiedenmann[168], C. Wiel[50], M. Wielers[133], N. Wieseotte[99], C. Wiglesworth[42], L. A. M. Wiik-Fuchs[54], D. J. Wilbern[119], H. G. Wilkens[36], D. M. Williams[41], H. H. Williams[127], S. Williams[32], S. Willocq[102], P. J. Windischhofer[125], F. Winklmeier[122], B. T. Winter[54], M. Wittgen[142], M. Wobisch[96], A. Wolf[99], R. Wölker[125], J. Wollrath[158], M. W. Wolter[85], H. Wolters[129a,129c], V. W. S. Wong[162], A. F. Wongel[48], S. D. Worm[48], B. K. Wosiek[85], K. W. Woźniak[85], K. Wraight[59], J. Wu[14a,14d], M. Wu[64a], S. L. Wu[168], X. Wu[56], Y. Wu[62a], Z. Wu[134,62a], J. Wuerzinger[125], T. R. Wyatt[100], B. M. Wynne[52], S. Xella[42], L. Xia[14c], M. Xia[14b], J. Xiang[64c], X. Xiao[105], M. Xie[62a], X. Xie[62a], J. Xiong[17a], I. Xiotidis[145], D. Xu[14a], H. Xu[62a], H. Xu[62a], L. Xu[62a], R. Xu[127], T. Xu[105], W. Xu[105], Y. Xu[14b], Z. Xu[62b], Z. Xu[142], B. Yabsley[146], S. Yacoob[33a], N. Yamaguchi[88], Y. Yamaguchi[153], H. Yamauchi[156], T. Yamazaki[17a], Y. Yamazaki[83], J. Yan[62c], S. Yan[125], Z. Yan[25], H. J. Yang[62c,62d], H. T. Yang[17a], S. Yang[62a], T. Yang[64c], X. Yang[62a], X. Yang[14a], Y. Yang[44], Z. Yang[62a,105], W.-M. Yao[17a], Y. C. Yap[48], H. Ye[14c], J. Ye[44], S. Ye[29], X. Ye[62a], I. Yeletskikh[38], M. R. Yexley[90], P. Yin[41], K. Yorita[166], C. J. S. Young[54], C. Young[142], M. Yuan[105], R. Yuan[62b,j], X. Yue[63a], M. Zaazoua[35e], B. Zabinski[85], E. Zaid[52], T. Zakareishvili[148b], N. Zakharchuk[34], S. Zambito[56], J. Zang[152], D. Zanzi[54], O. Zaplatilek[131], S. V. Zeißner[49], C. Zeitnitz[169], J. C. Zeng[160], D. T. Zenger Jr[26], O. Zenin[37], T. Ženiš[28a], S. Zenz[93], S. Zerradi[35a], D. Zerwas[66], B. Zhang[14c], D. F. Zhang[138], G. Zhang[14b], J. Zhang[6], K. Zhang[14a,14d], L. Zhang[14c], R. Zhang[168], S. Zhang[105], T. Zhang[152], X. Zhang[62c], X. Zhang[62b], Z. Zhang[66], H. Zhao[137], P. Zhao[51], T. Zhao[62b], Y. Zhao[135], Z. Zhao[62a], A. Zhemchugov[38], Z. Zheng[142], D. Zhong[160], B. Zhou[105], C. Zhou[168], H. Zhou[7], N. Zhou[62c], Y. Zhou[7], C. G. Zhu[62b], C. Zhu[14a,14d], H. L. Zhu[62a], H. Zhu[14a], J. Zhu[105], Y. Zhu[62a], X. Zhuang[14a], K. Zhukov[37], V. Zhulanov[37], N. I. Zimine[38], J. Zinsser[63b], M. Ziolkowski[140], L. Živković[15], A. Zoccoli[23a,23b], K. Zoch[56], T. G. Zorbas[138], O. Zormpa[46], W. Zou[41], L. Zwalinski[36]

[1] Department of Physics, University of Adelaide, Adelaide, Australia
[2] Department of Physics, University of Alberta, Edmonton, AB, Canada
[3] [(a)]Department of Physics, Ankara University, Ankara, Türkiye; [(b)]Division of Physics, TOBB University of Economics and Technology, Ankara, Türkiye
[4] LAPP, Univ. Savoie Mont Blanc, CNRS/IN2P3, Annecy, France
[5] APC, Université Paris Cité, CNRS/IN2P3, Paris, France
[6] High Energy Physics Division, Argonne National Laboratory, Argonne, IL, USA
[7] Department of Physics, University of Arizona, Tucson, AZ, USA
[8] Department of Physics, University of Texas at Arlington, Arlington, TX, USA
[9] Physics Department, National and Kapodistrian University of Athens, Athens, Greece
[10] Physics Department, National Technical University of Athens, Zografou, Greece
[11] Department of Physics, University of Texas at Austin, Austin, TX, USA

[12] Institute of Physics, Azerbaijan Academy of Sciences, Baku, Azerbaijan
[13] Institut de Física d'Altes Energies (IFAE), Barcelona Institute of Science and Technology, Barcelona, Spain
[14] [(a)]Institute of High Energy Physics, Chinese Academy of Sciences, Beijing, China; [(b)]Physics Department, Tsinghua University, Beijing, China; [(c)]Department of Physics, Nanjing University, Nanjing, China; [(d)]University of Chinese Academy of Science (UCAS), Beijing, China
[15] Institute of Physics, University of Belgrade, Belgrade, Serbia
[16] Department for Physics and Technology, University of Bergen, Bergen, Norway
[17] [(a)]Physics Division, Lawrence Berkeley National Laboratory, Berkeley, CA, USA; [(b)]University of California, Berkeley, CA, USA
[18] Institut für Physik, Humboldt Universität zu Berlin, Berlin, Germany
[19] Albert Einstein Center for Fundamental Physics and Laboratory for High Energy Physics, University of Bern, Bern, Switzerland
[20] School of Physics and Astronomy, University of Birmingham, Birmingham, UK
[21] [(a)]Department of Physics, Bogazici University, Istanbul, Türkiye; [(b)]Department of Physics Engineering, Gaziantep University, Gaziantep, Türkiye; [(c)]Department of Physics, Istanbul University, Istanbul, Türkiye; [(d)]Istinye University, Sariyer, Istanbul, Türkiye
[22] [(a)]Facultad de Ciencias y Centro de Investigaciónes, Universidad Antonio Nariño, Bogotá, Colombia; [(b)]Departamento de Física, Universidad Nacional de Colombia, Bogotá, Colombia
[23] [(a)]Dipartimento di Fisica e Astronomia A. Righi, Università di Bologna, Bologna, Italy; [(b)]INFN Sezione di Bologna, Bologna, Italy
[24] Physikalisches Institut, Universität Bonn, Bonn, Germany
[25] Department of Physics, Boston University, Boston, MA, USA
[26] Department of Physics, Brandeis University, Waltham, MA, USA
[27] [(a)]Transilvania University of Brasov, Brasov, Romania; [(b)]Horia Hulubei National Institute of Physics and Nuclear Engineering, Bucharest, Romania; [(c)]Department of Physics, Alexandru Ioan Cuza University of Iasi, Iasi, Romania; [(d)]Physics Department, National Institute for Research and Development of Isotopic and Molecular Technologies, Cluj-Napoca, Romania; [(e)]University Politehnica Bucharest, Bucharest, Romania; [(f)]West University in Timisoara, Timisoara, Romania
[28] [(a)]Faculty of Mathematics, Physics and Informatics, Comenius University, Bratislava, Slovak Republic; [(b)]Department of Subnuclear Physics, Institute of Experimental Physics of the Slovak Academy of Sciences, Kosice, Slovak Republic
[29] Physics Department, Brookhaven National Laboratory, Upton, NY, USA
[30] Departamento de Física, y CONICET, Facultad de Ciencias Exactas y Naturales, Instituto de Física de Buenos Aires (IFIBA), Universidad de Buenos Aires, Buenos Aires, Argentina
[31] California State University, CA, USA
[32] Cavendish Laboratory, University of Cambridge, Cambridge, UK
[33] [(a)]Department of Physics, University of Cape Town, Cape Town, South Africa; [(b)]iThemba Labs, Western Cape, South Africa; [(c)]Department of Mechanical Engineering Science, University of Johannesburg, Johannesburg, South Africa; [(d)]National Institute of Physics, University of the Philippines, Diliman, Philippines; [(e)]Department of Physics, University of South Africa, Pretoria, South Africa; [(f)]University of Zululand, KwaDlangezwa, South Africa; [(g)]School of Physics, University of the Witwatersrand, Johannesburg, South Africa
[34] Department of Physics, Carleton University, Ottawa, ON, Canada
[35] [(a)]Faculté des Sciences Ain Chock, Réseau Universitaire de Physique des Hautes Energies, Université Hassan II, Casablanca, Morocco; [(b)]Faculté des Sciences, Université Ibn-Tofail, Kénitra, Morocco; [(c)]Faculté des Sciences Semlalia, Université Cadi Ayyad, LPHEA-Marrakech, Morocco; [(d)]LPMR, Faculté des Sciences, Université Mohamed Premier, Oujda, Morocco; [(e)]Faculté des sciences, Université Mohammed V, Rabat, Morocco; [(f)]Institute of Applied Physics, Mohammed VI Polytechnic University, Ben Guerir, Morocco
[36] CERN, Geneva, Switzerland
[37] Affiliated with an institute covered by a cooperation agreement with CERN, Geneva, Switzerland
[38] Affiliated with an international laboratory covered by a cooperation agreement with CERN, Geneva, Switzerland
[39] Enrico Fermi Institute, University of Chicago, Chicago, IL, USA
[40] LPC, Université Clermont Auvergne, CNRS/IN2P3, Clermont-Ferrand, France
[41] Nevis Laboratory, Columbia University, Irvington, NY, USA
[42] Niels Bohr Institute, University of Copenhagen, Copenhagen, Denmark

[43] [(a)]Dipartimento di Fisica, Università della Calabria, Rende, Italy; [(b)]INFN Gruppo Collegato di Cosenza, Laboratori Nazionali di Frascati, Frascati, Italy
[44] Physics Department, Southern Methodist University, Dallas, TX, USA
[45] Physics Department, University of Texas at Dallas, Richardson, TX, USA
[46] National Centre for Scientific Research "Demokritos", Agia Paraskevi, Greece
[47] [(a)]Department of Physics, Stockholm University, Stockholm, Sweden; [(b)]Oskar Klein Centre, Stockholm, Sweden
[48] Deutsches Elektronen-Synchrotron DESY, Hamburg and Zeuthen, Germany
[49] Fakultät Physik , Technische Universität Dortmund, Dortmund, Germany
[50] Institut für Kern- und Teilchenphysik, Technische Universität Dresden, Dresden, Germany
[51] Department of Physics, Duke University, Durham, NC, USA
[52] SUPA-School of Physics and Astronomy, University of Edinburgh, Edinburgh, UK
[53] INFN e Laboratori Nazionali di Frascati, Frascati, Italy
[54] Physikalisches Institut, Albert-Ludwigs-Universität Freiburg, Freiburg, Germany
[55] II. Physikalisches Institut, Georg-August-Universität Göttingen, Göttingen, Germany
[56] Département de Physique Nucléaire et Corpusculaire, Université de Genève, Geneva, Switzerland
[57] [(a)]Dipartimento di Fisica, Università di Genova, Genoa, Italy; [(b)]INFN Sezione di Genova, Genoa, Italy
[58] II. Physikalisches Institut, Justus-Liebig-Universität Giessen, Giessen, Germany
[59] SUPA-School of Physics and Astronomy, University of Glasgow, Glasgow, UK
[60] LPSC, Université Grenoble Alpes, CNRS/IN2P3, Grenoble INP, Grenoble, France
[61] Laboratory for Particle Physics and Cosmology, Harvard University, Cambridge, MA, USA
[62] [(a)]Department of Modern Physics and State Key Laboratory of Particle Detection and Electronics, University of Science and Technology of China, Hefei, China; [(b)]Institute of Frontier and Interdisciplinary Science and Key Laboratory of Particle Physics and Particle Irradiation (MOE), Shandong University, Qingdao, China; [(c)]School of Physics and Astronomy, Shanghai Jiao Tong University, Key Laboratory for Particle Astrophysics and Cosmology (MOE), SKLPPC, Shanghai, China; [(d)]Tsung-Dao Lee Institute, Shanghai, China
[63] [(a)]Kirchhoff-Institut für Physik, Ruprecht-Karls-Universität Heidelberg, Heidelberg, Germany; [(b)]Physikalisches Institut, Ruprecht-Karls-Universität Heidelberg, Heidelberg, Germany
[64] [(a)]Department of Physics, Chinese University of Hong Kong, Shatin, N.T., Hong Kong; [(b)]Department of Physics, University of Hong Kong, Pok Fu Lam, Hong Kong; [(c)]Department of Physics and Institute for Advanced Study, Hong Kong University of Science and Technology, Clear Water Bay, Kowloon, Hong Kong, China
[65] Department of Physics, National Tsing Hua University, Hsinchu, Taiwan
[66] IJCLab, Université Paris-Saclay, CNRS/IN2P3, 91405 Orsay, France
[67] Department of Physics, Indiana University, Bloomington, IN, USA
[68] [(a)]INFN Gruppo Collegato di Udine, Sezione di Trieste, Udine, Italy; [(b)]ICTP, Trieste, Italy; [(c)]Dipartimento Politecnico di Ingegneria e Architettura, Università di Udine, Udine, Italy
[69] [(a)]INFN Sezione di Lecce, Lecce, Italy; [(b)]Dipartimento di Matematica e Fisica, Università del Salento, Lecce, Italy
[70] [(a)]INFN Sezione di Milano, Milan, Italy; [(b)]Dipartimento di Fisica, Università di Milano, Milan, Italy
[71] [(a)]INFN Sezione di Napoli, Naples, Italy; [(b)]Dipartimento di Fisica, Università di Napoli, Naples, Italy
[72] [(a)]INFN Sezione di Pavia, Pavia, Italy; [(b)]Dipartimento di Fisica, Università di Pavia, Pavia, Italy
[73] [(a)]INFN Sezione di Pisa, Pisa, Italy; [(b)]Dipartimento di Fisica E. Fermi, Università di Pisa, Pisa, Italy
[74] [(a)]INFN Sezione di Roma, Rome, Italy; [(b)]Dipartimento di Fisica, Sapienza Università di Roma, Rome, Italy
[75] [(a)]INFN Sezione di Roma Tor Vergata, Rome, Italy; [(b)]Dipartimento di Fisica, Università di Roma Tor Vergata, Rome, Italy
[76] [(a)]INFN Sezione di Roma Tre, Rome, Italy; [(b)]Dipartimento di Matematica e Fisica, Università Roma Tre, Rome, Italy
[77] [(a)]INFN-TIFPA, Povo, Italy; [(b)]Università degli Studi di Trento, Trento, Italy
[78] Department of Astro and Particle Physics, Universität Innsbruck, Innsbruck, Austria
[79] University of Iowa, Iowa City, IA, USA
[80] Department of Physics and Astronomy, Iowa State University, Ames, IA, USA
[81] [(a)]Departamento de Engenharia Elétrica, Universidade Federal de Juiz de Fora (UFJF), Juiz de Fora, Brazil; [(b)]Universidade Federal do Rio De Janeiro COPPE/EE/IF, Rio de Janeiro, Brazil; [(c)]Instituto de Física, Universidade de São Paulo, São Paulo, Brazil; [(d)]Rio de Janeiro State University, Rio de Janeiro, Brazil
[82] KEK, High Energy Accelerator Research Organization, Tsukuba, Japan
[83] Graduate School of Science, Kobe University, Kobe, Japan

[84] [(a)]Faculty of Physics and Applied Computer Science, AGH University of Science and Technology, Kraków, Poland; [(b)]Marian Smoluchowski Institute of Physics, Jagiellonian University, Kraków, Poland
[85] Institute of Nuclear Physics Polish Academy of Sciences, Kraków, Poland
[86] Faculty of Science, Kyoto University, Kyoto, Japan
[87] Kyoto University of Education, Kyoto, Japan
[88] Research Center for Advanced Particle Physics and Department of Physics, Kyushu University, Fukuoka, Japan
[89] Instituto de Física La Plata, Universidad Nacional de La Plata and CONICET, La Plata, Argentina
[90] Physics Department, Lancaster University, Lancaster, UK
[91] Oliver Lodge Laboratory, University of Liverpool, Liverpool, UK
[92] Department of Experimental Particle Physics, Jožef Stefan Institute and Department of Physics, University of Ljubljana, Ljubljana, Slovenia
[93] School of Physics and Astronomy, Queen Mary University of London, London, UK
[94] Department of Physics, Royal Holloway University of London, Egham, UK
[95] Department of Physics and Astronomy, University College London, London, UK
[96] Louisiana Tech University, Ruston, LA, USA
[97] Fysiska institutionen, Lunds universitet, Lund, Sweden
[98] Departamento de Física Teorica C-15 and CIAFF, Universidad Autónoma de Madrid, Madrid, Spain
[99] Institut für Physik, Universität Mainz, Mainz, Germany
[100] School of Physics and Astronomy, University of Manchester, Manchester, UK
[101] CPPM, Aix-Marseille Université, CNRS/IN2P3, Marseille, France
[102] Department of Physics, University of Massachusetts, Amherst, MA, USA
[103] Department of Physics, McGill University, Montreal, QC, Canada
[104] School of Physics, University of Melbourne, Victoria, Australia
[105] Department of Physics, University of Michigan, Ann Arbor, MI, USA
[106] Department of Physics and Astronomy, Michigan State University, East Lansing, MI, USA
[107] Group of Particle Physics, University of Montreal, Montreal, QC, Canada
[108] Fakultät für Physik, Ludwig-Maximilians-Universität München, Munich, Germany
[109] Max-Planck-Institut für Physik (Werner-Heisenberg-Institut), Munich, Germany
[110] Graduate School of Science and Kobayashi-Maskawa Institute, Nagoya University, Nagoya, Japan
[111] Department of Physics and Astronomy, University of New Mexico, Albuquerque, NM, USA
[112] Institute for Mathematics, Astrophysics and Particle Physics, Radboud University/Nikhef, Nijmegen, The Netherlands
[113] Nikhef National Institute for Subatomic Physics and University of Amsterdam, Amsterdam, The Netherlands
[114] Department of Physics, Northern Illinois University, DeKalb, IL, USA
[115] [(a)]New York University Abu Dhabi, Abu Dhabi, United Arab Emirates; [(b)]United Arab Emirates University, Al Ain, United Arab Emirates; [(c)]University of Sharjah, Sharjah, United Arab Emirates
[116] Department of Physics, New York University, New York, NY, USA
[117] Ochanomizu University, Otsuka, Bunkyo-ku, Tokyo, Japan
[118] Ohio State University, Columbus, OH, USA
[119] Homer L. Dodge Department of Physics and Astronomy, University of Oklahoma, Norman, OK, USA
[120] Department of Physics, Oklahoma State University, Stillwater, OK, USA
[121] Joint Laboratory of Optics, Palacký University, Olomouc, Czech Republic
[122] Institute for Fundamental Science, University of Oregon, Eugene, OR, USA
[123] Graduate School of Science, Osaka University, Osaka, Japan
[124] Department of Physics, University of Oslo, Oslo, Norway
[125] Department of Physics, Oxford University, Oxford, UK
[126] LPNHE, Sorbonne Université, Université Paris Cité, CNRS/IN2P3, Paris, France
[127] Department of Physics, University of Pennsylvania, Philadelphia, PA, USA
[128] Department of Physics and Astronomy, University of Pittsburgh, Pittsburgh, PA, USA
[129] [(a)]Laboratório de Instrumentação e Física Experimental de Partículas-LIP, Lisbon, Portugal; [(b)]Departamento de Física, Faculdade de Ciências, Universidade de Lisboa, Lisbon, Portugal; [(c)]Departamento de Física, Universidade de Coimbra, Coimbra, Portugal; [(d)]Centro de Física Nuclear da Universidade de Lisboa, Lisbon, Portugal; [(e)]Departamento de Física, Universidade do Minho, Braga, Portugal; [(f)]Departamento de Física Teórica y del Cosmos, Universidad de Granada, Granada, Spain; [(g)]Instituto Superior Técnico, Universidade de Lisboa, Lisbon, Portugal

[130] Institute of Physics of the Czech Academy of Sciences, Prague, Czech Republic
[131] Czech Technical University in Prague, Prague, Czech Republic
[132] Faculty of Mathematics and Physics, Charles University, Prague, Czech Republic
[133] Particle Physics Department, Rutherford Appleton Laboratory, Didcot, UK
[134] IRFU, CEA, Université Paris-Saclay, Gif-sur-Yvette, France
[135] Santa Cruz Institute for Particle Physics, University of California Santa Cruz, Santa Cruz, CA, USA
[136] [(a)]Departamento de Física, Pontificia Universidad Católica de Chile, Santiago, Chile; [(b)]Millennium Institute for Subatomic physics at high energy frontier (SAPHIR), Santiago, Chile; [(c)]Instituto de Investigación Multidisciplinario en Ciencia y Tecnología y Departamento de Física, Universidad de La Serena, La Serena, Chile; [(d)]Department of Physics, Universidad Andres Bello, Santiago, Chile; [(e)]Instituto de Alta Investigación, Universidad de Tarapacá, Arica, Chile; [(f)]Departamento de Física, Universidad Técnica Federico Santa María, Valparaíso, Chile
[137] Department of Physics, University of Washington, Seattle, WA, USA
[138] Department of Physics and Astronomy, University of Sheffield, Sheffield, UK
[139] Department of Physics, Shinshu University, Nagano, Japan
[140] Department Physik, Universität Siegen, Siegen, Germany
[141] Department of Physics, Simon Fraser University, Burnaby, BC, Canada
[142] SLAC National Accelerator Laboratory, Stanford, CA, USA
[143] Department of Physics, Royal Institute of Technology, Stockholm, Sweden
[144] Department of Physics and Astronomy, Stony Brook University, Stony Brook, NY, USA
[145] Department of Physics and Astronomy, University of Sussex, Brighton, UK
[146] School of Physics, University of Sydney, Sydney, Australia
[147] Institute of Physics, Academia Sinica, Taipei, Taiwan
[148] [(a)]E. Andronikashvili Institute of Physics, Iv. Javakhishvili Tbilisi State University, Tbilisi, Georgia; [(b)]High Energy Physics Institute, Tbilisi State University, Tbilisi, Georgia; [(c)]University of Georgia, Tbilisi, Georgia
[149] Department of Physics, Technion, Israel Institute of Technology, Haifa, Israel
[150] Raymond and Beverly Sackler School of Physics and Astronomy, Tel Aviv University, Tel Aviv, Israel
[151] Department of Physics, Aristotle University of Thessaloniki, Thessaloniki, Greece
[152] International Center for Elementary Particle Physics and Department of Physics, University of Tokyo, Tokyo, Japan
[153] Department of Physics, Tokyo Institute of Technology, Tokyo, Japan
[154] Department of Physics, University of Toronto, Toronto, ON, Canada
[155] [(a)]TRIUMF, Vancouver, BC, Canada; [(b)]Department of Physics and Astronomy, York University, Toronto, ON, Canada
[156] Division of Physics and Tomonaga Center for the History of the Universe, Faculty of Pure and Applied Sciences, University of Tsukuba, Tsukuba, Japan
[157] Department of Physics and Astronomy, Tufts University, Medford, MA, USA
[158] Department of Physics and Astronomy, University of California Irvine, Irvine, CA, USA
[159] Department of Physics and Astronomy, University of Uppsala, Uppsala, Sweden
[160] Department of Physics, University of Illinois, Urbana, IL, USA
[161] Instituto de Física Corpuscular (IFIC), Centro Mixto Universidad de Valencia-CSIC, Valencia, Spain
[162] Department of Physics, University of British Columbia, Vancouver, BC, Canada
[163] Department of Physics and Astronomy, University of Victoria, Victoria, BC, Canada
[164] Fakultät für Physik und Astronomie, Julius-Maximilians-Universität Würzburg, Würzburg, Germany
[165] Department of Physics, University of Warwick, Coventry, UK
[166] Waseda University, Tokyo, Japan
[167] Department of Particle Physics and Astrophysics, Weizmann Institute of Science, Rehovot, Israel
[168] Department of Physics, University of Wisconsin, Madison, WI, USA
[169] Fakultät für Mathematik und Naturwissenschaften, Fachgruppe Physik, Bergische Universität Wuppertal, Wuppertal, Germany
[170] Department of Physics, Yale University, New Haven, CT, USA

[a] Also Affiliated with an Institute covered by a cooperation agreement with CERN., Geneva, Switzerland
[b] Also at Borough of Manhattan Community College, City University of New York, New York, NY, USA
[c] Also at Bruno Kessler Foundation, Trento, Italy
[d] Also at Center for High Energy Physics, Peking University, Beijing, China

[e] Also at Centro Studi e Ricerche Enrico Fermi, Rome, Italy
[f] Also at CERN, Geneva, Switzerland
[g] Also at Département de Physique Nucléaire et Corpusculaire, Université de Genève, Geneva, Switzerland
[h] Also at Departament de Fisica de la Universitat Autonoma de Barcelona, Barcelona, Spain
[i] Also at Department of Financial and Management Engineering, University of the Aegean, Chios, Greece
[j] Also at Department of Physics and Astronomy, Michigan State University, East Lansing, MI, USA
[k] Also at Department of Physics and Astronomy, University of Louisville, Louisville, KY, USA
[l] Also at Department of Physics, Ben Gurion University of the Negev, Beer Sheva, Israel
[m] Also at Department of Physics, California State University, East Bay, USA
[n] Also at Department of Physics, California State University, Sacramento, USA
[o] Also at Department of Physics, King's College London, London, UK
[p] Also at Department of Physics, University of Fribourg, Fribourg, Switzerland
[q] Also at Department of Physics, University of Thessaly, Thessaly, Greece
[r] Also at Department of Physics, Westmont College, Santa Barbara, USA
[s] Also at Hellenic Open University, Patras, Greece
[t] Also at Institucio Catalana de Recerca i Estudis Avancats, ICREA, Barcelona, Spain
[u] Also at Institut für Experimentalphysik, Universität Hamburg, Hamburg, Germany
[v] Also at Institute of Particle Physics (IPP), Toronto, Canada
[w] Also at Institute of Physics, Azerbaijan Academy of Sciences, Baku, Azerbaijan
[x] Also at Institute of Theoretical Physics, Ilia State University, Tbilisi, Georgia
[y] Also at Lawrence Livermore National Laboratory, Livermore, USA
[z] Also at Physics Department, An-Najah National University, Nablus, Palestine
[aa] Also at The City College of New York, New York, NY, USA
[ab] Also at The Collaborative Innovation Center of Quantum Matter (CICQM), Beijing, China
[ac] Also at TRIUMF, Vancouver, BC, Canada
[ad] Also at Università di Napoli Parthenope, Naples, Italy
[ae] Also at University of Chinese Academy of Sciences (UCAS), Beijing, China
[af] Also at Department of Physics, University of Colorado Boulder, Colorado, USA
[ag] Also at Yeditepe University, Physics Department, Istanbul, Türkiye
* Deceased